Climate impact on diatom size and distribution

Scott Andrew Burgan

A dissertation submitted to the University of Bristol in accordance with the requirements for award of the degree of Master of Science (by research) in the Faculty of Science

Geographical Sciences

November 2019

Word Count: 25546

Abstract

Diatoms are one of the ocean's key primary producers and are responsible for a large proportion of carbon export from the surface layer. With this, diatoms also play a vital role in the cycling of many key nutrient's, such as phosphate and nitrogen, and are the key driver of the silica cycle. However, changes to the Earth's climate can alter the distribution, abundance, and size classes of this organism, which in turn will impact global carbon export.

This study investigates the effect of two differing climates - simulated using EcoGENIE – on diatom distribution and size. Firstly, diatoms were incorporated into the ecological component of the model by parameterising their defining features (high growth rate, silica usage and protection from grazers). Opal export was also added to the model, where mortality and messy feeding on diatoms resulted in opal export, allowing it to be reintroduced into the biological model and redistributed as biogenic silica. Once included in the model, I ran experiments to look at how different climates influenced diatoms. The first of these was a cooler environment with an atmospheric CO_2 concentration of 190 ppm, in line with that of the LGM. The second, a warmer environment, with a pCO_2 concentration of 425 ppm. These two climates were run to reach a steady state, where the impact on diatom distribution and size was compared to that of a pre-industrial control (278 ppm). This study found that at 190 ppm, primary production (PP) and carbon export increased by 4.9% and 1.4% respectively, primarily driven by increased nutrients in the surface waters from increased upwelling (472% global increase), fuelling diatom growth. At 425 ppm, both PP and carbon export decreased with biomass decreasing by almost 11% and consequentially POC export decreases by 4.6%. This decrease was driven by a reduction in the nutrients in the surface waters, particularly in the North Atlantic, due to a reduction in mixing and stratification of the water column. From this it is clear to see that diatoms play an important role in the export of carbon in this model, with the changes to nutrient supply at different climate being the key driver of the change. One of the key findings from this study, was the impact on diatom size class. These did not respond as expected, with a cooler environment leading to an increase in smaller diatoms and the warmer climate seeing an increase in larger sized diatoms. The compliance of diatoms to the general temperature size rule suggested by Bergmann (1847), James (1970) and Atkinson (1995) has been subject to numerous studies (Li *et al.*, 2009; Morán *et al.*, 2010; Yvon-Durocher *et al.*, 2011; Rüger and Sommer, 2012; Adams *et al.*, 2013) with mixed results. I concluded that in this study however, being of a smaller size was not more advantageous – as suggested by Adams *et al* (2013) - therefore alterations to size with temperature change was not seen.

An additional experiment incorporating ballasting was also conducted on the pre-industrial time period. With this integrated into the model, it showed increased carbon export (by up to 175%) from smaller diatom size class in equatorial regions, highlighting their importance, and the importance of including multiple size classes when modelling diatoms in future studies.

Acknowledgements

Firstly, I would like to thank my supervisor Fanny Monteiro for her guidance and support throughout this project. Fanny always made time for me despite her numerous PhD students, busy work schedule and personal research. For that, I can't thank her enough.

I would also like to thank Jamie Wilson for his help throughout this project, helping me with any modelling related queries that I had and always providing valuable guidance. Finally, a thank you to the postgraduates in Brown's who made my time at Bristol enjoyable and helped me adapt to postgraduate life, as well as providing valuable knowledge and support when learning new skills.

Author's declaration

I declare that the work in this dissertation was carried out in accordance with the requirements of the University's *Regulations and Code of Practice for Research Degree Programmes* and that it has not been submitted for any other academic award. Except where indicated by specific reference in the text, the work is the candidate's own work. Work done in collaboration with, or with the assistance of, others, is indicated as such. Any views expressed in the dissertation are those of the author.

SIGNED:…….. DATE: ……

Table of Contents

Abstract iii
Acknowledgements v
Author's declaration vii
List of Figures xii
List of tables xvi
1 Introduction 2
2 Literature review 7
2.1 – Current Distribution 7
2.2 – Key groups of diatoms 8
2.3 - Controls on diatoms 9
2.3.1 Temperature 9
2.3.2 Nutrients 10
2.3.3 Light 11
2.3.4 Grazing 12
2.4 – Interactions between diatoms and climate 13
2.4.1 – Climates impacts on diatom biogeography 13
2.5 What can cause these changes in biogeography? 15
2.6 Past patterns 17
2.7 The use of diatoms in climate models 19
2.7.1 NPZD models 19
2.7.2 More complex PFT models 20
2.7.3 Darwin model 21
2.8 Use of models to predict future climate 22
3 Methodology 24
3.1 Model Description 24
3.1.1 Ocean physics component: C-GOLDSTEIN 24
3.1.2 Ocean biogeochemical cycling component: BIOGEM 25
3.1.3 Ecological component: ECOGEM 25
3.1.4 Diatom equation 31
3.1.5 State Variables 31
3.2 Size Dependant traits 33
3.3 Adding Diatoms into ECOGEM 36
3.4 Model runs 38
4 Results 39
4.1 Distribution under preindustrial conditions 39

4.1.1 Nutrients 39
4.1.2 Total phytoplankton and zooplankton 41
4.1.3 Diatoms 42
4.2 Effect of climate 45
4.2.1 Colder climate experiment (190ppm) 46
4.2.2 Warmer climate experiment (425ppm) 50
4.3 Causes of change 54
5 Discussion 60
5.1 – Cooler climate (190ppm) 61
5.2 – Warmer climate experiment (425ppm) 64
5.3 – Does size class matter? 67
5.4 – Future investigations 69
6 Conclusion 71
7 References 74
8 Appendix 104

List of Figures

Figure 1, the biogeographical distribution of diatoms illustrated by the MIT ecosystem model results. This shows the distribution of diatoms in the surface waters between April - June (a) and October - December (b) (Tréguer et al., 2018)..... 13

Figure 2, a visual representation of EcoGEnIE's size structured model (Ward et al., 2018), depicting important allometric relationships for (1) affinity to nutrients and carbon uptake rate, (2) cell quota for carbon, and (3) grazing. 36

Figure 3, a visual representation of the coupling between BIOGEM and ECOGEM, adapted from Ward et al. (2018). State variables shown: R represents a resource, B planktonic biomass, D diatom biomass, OM indicating organic matter, and OP showing opal. The subscripts (B and E) indicate if this is occurring in BIOGEM or ECOGEM and (δ) is rate of change. The adaptions made to this from Ward et al. (2018) are indicated by their blue colouring with these processes only occurring in diatoms. ... 37

Figure 4, global phosphate concentration (µmol P kg^{-1}) in cGEnIE surface waters (80.8m) during preindustrial simulation (left) compared to phosphate concentrations (µmol P Kg^{-1}) from global observations from NOAA (WOA) (Garcia et al., 2019)..... 39

Figure 5, global silicate concentration (µmol Kg-1) in cGEnIE surface waters (80.8m) during preindustrial simulation (left) compared to silicate concentrations (µmol Kg-1) from global observations from NOAA (WOA) (Garcia et al., 2019)..... 40

Figure 6, the surface (80.8m) concentration of iron (nmol Fe Kg^{-1}) in our model when under preindustrial conditions 41

Figure 7, phytoplankton (left) and zooplankton (right) concentrations (µmol C l^{-1}) in our model when under preindustrial conditions..... 42

Figure 8, concentration of diatoms (µmol C l^{-1}) in cGEnIE (left) under preindustrial conditions, compared to the MIT Darwin model (right). The Darwin model uses mmol C m^{-3}, however when converted, this is the same as µmol C l^{-1}- which is used in the cGEnIE model. 43

*Figure 9, the contribution of size classes (%) to the global concentration depicted in figure 8. Showing 1µm diatoms (top left), 10µm diatoms (top right) and 100µm diatoms (bottom). The contribution of each size class was calculated using a simple percentage calculation ((x / y) * 100) where x is the concentration of the selected size class and y is the overall diatom concentration..... 45*

*Figure 10, results showing the change in PFT concentrations between a cool climate and the preindustrial environment. The percentage change in concentration was calculated as follows: ((concentration at 190ppm – concentration at 278ppm) / concentration at 278ppm) *100. A full*

comparison of these functional type's concentration with the preindustrial environment can be found in Appendix 1.....47

*Figure 11, changes in diatom size class concentrations between the cooler environment and the preindustrial run – with blue indicating a reduciton in concentration and red showing an increase. These changes were calculated as follows: ((size class concetration at 190ppm - size class concetration at 278ppm) / size class concetration at 278ppm) * 100.....48*

*Figure 12, changes to POC export between the cooler environment and the preindustrial environment, with blue indicating a reduction in export and red an increase. This was calculated as follows: ((POC export in cooler environment – POC export in preindustrial environment) / POC export in preindustrial environment * 100.....49*

*Figure 13, results showing the change in PFT concentrations between a warm climate and the preindustrial environment. The percentage change in concentration was calculated as follows: ((concentration at 425ppm – concentration at 278ppm) / concentration at 278ppm) *100. A full comparison of these functional type's concentration with the preindustrial environment can be found in Appendix 2.....51*

*Figure 14, changes in diatom size class concentrations between the warmer environment and the preindustrial run – with blue indicating a reduciton in concentration and red showing an increase. These changes were calculated as follows: ((size class concetration at 425ppm - size class concetration at 278ppm) / size class concetration at 278ppm) * 100.....52*

*Figure 15, changes to POC export between the warmer environment and the preindustrial environment, with blue indicating a reduction in export and red an increase. This was calculated as follows: ((POC export in warmer environment – POC export in preindustrial environment) / POC export in preindustrial environment * 100 .....53*

*Figure 16, the change in upwelling velocity between the preindustrial climate (top) and the cooler (bottom left) and warmer climate (bottom right). Changes were calculated as follows: ((Upwelling in cooler / warmer climate – upwelling in preindustrial conditions) / upwelling in preindustrial conditions) *100. The changes in upwelling are limited to between -100% and 100%. This is due to a few select points showing dramatic changes in velocity thus, when the scale is set to include these, numerous other data points become ineligible. 55*

*Figure 17, changes in convective mixing between preindustrial (top) and cooler (bottom left) and warmer environment (bottom right). Changes were calculated as follows: ((Convective mixing in cooler / warmer climate – convective mixing in preindustrial conditions) / convective mixing in preindustrial conditions) *100. .....56*

*Figure 18, changes in MLD between the preindustrial environment and the cooler (left) and warmer (right) environment. This was calculated as follows: ((MLD in cooler / warmer climate – MLD in preindustrial conditions) / MLD in preindustrial conditions) *100. .....58*

*Figure 19, change in surface PO_4 concentration between preindustrial climate and the cooler (left) and warmer (right) environments. This was calculated as follows: ((PO_4 in cooler / warmer climate – PO_4 in preindustrial conditions) / PO_4 in preindustrial conditions) *100. .....58*

*Figure 20, changes to sea ice cover between the preindustrial environment and the cooler (left) and warmer (right) environments. This was calculated as follows: ((sea ice in cooler / warmer climate – sea ice in preindustrial conditions) / sea ice in preindustrial conditions) *100. .....59*

Figure 21, the total flux of POC (solid line) and the POC flux associated with ballast materials (dashed line). The crosshatched partition of these two lines represents "excess" POC that would be remineralized in the surface / upper water column (image taken from Armstrong et al., (2001)).....67

*Figure 22, a comparison of POC export with ballasting effect off (top left) and when it is switched on (top right) under pre-industrial conditions. The percentage change between these two states is also shown, and was calculated as follows; ((POC with ballasting - POC export without ballasting) / POC export without ballasting) *100.....69*

List of tables

Table 1, Index notation for the state variables in ECOGEM (adapted from (Ward et al., 2018)).....32

Table 2, PFTs and their associated size classes (adapted from Ward et al., (2018)).....32

Table 3, Size-dependant ecophysiological parameters (p) and associated units, with their size scaling coefficients (a, b, c). (adapted from (Ward et al., 2018)) 34

List of equations

(1) Nutrient uptake before silica addition *26*

(2)Nurtient uptake with addition of silica *26*

(3)Temperature limitation *27*

(4)Light Limitation *27*

(5)Maximum light-saturated growth rate *28*

(6)Photosynthetic rate *28*

(7)Cell quota *29*

(8)Nutrient uptake *29*

(9)Grazing rate *30*

(10)Mortality *30*

(11)Diatom growth (simplified) *31*

(12)Diatom growth *31*

(13)Ballasting *67*

1 Introduction

Diatoms (Bacillariophyceae) are unicellular eukaryotic algae found in freshwater and marine systems around the world. These silicified organisms can appear as single cells, but also as filaments, chains, and in colonies - in both the water column and on benthos. They are particularly important for the marine system, as they account for 40% of the total primary production (PP) in the world's oceans (Nelson *et al.*, 1995; Treguer *et al.*, 1995). Diatom's are also responsible for a large proportion of organic carbon export from the surface to deeper waters (Rynearson *et al.*, 2013; Assmy *et al.*, 2013), critical for the carbon cycle and climate change. Diatoms importance comes from advantageous traits that distinguish them from other phytoplankton. These include a silica cell wall, known as the frustule, which encompasses the organs of the cell and offers protection against grazing (Hamm *et al.*, 2003), higher relative growth rates (Banse, 1982) and their ability to store nutrients due to their larger size (Smetacek, 1999; Litchman, Klausmeier and Yoshiyama, 2009). This cell wall is ornate and complex in structure as well as being transparent and perforated, allowing for the passing of both light and diffusion of materials (Sabater, 2009). With their silica frustule, and contribution to PP, diatoms not only influence the cycling of many of the ocean's key nutrients such as phosphorous (P), nitrogen (N), but they also are a key driver of the silica (Si) cycle; often governing export production (Buesseler, 1998).

The ballasting of inorganic opal, calcium carbonate and lithogenic materials needs to be considered when looking at carbon export. If diatoms were the main cause of organic carbon export, we would expect to see regional variability in rain ratios, which is not seen in sediment trap data (Archer, 1996). The proposed mechanism of ballasting (Armstrong *et al.,* 2001) was developed based on observations linking carbon export with fluxes in these ballast minerals. These minerals can contribute up to half of sinking particles from the surface waters (Honjo, Manganini and Cole, 1982) and have a greater density than both seawater and other organic materials (McCave, 1975; Smayda, 1971). Therefore, as these ballast minerals sink, pick up more organic material and increase in

density, you would expect to see an increase in their sinking rate, as well as potentially protecting the organic material being exported (Armstrong *et al.*, 2001).

Diatoms are the one of the few phytoplankton group to use silicic acid to produce a biomineral silica cell wall (Lewis, 1955) also known as a frustule. This cell wall provides protection from grazers (Hamm *et al.*, 2003) and also supports the formation of a large vacuole used for nutrient storage in larger species (Smetacek, 1999). However, a trade-off of using silica, is that it's an additional limiting nutrient. This limitation leads to distinct regional distribution due to the varying availability of silica, from basins to basins (Moore and Abbott, 2002).

Diatoms can vary dramatically in size, with the smallest being the *Minidiscus* genus - which can be as small as 1.9 μm in diameter (Aké-Castillo *et al.*, 2001). These tiny diatoms have a wide distribution with some species being cosmopolitan and other confined to specific regions. In contrast, one of the largest diatom genus is *Ethmodiscus* can grow 4-5 orders of magnitude larger (Sommer *et al.*, 2016) and favours stratified oligotrophic water masses (Luo *et al.*, 2018), and unlike certain *Minidiscus* spp*.,* these are not cosmopolitan. The varying distribution of size classes is constrained by resource competition, biochemistry, and the climate. Cell size and morphology often govern an organisms eco-physiological traits (Litchman *et al.*, 2007) such as nutrient uptake, growth rate and their minimum nutrient quota (Litchman *et al.*, 2006). For example, smaller cells with a higher surface area to volume ratios often fare best in nutrient poor environments - due to a reduced diffusion boundary, higher photosynthesis rates, lower sinking rates and faster reproduction / cell division when compared to larger cells (Litchman *et al.*, 2006). However, in a well-mixed nutrient-rich environment larger cells would often be the dominant class (Bell and Kalff, 2001). As a result, changes in distribution can tell us a lot about ocean chemistry, changes under different climate scenarios and changes in diatom size class distribution – all of which will be important factors to look at.

In recent decades, studies have begun to uncover the strong relationship between the silica cycle and other biogeochemical cycles such as carbon and nitrogen cycles (Tréguer and De La Rocha, 2013).The tight coupling to these key biogeochemical cycles, especially that of carbon, make silica a fundamental element when looking at climate change. Atmospheric CO_2 concentration plays a fundamental role in changes to the earth's climate and is focal point in the latest IPCC report (Masson-Delmotte *et al.*, 2018). Therefore, removing CO_2 from the atmosphere and sequestering it in the deep ocean may be essential in slowing the impacts of climate change. With diatom's high relative abundance and export production, we need to have a good understanding of their response to climate change; as changes in their distribution, abundance and diversity could impact the removal of atmospheric CO_2.

Evidence exists also for diatoms to play a key role in regulating paleoclimatic events (Matsumoto and Sarmiento, 2008; Matsumoto, Sarmiento and Brzezinski, 2002). In particular during the last glacial maximum (LGM), the peak of which was roughly 21 500 years ago, there is a hypothesis that changes in diatoms were responsible for some of the draw-down of atmospheric CO_2 observed during that period, referred to as the Si leakage hypothesis (Brzezinski *et al.*, 2002; Matsumoto, Sarmiento and Brzezinski, 2002). This hypothesis explains the CO_2 draw-down due to the reduction of Si-limitation in the lower latitudes (Matsumoto, Sarmiento and Brzezinski, 2002), allowing for the formation of diatom blooms, and increasing the export of carbon into the deep ocean (Kienast *et al.*, 2006). It is believed that iron could be the cause of this shift in silica. Alleviating iron limitation in the high-nutrient low-chlorophyll regions of the Southern Ocean (SO) would allow for an increase in phytoplankton, especially diatoms, increasing carbon export (Buesseler and Boyd, 2003). Additionally it was shown that diatom's Si:N ratio was reduced from 4:1 to 1:1 in nutrient and light replete diatoms (Sarthou *et al.*, 2005; Brzezinski, 1985). This decrease in the utilisation of silica allows for an increase in its export to the lower latitudes and other upwelling regions (Kienast *et al.*,

2006). An influx of silica into silica limited regions such as the equatorial eastern Pacific, could lead to a shift in community dynamics and allow for increased carbon export in the lower latitudes.

Having possibly had an impact on past climates, it is likely diatoms will play a role in future climates as well. With a gradually warming climate, we would expect to see changes to the distribution, abundance, and carbon export from diatoms over the coming decades as alterations to the ocean's biochemistry occur. The exact nature of these changes has been investigated in several studies (Richardson and Schoeman, 2004; Hays, Richardson and Robinson, 2005; Masson-Delmotte *et al.*, 2018) with the use of computer modelling. This will also be used in this study to look at the effect of both a warmer and colder climate on diatoms. Using a size-based ecosystem model embedded into an Earth system model (EcoGENiE) I will be able to run simulations of both warmer and colder climates and compare the results to current literature to test its validity.

The overall aim of this thesis is to determine how differing climatic scenarios will affect the distribution, abundance and export abilities of marine diatoms of varying sizes. This will be done by running a series of climate simulations on EcoGENIE, depicting pre-industrial (278 ppm), future warm climate (425 ppm) and cold climate (190 ppm) conditions. With this, I will be able to compare changes to these outputs and investigate the top-down/bottom-up controls that may be responsible. In this thesis I expect to see an increase in both abundance and POC export from marine diatoms in a cooler paleoclimate - particularly in the mid-latitudes - with larger size classes becoming more dominant. This is due to cooler surface waters allowing for greater upwelling thus increasing the delivery of nutrients to the surface - allowing for increased diatom growth. As pCO_2 increases I would expect to see contrasting results, with a POC export reduction (especially in the low latitudes) as the oceans become more stratified and as a result, nutrients become more limited. Additionally, I expect to see a shift in distribution to the lower latitudes as pCO_2 increases and temperature limitations are reduced, as well as an increase in the abundance of smaller size classes, that are better adapted to the lower nutrient conditions.

A summary of my hypothesis:

- In the cooler climate experiments;
    - *Diatom abundance will increase, as will POC export.*
    - *Larger size classes will become more prominent and dominate diatom biomass.*
- In the warmer climate experiments;
    - *Diatom abundance will decrease along with POC export.*
    - *Smaller size classes will become more prominent and dominate the diatom biomass.*

2 Literature review

2.1 – Current Distribution

Diatoms are diverse in their distribution, being found in terrestrial, fresh water and marine environments (Mann and Droop, 1996), with many being endemic to specific geographical locations - especially marine diatoms (Vanormelingen, Verleyen and Vyverman, 2008). This study focuses on marine diatoms, which are often dominant in high-nutrient systems, areas of coastal upwelling, the Southern Ocean and in spring blooms (Wilson, Smith and Nelson, 1986).

With their dependence on silica, diatoms are expected to be found in areas with a higher silica concentration. *Tréguer and De La Rocha. (2013)* list the main external inputs of silicic acid (DSi) to the world's oceans, these being:

- **Continental inputs**– silicic acid and biogenic silica flux from rivers, estuaries, reverse weathering and submarine groundwater discharge. (7.1 ± 2.0 Tmol Si y^{-1})
- **Aeolian inputs** – lithogenic and biogenic silica found in dust (0.5 ± 0.5 Tmol Si y^{-1})
- **Hydrothermal inputs** – leaching of silicon from the oceanic crust (0.6 ± 0.4 Tmol Si y^{-1})
- **Dissolution of terrestrial materials and sea floor basalt** – (1.9 ± 0.7 Tmol Si y^{-1})

These inputs help explain the dominance of diatoms in coastal regions; with upwelling bringing nutrients to potentially DSi rich environments (supplied by continental inputs) and aeolian inputs combining with the additional nutrients accompanying spring blooms and high nutrient systems.

The Southern Ocean, although not effected by river or submarine groundwater flow, does have a unique source of DSi not previously considered by *Tréguer and De La Rocha. (2013).* This was input from processes linked with the melting of the Antarctic ice sheets such as basal melting, subglacial meltwaters and melting of icebergs (Tréguer, 2014). The Southern Ocean in fact, has been identified

as having a vital role in the world ocean silica cycle (Pondaven *et al.*, 2000a; Treguer *et al.*, 1995; DeMaster, 2002), with Antarctic Bottom water exporting large amounts of DSi to deep regions in the Atlantic, Pacific and Indian basins (Anderson *et al.*, 2002).

Satellite imagery is a method used in multiple studies to depict the distribution of selected phytoplankton groups (Lehahn, D'Ovidio and Koren, 2018; Di Cicco *et al.*, 2017; Alvain *et al.*, 2008). These studies use ocean colour sensors to measure chlorophyll *a* (Chl *a*) in the surface waters to determine phytoplankton locations. In order to distinguish between groups of phytoplankton, *Alvain et al., (2008)* looked at the water-leaving radiance measured in the ocean colour sensor. Like in situ data had shown, significant variation in wavelengths were seen for different Chl *a*, which in turn distinguishes between the different groups of phytoplankton. However, ground-truthing of methods, such as the Lagrangian method (Lehahn, D'Ovidio and Koren, 2018) is rare, with studies often focussing on physical tracers (Prants *et al.*, 2016). Additionally methods using altimetry can also be subject to uncertainties due to them being infamously unreliable (Cipollini, Vignudelli and Benveniste, 2014).

2.2 – Key groups of diatoms

The number of diatom species is still debated with estimates ranging from 20 000 (Guiry, 2012) to 200 000 (Mann and Droop, 1996), but this was revisited by *Mann and Vanormelingen (2013)* with a new estimation of 30 000 – 100 000 species. The earliest fossil record of diatoms is believed to be 180 million years old (Myr) and during this time there was only one class of diatoms, the centric diatoms who were characterised by their radial symmetry. It wasn't until 90 million years later that the second class of diatom that we see today was derived, the pennate diatom (Kooistra *et al.*, 2007), identifiable by their bilateral symmetry.

Diatom identification and classification can be done in numerous was such as PCA analysis (Pappas and Stoermer, 2003), looking at contour shape and texture change during life cycles (Sánchez,

Cristóbal and Bueno, 2019), but the most common is taking into account morphometric measures (length and width) and frustule characteristics (Blanco, Borrego-Ramos and Olenici, 2017). One such frustule characteristic is the presence of a raphe system found in certain pennate diatoms. These raphe systems allow for movement along surfaces by using a cytoplasmic contractile system and a secretion system (Drum and Hopkins, 1966). This is not found in all pennate diatoms with Araphid pennate diatoms lacking this, and for that reason, it's considered that these should be a separate class.

Further distinguishing features found in diatoms can include their ability to form chains, regulate their buoyancy and even fix nitrogen. Chain formation has been shown to have a control on the sinking rate of the diatoms, with a larger chain lengths leading to higher sinking rates (Bannon and Campbell, 2017). As well as chain formation altering sinking rates, some diatom species can also regulate their buoyancy and consequentially modify their sinking speed. This was noted by *Villareal (1992)* who found *Ethmodiscus* spp. to have a positive buoyancy, with an average accent rate of 1.4 m d^{-1}. The ability to modify buoyancy is believed to require energy (Waite, Thompson and Harrison, 1992) therefore, we would expect this ability to cease once certain environmental variables caused metabolic inhibition (Waite *et al.*, 1997).

Finally, diatom diazotroph associations (DDA) are another unique variation of diatoms; which is the ability to fix nitrogen. These diatoms act as a host for either an endosymbiotic or ectosymbiotic heterocystous cyanobacteria (Villareal *et al.*, 2012) and have a global distribution (Foster, Subramaniam and Zehr, 2009). However, DDA will not be included in this study as the Earth system model being used is yet to incorporate the nitrogen cycle.

2.3 - Controls on diatoms

2.3.1 Temperature

The effect of temperature on diatoms has long been studied, with sometime conflicting results. The growth rates of cells, including diatoms, is widely accepted to increase linearly with temperature

(Javaheri *et al.*, 2015; Montagnes and Franklin, 2001). One adaptation that is debated, is temperature's influence on cell volume and size. It has been shown that diatom cell volume decreases with increasing temperature (Li, Beardall and Gao, 2018), but there are also contradictory papers in the past, such as that by *Durbin (1977)*, who found there to be an increase in cell volume, and *Yoder (1979)*, who found no distinct pattern in relation to cell volume. In general, with a few exceptions, diatoms typically follow the temperature-size rule proposed by *Atkinson (1995)*. However, the cause of this is still not clear, with numerous explanations being proposed, but none widely accepted. One hypothesis is that a reduced cell size is an adaptation implemented to reduce their sinking rate, but this cannot be applied to ectotherms in a general sense (Atkinson, 1995). Another possible cause of a decreased cell volume is due to an increased metabolism and growth rate associated with increased temperatures, which in turn, requires more nutrients. Consequently an increased surface ratio to cell mass would be advantageous (Atkinson, Ciotti and Montagnes, 2003).

2.3.2 Nutrients

Nutrient limitation is described by at least three hypotheses. The first is the rate at which phytoplankton nutrient uptake occurs, which often fits with the Michaelis-Menten- kinetics (Turpin, 1988). Secondly, the relationship between the cell quota of a limiting nutrient and an organism's growth rate (Droop, 1968), sometimes referred to as Droops cell quota model. Finally, Leibig's law, which states that the growth of a cell is dependent on the internal concentration of the most limiting nutrient (Rhee, 1978; Droop, 1974).

Nitrogen and phosphorus are two macro nutrients that are thought to limit all phytoplankton (Watson, McCauley and Downing, 1997) and in addition to these, due to diatom's dependence on silicic acid, silica is also a limiting nutrient. Silicon is a key factor in the cell cycle and DNA formation,

thus a reduction in the availability of silicon will dramatically reduce growth and cell division (Brzezinski, Olson and Chisholm, 1990).

Like macronutrients, micronutrients play an important role in the development of diatom blooms and their life cycle. It is thought that iron has previously played an important role in oceanic primary production, as well as the export and subsequent absorption of atmospheric CO_2 (Martin, 1990; Falkowski, Barber and Smetacek, 1998). This is likely due to a past climate with an increased aridity, thus causing an increased dust flux, a pattern that may occur again due to anthropogenic changes (Asadi Zarch *et al.*, 2017). Many of the ocean's HNLC regions are iron limited leaving phytoplankton unable to utilise these rich nutrient sources. Iron is vital in many oceanic plant processes including the synthesis of chlorophyll and nitrate reduction (Rueler and Ades., 1987). Due to the profound impact of iron on diatom blooms, it has been a focus for numerous studies and fertilisation experiments (Smetacek *et al.*, 2012; Boyd *et al.*, 2000; Coale *et al.*, 1996) and is linked to the Si leakage hypothesis.

The chosen method of nutrient uptake used for my study is based on the cell quota model (Droop, 1968). This was chosen as it is more flexible and allows for plankton to take up nutrients depending on their availability. This was chosen over a fixed cellular stichometry as it increases the model's realism.

2.3.3 Light

Light is another control on diatoms, due to their dependence on photosynthesis. Diatoms are exposed to fluctuating light intensities due to varying degrees of light irradiation and their vertical movement through the photic zone (Kemp and Villareal, 2018). These fluctuations usually occur on daily or seasonal time scales but can also vary over the course of just a few seconds (Litchman and Klausmeier, 2001). At lower light intensities, these organisms will have a reduced ability to photosynthesize unless properly adapted to the conditions. Likewise, it has been shown that

excessive light exposure can also have a detrimental effect on phytoplankton's productivity (Long, Humphries and Falkowski, 1994), however, this can be managed by dissipating excess energy resulting from over exposure (Niyogi, 2000). Therefore, the plasticity of these organisms will play a key role in determining their distribution. *Litchman and Klausmeier (2001)* showed this when they found that phytoplankton species express a gleaner-opportunist trade-off between competitive ability and their ability to reach carrying capacity quickly.

Diatoms plasticity allows them to maintain a higher growth rate through various light intensities (Li and Campbell, 2013) due to their ability to adjust their photosynthetic apparatus (Lavaud, Rousseau and Etienne, 2004). It is also hypothesised that their biogenic silica frustule could have light-trapping capabilities, enhancing their photosynthetic efficiency in low light conditions (Romann *et al.*, 2015). These attributes allow diatoms to inhabit hugely diverse ecosystems from below sea ice to surface waters. However, they are still limited by light availability and consequentially, seasonal and daily light fluctuations will affect diatoms abundance. In the model used for this study, light will not undergo daily changes due to the time scales being used not accounting for this. However, the photosynthetic rate of organisms will vary depending on size. Therefore, certain size classes will be able to use light more efficiently than other classes making them more successful under a greater range of light intensities.

2.3.4 Grazing

A final key control on diatom abundance and distribution is the rate at which they are grazed by predators. One of the main predators of phytoplankton is zooplankton, often in the form of small copepods. Diatoms, however, have been shown to have a distinct biological advantage over other phytoplankton groups. This is due to the protection given by their unique silica frustules, which have been shown to require large amounts of force to break (Hamm *et al.*, 2003).

Studies have shown that diatoms have also developed other adaptions to reduce predation. A study by *Pondaven et al (2007)* found diatoms can alter their degree of silicification depending on the abundance of predators, increasing the thickness of their frustule in the presents of predators. Furthermore, there is evidence to suggest that chain forming diatoms have some degree of plasticity when determining their chain length, decreasing their length in order to reduce predation (Bergkvist *et al.*, 2012). This is likely due to zooplankton's preference towards grazing larger prey when it is available (Richman and Rogers, 1969), thus smaller sized diatoms may also have an advantage over larger diatom species.

2.4 – Interactions between diatoms and climate

2.4.1 – Climate impacts on diatom biogeography

For this study we will focus on the climatic impacts on diatom biogeography, which is well documented and can have a large impact on diatom distribution. The degree to which diatoms respond to environmental changes can be seen over small timescales, with seasonal variations altering their distributions and abundance (figure 1). This is due to changes in ocean temperature and nutrient supply associated with the seasons. In fact it has been hypothesised, that due to phytoplankton's sensitivity to changes

Figure 1, the biogeographical distribution of diatoms illustrated by the MIT ecosystem model results. This shows the distribution of diatoms in the surface waters between April - June (a) and October - December (b) (Tréguer *et al.*, 2018)

in their environment, they could be a better indicator of climatic changes than environmental variables themselves, due to their ability to amplify small, and difficult to detect environmental fluctuations (Taylor, Allen and Clark, 2002). This sensitivity could shift the global distribution of diatoms altering their biogeography, with knock on effects.

Due to diatoms being a main primary producer in the global oceans, their distribution can have a profound effect on the oceanic food web. Therefore an alteration of their biogeography away from their normal bloom patterns, could impact energy transfer to organisms of a higher trophic level (Pierella Karlusich, Ibarbalz and Bowler, 2020). With this, it has been suggested that dramatic shifts could lead to the removal of top predators and herbivores in the oceans (Smetacek and Cloern, 2008), thus altering ecosystem dynamics and community structure in the affected regions. It is likely that this bottom up control on the food web could be caused by the match-mismatch hypothesis suggested by *Cushing (1990)*, where food supply by phytoplankton does not match the food demand of zooplankton. With decreased food availability, it is likely zooplankton numbers would decline, and in turn, have a detrimental effect on fisheries.

In addition to a reduction in energy supply to higher trophic levels, changes in biogeography will also alter the drawdown and cycling of nutrients (Falkowski, Barber and Smetacek, 1998; Weber and Deutsch, 2010). This is important for primary productivity and could potentially enhance the negative effects on diatom distribution. Finally, we would expect to see changes to the distribution of different size of plankton with altered temperatures. Previous climatic conditions have shown, that with increased temperatures, diatoms were, in general, a smaller size (Finkel *et al.*, 2005). With this, we would see increased recycling in the microbial loop (Azam *et al.*, 1983), causing a reduction in the export of nutrients and carbon.

2.5 What can cause these changes in biogeography?

Since the beginning of the industrial revolution, human activities have caused a 1°C global temperature increase, with this set to increase to 1.5°C by 2030 -2052 (Masson-Delmotte *et al.*, 2018). Atmospheric CO_2 concentrations continue to rise (from 384 ppm in January 2008 to 408 ppm by the end of 2018 (NOAA, 2018)), causing an increase in sea surface temperature (SST), alterations to ocean pH and other physical and chemical changes. A study by *Burrows et al (2014)* found that isotherms of SST are moving towards the higher latitudes at a rate of up to 40 km per year. With these changes in isotherms we would also expect to see changes in marine organism distribution.

As previously discussed (1.4.1.1), temperature acts as a control on diatom size and growth rate, with increased temperature decreasing the overall cell volume of diatoms. As well as this morphological change, temperature can affect the development of their silica frustule – increasing Si content in some species and decreasing it in others (Paasche, 1980). With their silica frustules being a possible mechanism for protection from grazing (Hamm *et al.*, 2003), a decrease in Si content could leave these diatoms more vulnerable to grazing, thus changing the community composition and possibly their diversity.

A key requirement for all phytoplankton is nutrients, with the dense, nutrient-rich deep waters often being the main supply to the photic zone. A change in the nutrient upwelling regime would lead to dramatic changes in the community affected as nutrient limitations reduce phytoplankton growth, and consequentially, primary production. Due to their inverse relationship, an increase in SST will cause the ocean's surface water density to decrease, which will cause an increase in the stratification of the water column - affecting both light availability and nutrient supply to surface waters. The effect of intensified stratification on primary production was modelled by *Steinacher et al (2010)* in a multi-model analysis and found an overall decrease in global primary productivity of between 2 – 20% by 2100, under the SRES A2 emissions scenario. They also found that following the

SRES A2 emissions scenario there would be two changes in primary productivity regimes. The first of these is a reduction in primary productivity for the low and mid-latitudes as well as the North Atlantic, due to the decrease in micro-nutrients reaching the euphotic zone caused by enhanced stratification. The second finding was an increase in primary productivity for the Southern Ocean due to the reduction in light and/ or temperature limitations. These regime shifts would be expected to cause a change in the biogeography of diatoms, as conditions in the Southern Ocean become more favourable with increasing SSTs. Smith *et al.* (2017) found that SST had the greatest influence on diatom biogeography in the Southern Ocean, however macro-nutrients and pCO_2 have also been found to be good statistical indicators.

My study will be focussing on the effect of these temperature changes on nutrient delivery and stratification, but there are still other factors that are worth consideration. One of these is outlined in section 1.4.1.3, which briefly touched upon diatom dependence on light and their plasticity in reacting to different levels of irradiance. With light intensities set to increase due to enhanced stratification (Boyd *et al.*, 2010), diatoms in shallow waters or close to the surface will be put under additional stress. If these light intensities are too high for certain diatom species, and photoinhibition does occur, we would expect to see their geographical locations to shift. Changes to wind patterns could also be considered as they are responsible, in regions such as the Southern Ocean, for the overturning of deep water and eddie formation which in turn can transport waters across the Antarctic Circumpolar Current (ACC) (Dufour *et al.*, 2015). Therefore, changes to wind intensity or direction would undoubtably have some influence on the mixing of the surface waters in these regions, effecting both nutrient supply and light penetration. Furthermore, the transport of continental dust to the iron-limited Southern Ocean will also be dependent on the intensity and direction of these winds, further demonstrating their importance.

2.6 Past patterns

Over time diatoms have been subject to numerous dramatic changes in climate, with the most recent being the last glacial maximum (LGM). This period, when compared to the modern-day climate, is a good indicator of the effect a changing environment can have on the distribution and abundance of diatom populations.

One of the key regions when looking at diatoms in the LGM is the Southern Ocean. With lower ocean and atmospheric temperatures as well as increased wind speeds, ice cover and continental dust fluxes (Hays, 1977), this region would have had a different ecological structure to what we see today. A study by *Martin (1990)* argued that due to an increase in primary production in the LGM, Antarctica and the Southern Ocean were a far stronger sink for CO_2 in this period than they are today. With this, numerous hypotheses have been developed arguing both for and against this claim, many of which involve the export of CO_2 via diatoms.

The study by *Martin (1990)* is the fundamental hypothesis that many others build upon, the Iron Hypothesis. It was proposed that widespread iron limitation in our oceans, especially in the Southern Ocean and other HNLC regions, is causing a lower rate of productivity. This is due to iron being an essential nutrient for photosynthesis and nitrogen fixation (Jickells *et al.*, 2005). Therefore, the higher rate of aeolian dust transport in the LGM would have increase iron-fertilisation, thus increasing productivity and a reducing atmospheric CO_2. This is now a widely accepted hypothesis, with numerous iron-fertilisation experiments providing evidence for increased productivity with the addition of iron (Boyd *et al.*, 2007).

When looking specifically at diatoms, there are a couple hypotheses regarding the effect iron had on their distribution and its ecological impacts. During periods of iron limitation, it has been shown that diatoms reduce both their carbon and nitrogen content, and increase their silica, thickening their frustules (Hutchins and Bruland, 1998). Because of this, the Si:N in the Southern Ocean is currently

~4:1 (Pondaven *et al.*, 2000) compared to the 1:1 ratio found under adequate light and nutrient levels (Brzezinski, 1985). Therefore, when iron is added to these HNLC areas and nutrients are no longer limiting, we would expect to see a shift in the Si:N towards 1:1, allowing for the distribution of excess silica via ocean currents. This is the basis of the silicic acid leakage hypothesis (SALH), where an increase in Si to equatorial oceans will allow for greater diatom numbers; leading to them outcompeting other groups of phytoplankton such as coccoliths and reducing pCO_2 in equatorial oceans (Matsumoto, Sarmiento and Brzezinski, 2002; Brzezinski *et al.*, 2002). This has been studied in numerous iron fertilisation experiments with arguments for (Assmy *et al.*, 2013) and against it (Beucher, Brzezinski and Crosta, 2007). There are two other theories similar to SALH, both involving the reduction in pCO_2 via out competing coccoliths. One of these is the silica hypothesis suggested by *Harrison (2007)* who looked at the possibility of increased silica via aeolian dust fluxes in the LGM. With this, he hypothesised that there would be an increase in the abundance of diatoms at the expense of coccoliths, reducing the production of calcite, and therefore lowering pCO_2 levels. The silicon induced alkalinity pump hypothesis, uses this to also explain how diatoms could consequentially cause an increased alkalinity in the regions affected (Nozaki and Yamamoto, 2001). Both are very similar to each other and the SALH, but neither study talks in detail about the propagation of silica out of the Southern Ocean into mid - latitudes, the fundamental factor behind SALH.

A final hypothesis regarding the LGM and diatoms, is that there were El Niño-like conditions (Beaufort *et al.*, 2001). This study found reduced productivity in the Eastern Equatorial Pacific (EEP) and an increase in the Western Equatorial Pacific (WEP) that is associated with El Niño events. This was further backed up by *Bradtmiller et al (2006)* who also found this pattern but when looking specifically at glacial diatom productivity.

Past climates have had a profound impact on the distribution and ecological impact of diatoms. However, there is much speculation around which hypothesis is correct and further research into LGM circulation patterns and conditions is likely needed.

2.7 The use of diatoms in climate models

The ability to model the marine environment has proven to be a useful tool in understanding our complex marine ecosystems, filling the gap in observations and making predictive estimates for the future and the past. Early Earth system models proved to be reasonably successful in computing large scale system qualities such as chlorophyll levels and primary production rates, as well as the constraints on these (Anderson, 2005). However, due to their simplicity, they could also be prone to producing unrealistic behaviours (Fulton, Smith and Johnson, 2003). As our understanding of the marine environment developed, so did the demand for increasingly complex system models. With diatoms known to play a key role in the export of nutrients (Kemp *et al.*, 2000), being able to model the complexity of the diatom community structure would prove vital.

2.7.1 NPZD models

Among the first models to be used, NPZD models are used to look at four variables, nutrients (N), phytoplankton (P), zooplankton (Z) and detritus (D). These models can vary in their complexity, looking at one limitation, for example the limitation of temperature on phytoplankton growth rate, or multiple factors and their impact (Heinle and Slawig, 2013). One of the earlier uses of this type of model was by *Wroblewski, Sarmiento and Flierl (1988)* who looked at the geographical distributions of plankton in the North Atlantic in relation to nitrate distribution. These early studies have developed over the years and now are often incorporated into 3D general circulation models (GCM)

and have proven to show good correlation with data and observations. For example, when looking at the regional difference in pCO_2 over differing seasons in the Pacific, *Six and Maier-Reimer (1996)* found their model predicted the seasonal turnover of organic material reliably. They believed this was another step towards "a complete description of the ocean carbon cycle" but additional data and adjustments would be key to look at specific climatic conditions.

2.7.2 More complex PFT models

As our understanding of the marine system improved, it was determined that looking at plankton functional types (PFT) would improve the accuracy of these models in simulating the complex marine environment. One of the first PFT models was the FYFY model which included six functional types - diatoms, N specialists and P specialists in grazed and non-grazed forms (Van Den Berg *et al.*, 1996). This model was used to look at the composition and succession of these groups in the southern North Sea and although changes in mean biomass of plankton were inconclusive, variability in dominance and abundance of plankton types could be interpreted and linked to nutrient supply.

The European Regional Seas Ecosystem Model (ERSEM) eventually replaced the FYFY model used by *Van Den Berg et al (1996)* and was developed by *Baretta, Ebenhöh and Ruardij (1995)*. This is a model now widely used and was initially developed with the aim of simulating biogeochemical seasonal cycling of key nutrients in both the benthic and pelagic food webs of the North Sea. This model was not always successful with some study results not always conforming with observed data (Lenhart, Radach and Ruardij, 1997). However, as it developed, it proved to be a powerful model for not only modelling of the North Sea ecosystems, but global oceans and coastal areas (Butenschön *et al.*, 2016). This model has numerous categories, these being primary producers, consumers, bacterial decomposers, as well as particulate and dissolved organic matter (POM, DOM). These categories are found in the pelagic system with primary producers not being present in the benthic

model. These are split into further subcategories with most categories having a fully dynamic stoichiometry to increase the plasticity of the system (Butenschön *et al.*, 2016).

As these developed, models began to incorporate a larger number of functional types, with diatoms often being a key group. But with increased PFTs comes increased complexity and room for error. Some models have struggled to accurately portray certain groups, coccolithophores in particular (Quere *et al.*, 2005; Gregg *et al.*, 2003) due to their more difficult ecology and resulting parameterisations. Diatoms however, are often considered easier to model and have successfully been used in PFT models to look at primary production and community shifts as a result of climate change (Moore, Doney and Lindsay, 2004) and in numerous other studies looking at diatom blooms and primary production (Lancelot *et al.*, 2005).

2.7.3 Darwin model

One of the most recent and complex marine ecosystem models in use today is the DARWIN model. Recent developments in this model, have allowed for the implementation of the Droop-style approach when looking at the internal stores of elements within a cell – this is then used in the parameterisation of photoautotrophs (Ward *et al.*, 2012). This, and the addition of multiple cell sizes (Ward, Dutkiewicz and Follows, 2014) has allowed this model to look at more complex ecosystem properties, such as zooplankton-to-phytoplankton ratio, among different sized organisms. Additionally, this trait-based model allows for plankton communities to be defined by ecological and physiological rules, rather than basing them off current ecology, as these factors are far less likely to change over time. Therefore, a plankton communities' ability to compete for resources and combat grazing pressure, will be driven by their predefined traits and the trade-offs associated with these.

The most recent study using this model was a review by *Tréguer et al., (2018)* which looked at the impact of diatom diversity on the oceans biological pump. In order to define diatoms as a separate

organism from non-siliceous phytoplankton - key traits and their associated trade-offs would have had to be considered. This would have included their additional nutrient limitation (silica) as well as a potentially higher sinking rate meaning less time in the surface waters. This would have been balanced by their faster growth rate, larger size and protection from grazing. This model projected a decline in the primary production by diatoms, although it was concluded, that more work would be needed in order to truly assess any alterations to their biological input.

2.8 Use of models to predict future climate

With an abundance of oceanographic models now at our disposal, people have begun to attempt to model future climate scenarios, as summarised in the recent IPCC report (Masson-Delmotte *et al.*, 2018). It showed with just a 1.5^{o}C SST warming there would be an increase in ocean acidification, increases in stratification, alterations to the carbon pump, damage and loss of ecosystems such as coral reefs and changes to the biogeography of marine plankton. In addition to this, it is predicted that increases in SST will lead to not only reductions in phytoplankton and diatom abundance, but also a change in size class distribution, with lower nutrient supply favouring smaller size classes as previously discussed, (2.3.1). Even if the conservative RPC2.6 scenario was followed, it is expected that diatoms will be largely effected with decreases in growth rate and carbon carrying capacity (Krause and Lomas, 2020), reducing global carbon export. There have been numerous studies into the future of diatoms, with many predicting reductions in both global primary productivity and export (Bopp *et al.*, 2013; Cabré, Marinov and Leung, 2015; Fu, Randerson and Moore, 2016), and only a few showing an increase in PP (Sarmiento *et al.*, 2004; Schmittner *et al.*, 2008). These impacts are also predicted to vary between ocean basins (Nakamura and Oka, 2019) increasing modelling complexity. Future predictions by models have a large spread in results due to the utilisation of

differing circulation models and parameterisations, however, this data is still extremely valuable and helps us to improve current models and better predict future trends (Laufkötter *et al.*, 2015).

To limit the globe to just 1.5^{o}C SST warming would require large scale mitigation efforts globally and it is likely that this threshold will be exceeded. My report looks at an increase in pCO_2 to 425ppm which sees the oceans SST increase on average by almost 1.5^{o}C, allowing further investigation into the effect of this increase on diatoms.

3 Methodology

3.1 Model Description

The model used for this project is a simplified atmosphere and carbon-centric version of GEnIE, cGENIE (Ward *et al.*, 2018). This Earth system model represents different components of the Earth system – such as ocean circulation, ocean biogeochemistry, deep-sea sediments, and geochemistry, allows them to be combined (Lenton *et al.*, 2007), and has previously been used to look at interactions between biological productivity, biogeochemistry, and climate over diverse timescales (Ridgwell and Schmidt, 2010; Monteiro *et al.*, 2012; Cao *et al.*, 2009; Meyer, Ridgwell and Payne, 2016). cGEnIE features a reduced spatial resolution and simplified physics, enabling an efficient simulation of these interacting variables over a range of timescales.

3.1.1 Ocean physics component: C-GOLDSTEIN

The physical ocean model, C-GOLDSTEIN, features a 3-D ocean circulation model found in *Edwards and Marsh* (2005) and a 2-D model of the atmosphere and the dynamic-thermodynamic sea-ice model (Marsh *et al.*, 2011). Our model uses a 36x36 equal-area horizontal grid in uniform spaced increments of 10^{o} in longitude and increasing in the latitude, the resolution varies from equator to pole, from ~3.2^{o} to 19.2^{o}, allowing for a uniform surface grid area. The vertical ocean resolution has 16-levels with a logarithmically-spaced grid with the thickness of the grid increasing with depth (starting at 80.8 m in the surface waters and increasing to ~765 m at depth). The parameters for the physical model were calibrated using the ensemble Kalman filer (EnKF) against mean climatic data (Ridgwell *et al.*, 2007; Hargreaves *et al.*, 2004). For this study the model will be using the parameter values found in *Cao et al.* (2009), referred to as GENIE16.

3.1.2 Ocean biogeochemical cycling component: BIOGEM

The biochemical model used in cGENIE (BIOGEM) resolves the cycling of major nutrients involved in biological uptake in the surface waters and remineralisation/redissolution at depth. The compounds used in this model are carbon (C), phosphorus (P), Iron (Fe) and silica (Si), as well as their associated tracer compounds.

3.1.3 Ecological component: ECOGEM

BIOGEM will transform surface inorganic nutrients straight into exported nutrients or dissolved inorganic matter (DOM) but does not explicitly resolve a biological community. With the addition of the dynamic plankton community in ECOGEM, trophic interactions and mortality will add additional organic matter and inorganic compounds into the system. This switches the model from a flux-based parameterisation of a plankton community, into a complex and well-defined dynamic representation of the community.

BIOGEM:

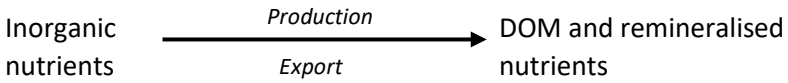

ECOGEM:

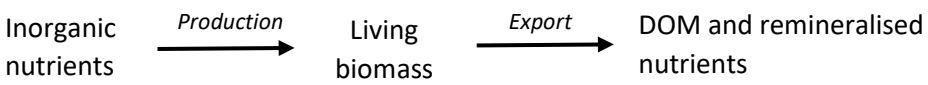

All the planktonic groups within this component are modelled as spherical shaped and are constrained to growing in the upper layer of the model (0 – 80.8m depth). The following sections contain the key formulas used to simulate plankton growth within the ECOGEM component however, the full list of ECOGEM formulas can be found in *Ward et al*. (2018).

3.1.3.1 Nutrient uptake

The biological uptake of compounds (PO_4^{3-}, Fe^T, H_4SiO_4) (mol kg^{-1} yr^{-1}) is a function of their micro- and macro- availability, sea ice, temperature and irradiance. For non-siliceous organisms, the equations for the growth limitation term for uptake is as follows:

(1)

$$\Gamma = k_{ice} \cdot k_T \cdot k_I \cdot k_{(PO_4)} \cdot k_{(\mathrm{Fe}^T)} \cdot \tau \cdot \min(PO_4, Fe^T)$$

However, for diatoms this formula is modified to include the silicic acid half saturation constant:

$k_{(H_4SiO_4)}$:

(2)

$$\Gamma = k_{ice} \cdot k_T \cdot k_I \cdot k_{(PO_4)} \cdot k_{(\mathrm{Fe}^T)} \cdot k_{(H_4SiO_4)} \cdot \tau \cdot \min(\mathrm{PO_4}, \mathrm{Fe^T}, H_4SiO_4)$$

For these equations the term τ represents the net nutrient uptake timescale, which is modified by the first 4 terms: modifiers for sea-ice (k_{ice}), temperature (k_T), irradiance (k_I), and nutrient limitation upon biological activity ($k_{(PO_4Fe^T)}$). A full break down of these terms can be found in Jones *et al.* (in prep).

3.1.3.2 Calculating temperature limitation

Temperature can be a limiting factor due to its effect on metabolic processes within cells, and consequentially, this will impact diatoms growth. In this model, all plankton functional types have the same temperature limitation value.

(3)

$$\gamma^T = e^{A(T - T_{ref})}$$

Here the parameter A is temperature sensitivity, *T i*s ambient water temperature in °C and T_{ref} is a reference temperature, at which γ^T is equal to 1°C.

3.1.3.3 Calculating light limitation

Firstly, photosynthesis for phytoplankton in ECOGEM is modified from *Geider, MacIntyre and Kana* (1998) and *Moore et al.* (2002). Limitation itself is established using a Poisson function of local irradiance (*I*), which is then altered by the iron-dependant initial slope of the P-I curve ($-\alpha \cdot \gamma_{j,Fe}$), the cells photosynthetic proficiency and the chlorophyll α : carbon ratio($Q_{j,chl}$). This is then divided by the maximum light-saturated growth rate ($P_{j,C}^{sat}$) which is described further in Ward et al. (2018).

(4)

$$\gamma_j^I = 1 - \exp\left(\frac{-\alpha \cdot \gamma_{j,Fe} \cdot Q_{j,chl} \cdot I}{P_{j,C}^{sat}}\right)$$

Where;

(5)

$$P_{j,C}^{stat} = P_{j,C}^{max} \cdot \gamma^{t} \cdot \min\left[\gamma_{j,P}, \gamma_{j,Fe}\right]$$

Therefore, the overall gross photosynthetic rate can be calculated with the following formula:

(6)

$$P_{j,C} = \gamma_{j,I} P_{j,C}^{sat}$$

3.1.3.4 Calculating nutrient limitation

Nutrients are key in almost all biological processes. The growth of each phytoplankton functional type in this model is therefore the result of carbon attribution, as well as other essential elements needed by the cell.

3.1.3.4.1 The plankton quota saturation term

To calculate the uptake capacity - and the consequential storage of nutrients - the following equation is used. In order to prevent the over accumulation of N or Fe biomass in relation to C, the uptake capacity of each nutrient decreases to zero when the quota is filled (Ward *et al.*, 2012).

(7)

$$Q_{j,i_b}^{stat} = \left(\frac{Q_{j,i_b}^{max} - Q_{j,i_b}}{Q_{j,i_b}^{max} - Q_{j,i_b}^{min}}\right)^{0.1}$$

The cellular nutrient quota (Q) is the ratio of nutrients to carbon biomass and is defined in Ward et al. (2018). The general uptake rule for element i_b, is a linear function of the nutrient status, which is then altered by the additional shape parameter (0.1; Geider, MacIntyre and Kana, 1998).

3.1.3.4.2 Nutrient uptake

Nutrients in this model are taken up as a function of their environmental availability ($[R_{i_r}]$), maximum uptake rate (V_{j,i_b}^{max}), nutrient affinity (α_{j,i_r}), the quota saturation term (Q_{j,i_b}^{stat}) and temperature limitation (γ^T). This is used for P and Fe in phytoplankton, but in the case of diatoms, Si uptake is also calculated.

(8)

$$V_{j,i_r} = \frac{V_{j,i_b}^{max} \alpha_{j,i_r}[R_{i_r}]}{V_{j,i_r}^{max} - \alpha_{j,i_r}[R_{i_r}]} Q_{j,j_b}^{stat} \cdot \gamma^T$$

This formula is created by modifying the Michaelis-Menten-type response, replacing the half saturation constant with nutrient affinity.

3.1.3.5 Calculating the grazing rate

The predator-biomass-specific grazing rate of a predator (j_{pred}) on its prey (j_{prey}) is calculated by looking at the overall grazing rate, the prey switching term and prey refuge.

(9)

$$G_{j_{pred},j_{prey},C} = \gamma^T \cdot \underbrace{G^{max}_{j_{pred},C} \cdot \frac{f_{j_{pred},C}}{k_{j_{pred},C} + f_{j_{pred},C}}}_{\text{overall grazing rate}} \cdot \underbrace{\Phi_{j_{pred},j_{prey}}}_{\text{switching}} \cdot \underbrace{(1 - e^{\Lambda \cdot f_{j_{pred},C}})}_{\text{prey refuge}}$$

Here, $G^{max}_{j_{pred},C}$ is the maximum grazing rate of the predator, which is influenced by temperature limitation (γ^T). Also found within the overall grazing rate calculation is the total food available to the predator ($f_{j_{pred},C}$) and the half-saturation constant for all available prey ($k_{j_{pred},C}$). The switching term is calculated through a matrix-form equation that is explained in Ward et al. (2018). For this paper, active switching is assumed, whereby predators have a preference towards attacking prey that is more readily available (*s* = 2; Ward et al 2018). Finally, prey refuge is added so that when prey availability is low, the overall grazing rate will decrease.

3.1.3.6 Mortality

The final loss term in the ECOGEM component is plankton mortality rate.

(10)

$$m_j = m_p \left(1 - e^{-10^{10} \cdot B_{j,C}}\right)$$

The linear mortality rate (m_p) here is decreased at low biomass levels (where the population's carbon biomass is ~< 10^{-10} mmol C m^{-3}). This is done to maintain a viable population in each surface grid whilst having a negligible effect on the ecosystem itself.

3.1.4 Diatom equation

The abundance of diatoms over time, in its simplest derivative term can be defined as abundance being equal to growth of the diatom community subtracted from the losses.

(11)

$$\frac{Diatom}{dt} = growth - \ losses$$

When broken down, the equation can be written as below, with the growth term being dependant on temperature (γ^T), light (γ^I) and nutrient limitations (γ^{Nut}), as well as their growth rate (η_{max}). The losses can be calculated by looking at the sum of grazing from predators and their mortality rate.

(12)

$$\frac{Diatom}{dt} = \gamma^T \cdot \gamma^I \cdot \gamma^{Nut} \cdot \eta_{max} - (Grazing + Mortality)$$

3.1.5 State Variables

State Variable	**Dimensions**	**Index**	**Size**	**Available elements**

R	Resource element	i_r	I_r	DIC, PO_4, Fe, Si
B	Plankton Class Cellular quota	j i_b	J I_b	1, 2, …, J C, P, Fe, Si, Chl
D	Organic matter size Detrital nutrient element	k i_d	K I_d	DOM, POM C, P, Fe, Si

Table 1, Index notation for the state variables in ECOGEM (adapted from Ward et al., 2018)

The mathematical state of this dynamic system is split into three matrices, nutrient resources (**R**), plankton biomass (**B**) and organic matter (**D**) (Table 1). The **R** vectors include distinct organic resources (I_r). The plankton community (**B**) is composed of individual populations (J), which are linked to a cellular nutrient quota (I_b). Organic matter (**D**) is not resolved as a state variable in

ECOGEM as there is no grazing on detrital organic matter. A full description of this variable and the calculations for **R**, **B** and **D** are outlined in *Ward et al.* (2018).

Table 2, PFTs and their associated size classes (adapted from Ward *et al.*, (2018))

3.2 Size Dependant traits

One of the key aspects to this study is the size-dependant traits that can be used to distinguish between plankton of differing sizes. For the purpose of this investigation four diatom size classes and five zoo- and phyto- plankton classes (Table 2) have been used. When running these experiments, it was clear that the model underestimates the distribution and abundance of mesoplankton (>1000 μm in this instance) as well as 0.1 μm phytoplankton. For this reason, all results from these groups were not included as they would not accurately represent the size classes

Plankton functional type (PFT)	**Estimated spherical diameter (ESD) (μm)**
Diatom	1, 10, 100, 1000
Phytoplankton	0.1, 1, 10, 100, 1000
Zooplankton	1, 10, 100, 1000, 10000

associated. Table 2 lists these ecophysiological parameters, which have been assigned as power-law functions of an organism's volume (Ward *et al.*, 2018). The only exception to this rule is the maximum photosynthetic rate which deviates from the standard power law given in *Ward et al. (2018)* and instead a unimodal curve derived from a study by Marañón *et al.* (2013) is used.

With these parameters (table 2), EcoGEnIE can determine not only different functional types, but the size classes show in table 2. Figure 2 shows how alterations to cell volume / size class will affect

key processes within the community, thus selecting organisms that favour current conditions. Maximum nutrient uptake and affinity are both size-dependant functions, with smaller size classes having a higher affinity to nutrients than larger cells (figure 2). Photosynthesis follows a similar rule in our model, but with small cell sizes seeing a reduced rate, indirectly reflecting that nitrogen demand is high but their uptake, storage and efficiency in converting this to biomass is reduced (Marañón *et al.*, 2012). Larger cells, although being efficient in their uptake and storage of nutrients, are also limited by their ability to convert this into biomass.

Grazing by zooplankton is also a function of size. It is dependent on the concentration of available prey and has a size-dependant maximum grazing rate. In our model, zooplankton will predominantly graze upon phytoplankton that are 10 times smaller than themselves. This is due to these phytoplankton being less likely to escape grazing, as well as being easier to digest (Kiørboe, 2008). Prey palatability in figure 2 shows (in black) an example of the size preference of prey given a zooplankton's cell volume.

Table 3, Size-dependant ecophysiological parameters (p) and associated units, with their size scaling coefficients (a, b, c). (adapted from (Ward et al*., 2018))*

Parameter	**Symbol**	**Size-scaling coefficients**			**Units**
	p	***a***	***b***	***c***	
Maximum photosynthetic rate	P_C^{max}	3.08	5.00	-3.80	mmol N (mmol C) −1 d−1
Maximum nutrient uptake rates	$V_{PO_4}^{max}$	4.4×10^{-2}	-0.06		mmol P (mmol C) −1 d−1
	V_{Fe}^{max}	1.4×10^{-4}	-0.09		mmol Fe (mmol C) −1 d−1
	$V_{SiO_2}^{max}$	0.077	-0.27		mmol Si (mmol C) −1 d−1

Nutrient affinities	α_{PO_4}	1.10	-0.35	m^3 (mmol C) −1 d−1
	α_{Fe}	0.175	-0.36	m^3 (mmol C) −1 d−1
	α_{SiO_2}	0.024	-0.27	m^3 (mmol C) −1 d−1
Cell carbon content	Q_C	1.45×10^{-11}	0.88	Mmol C $cell^{-1}$
Maximum prey ingestion rate	G_C^{max}	21.9	-0.16	d^{-1}

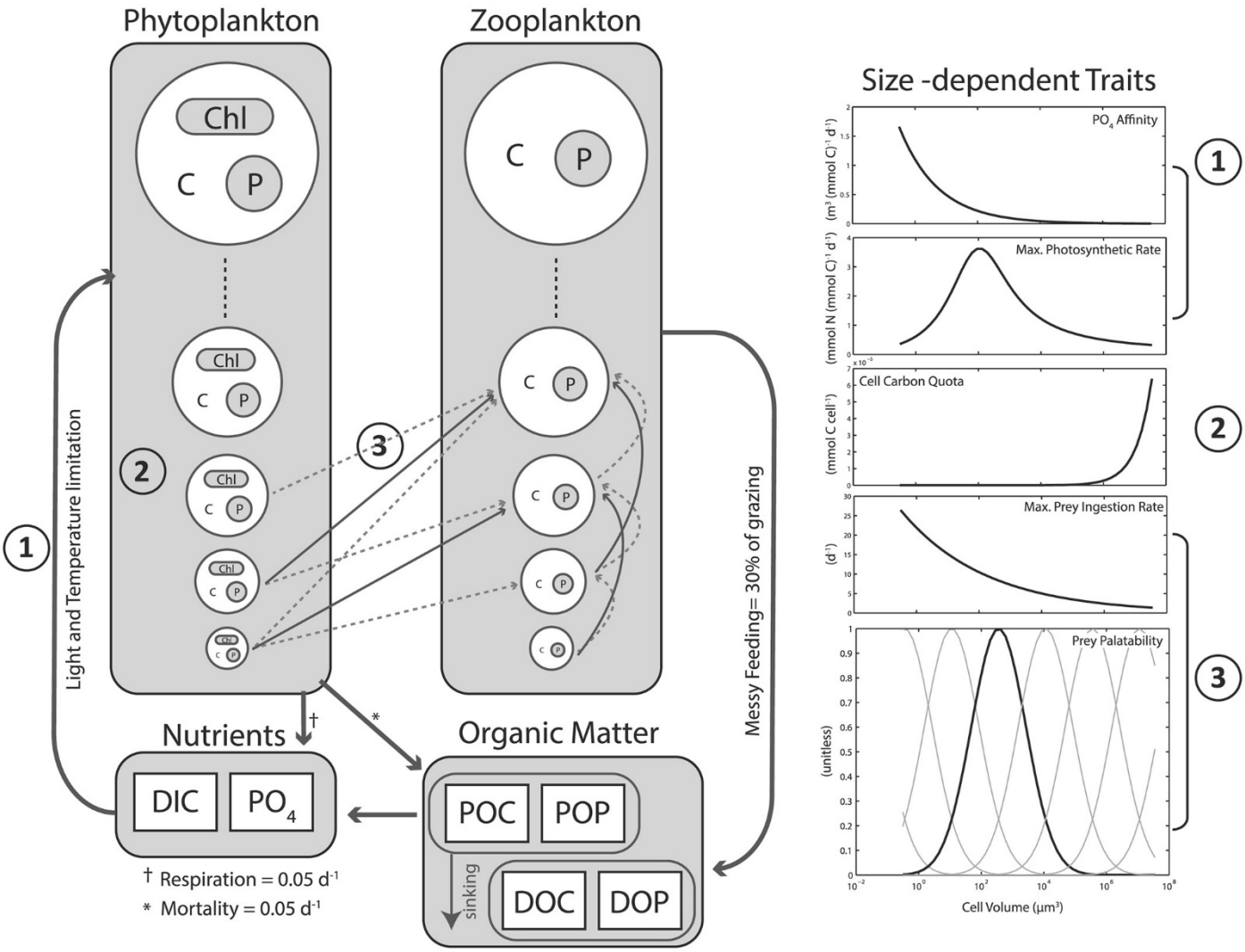

Figure 2, a visual representation of EcoGEnIE's size structured model (Ward et al., 2018), depicting important allometric relationships for (1) affinity to nutrients and carbon uptake rate, (2) cell quota for carbon, and (3) grazing.

3.3 Adding Diatoms into ECOGEM

Diatom's use of silica and reduced palatability, due to the protection from grazers (Hamm *et al.*, 2003), and high growth rates are the defining traits when comparing them to other functional types within ECOGEM. For this thesis, these defining traits had to be incorporated into the model as well as other key processes. This simply involved switching on traits - already implemented in the model for other plankton groups - that related to them, and as a result, separating them from non-siliceous phytoplankton. Firstly, the use of silica was implemented, making this a limiting nutrient for diatom

growth, unlike for other phytoplankton. Palatability was reduced to simulate the protection acquired through the silica frustule of diatoms, thus reducing grazing pressure.

To do this, palatability – seen in figure 2 – was halved for diatoms meaning grazing on them should be reduced by 50%. Finally, the export of opal from diatoms had to be accounted for. Due to diatoms being the only plankton in the model to use silica, this had not been added into the code before.

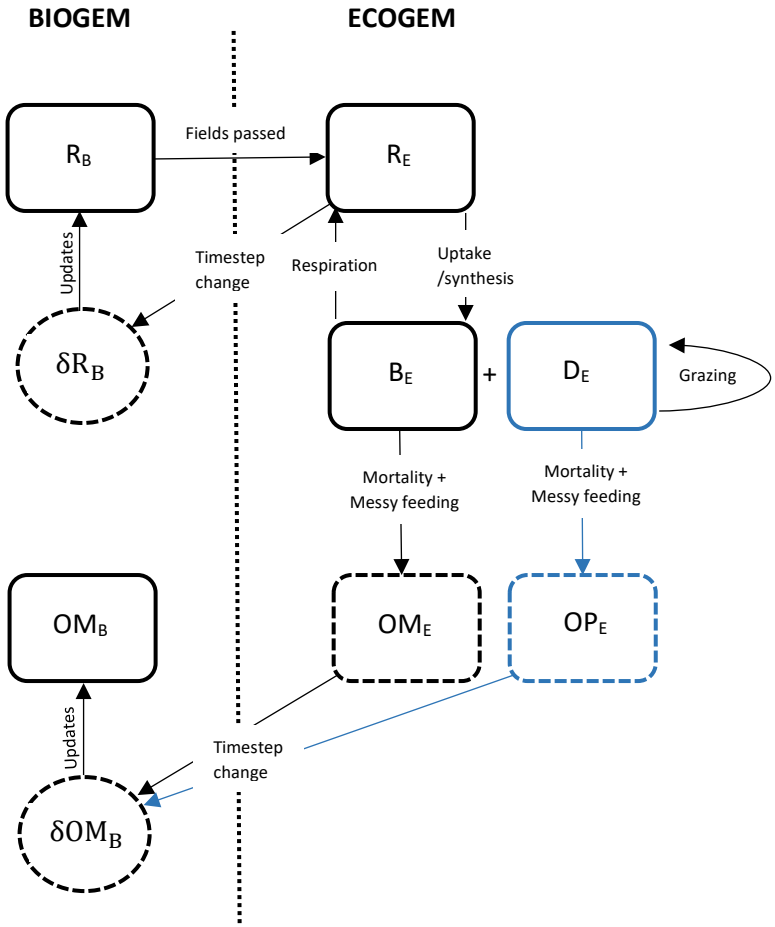

*Figure 3, a visual representation of the coupling between BIOGEM and ECOGEM, adapted from Ward et al. (2018). State variables shown: **R** represents a resource, **B** planktonic biomass, **D** diatom biomass, **OM** indicating organic matter, and **OP** showing opal. The subscripts (B and E) indicate if this is occurring in BIOGEM or ECOGEM and (δ) is rate of change. The adaptions made to this from Ward et al. (2018) are indicated by their blue colouring with these processes only occurring in diatoms.*

In order to account for silica uptake and use by diatoms, there had to be some form of export via mortality or messy feeding. This meant that opal (biogenic silica) had to be exported and

reintroduced into the BIOGEM component, separate from POM, to avoid a reduction in global SiO_2 (figure 3). This was a step that I added, as it wasn't currently implemented in the model due to silica not previously being used in ECOGEM. Once all organic matter and opal was reintroduced in to BIOGEM, it could be once again be reintroduced into ECOGEM. After all parameterisations were in place, a series of model runs were conducted to insure everything was working as expected. This also provided the opportunity to compare to both observational data and that of other models.

3.4 Model runs

In this thesis, I ran two differing scenarios, a warm climate and a cooler climate. These scenarios were run alongside a pre-industrial control, where atmospheric pCO_2 is at 278 ppm. All three runs were run for 10 000 years in order to reach steady ocean state. For the cooler experiment, atmospheric pCO_2 was lowered to 190 ppm in accordance with ice-core data from the LGM (Monnin *et al.*, 2001). This same process was used for the warmer climate scenario, but with pCO_2 being increased to 425 ppm, allowing me to investigate a low-level future warming, as required by the Paris Agreement. This concentration was based of the work of Davis, Caldeira and Matthews, (2010) who estimate pCO_2 levels just shy of 430 ppm by 2060, based on their calculations of cumulative future emissions (496 gigatons) between 2010 and 2060. This also complied with SSP1-2.6 scenario developed for CMIP6 (O'Neill *et al.*, 2016), an update of the previous RPC2.6. This scenario was implemented by O'Neill et al. (2016) to investigate the low-end of potential future warming pathways. With this scenario predicted to keep warming below the 2 ^oC level, and as low as <1.5 ^oC, it could be used to inform the Paris Agreement targets (warming below 1.5 ^oC and 2 ^oC).

By looking at the state of the ocean under both a warmer and cooler climate, I can compare the effects and any symmetry that may arise from in the results. For each of these experiments, both top-down and bottom-up controls are investigated, as well as key physical processes, such as

upwelling and mixed layer depth. This allows for a better understanding of the key drivers in diatom distribution, size and abundance, as well the impact this had on the biological export of carbon.

4 Results

4.1 Distribution under preindustrial conditions

4.1.1 Nutrients

In our pre-industrial run – where average SST is 17.5 °C - the model shows typical distribution of the macronutrient phosphate (PO_4) and micronutrient iron (Fe). PO_4 is highest in the Southern Ocean and North Atlantic Ocean with concentrations reaching up to 1.6 and 0.6 µmol kg^{-1} respectively, and the lowest concentrations in equatorial and mid latitude regions 0.01 – 0.2 µmol kg^{-1} (figure 4).

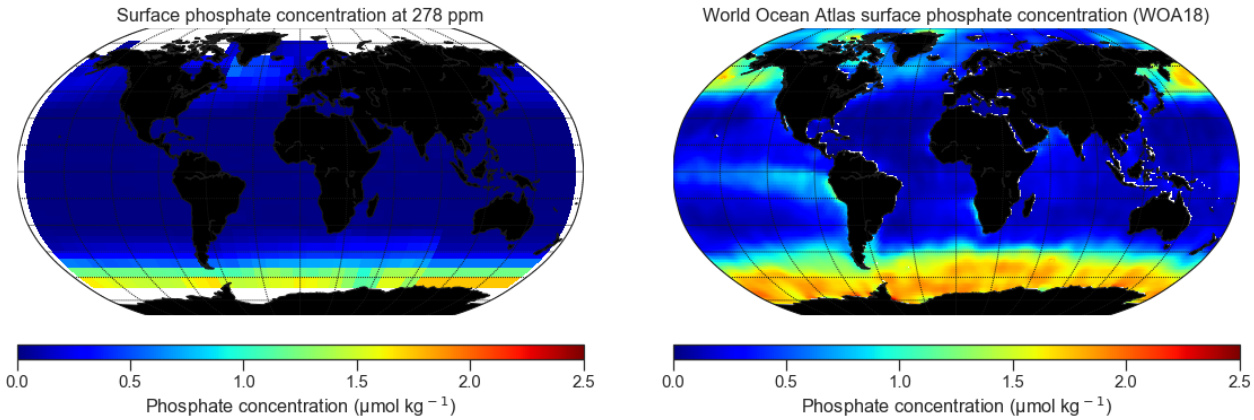

Figure 4, global phosphate concentration (µmol P kg^{-1}) in cGEnIE surface waters (80.8m) during preindustrial simulation (left) compared to phosphate concentrations (µmol P Kg^{-1}) from global observations from NOAA (WOA) (Garcia et al., 2019)

When comparing this to data from observations (figure 4) we can see similarities in both concentration value and distribution in the Southern Ocean and North Atlantic. However, in our model we do not see the same concentrations in upwelling regions off the west coast of South America and in the North Pacific – with our model giving much lower concentrations. This primarily due to the low resolution and simplification of ocean physics that are used in EcoGENIE, as well as a difference in time periods. Silica in the model covers a vast amount of surface waters, with its highest concentrations being in the Southern Ocean and Mediterranean (82 µmol l^{-1}) (figure 5). There is also a strong concentration found up through the Atlantic, with the lowest values being in the Arctic circle (72 µmol l^{-1}), N. Pacific (73 – 77 µmol l^{-1}) and around the coasts of Costa Rica and

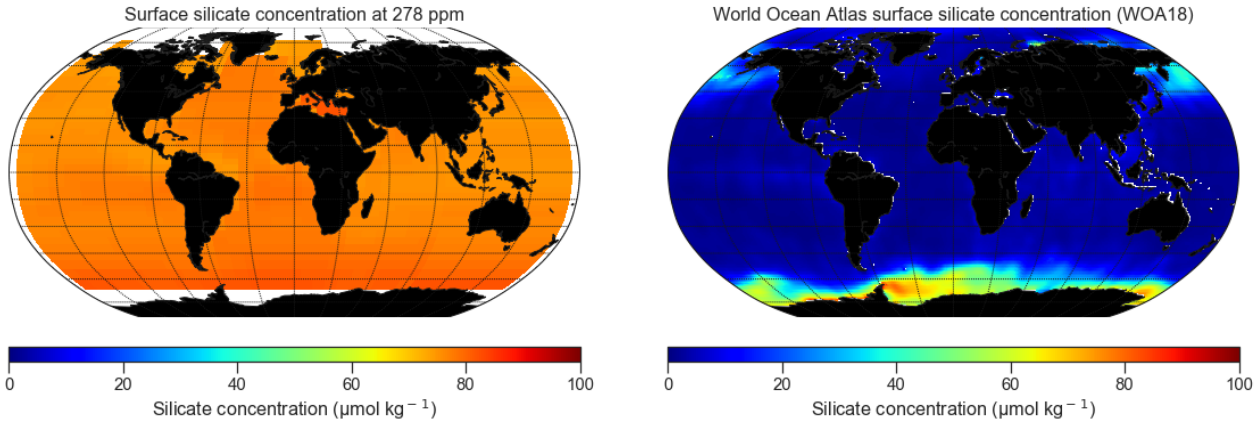

Figure 5, global silicate concentration (µmol Kg-1) in cGEnIE surface waters (80.8 m) during preindustrial simulation (left) compared to silicate concentrations (µmol Kg-1) from global observations from NOAA (WOA) (Garcia et al., 2019)

Nicaragua (74 µmol l^{-1}). When comparing the modelled silicate concentration with observations (figure 5), we see that the model overestimates global silicate concentration. This is particularly evident in the equatorial regions where observations put silicate at 0 – 10 µmol l^{-1} whereas in my model it is 79 µmol l^{-1}. There is, however, noticeable difference in the North Pacific concentrations. In observational data this is a region of high silicate, whereas in our model, it is low. This discrepancy is discussed further in section 3.1.3.

Iron concentrations are the highest around the North Atlantic Ocean, the Mediterranean Sea and in the most northern parts of the Indian Ocean (Arabian Sea) reaching highs of 1.8 nmol kg^{-1} (figure 6). This distribution matches the source of iron via atmospheric deposition (not shown). The Southern Ocean, as expected, has a low concentration of iron (average: 0.3 nmol Fe kg^{-1}). The Pacific Ocean, particularly around the ocean gyres, had extremely low iron concentrations dropping to 0.1 nmol Fe kg^{-1}.

4.1.2 Total phytoplankton and zooplankton

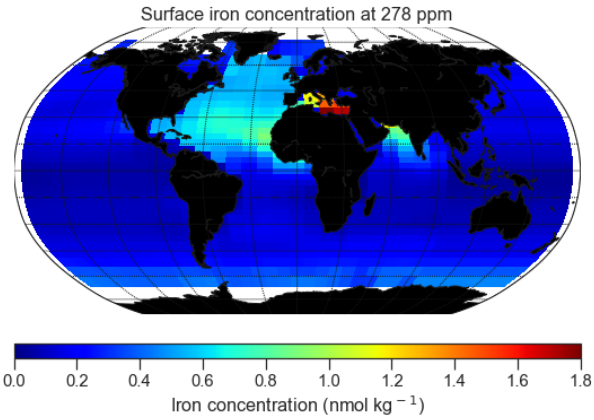

Figure 6, the surface (80.8 m) concentration of iron (nmol Fe Kg^{-1}) in our model when under preindustrial conditions

Preindustrial global biomass of phytoplankton in our model is 1.04 GtC, with a vast bulk of the population found in the higher latitudes (figure 7). The Southern Ocean presents the highest concentration of phytoplankton – with values up to 3.43 µmol C l^{-1}. The North Atlantic also has high concentrations, particularly south of Greenland (2.99 µmol C l^{-1}). These high concentrations correspond well with nutrient distribution, particularly of PO_4 (figure 4). Lowest concentrations of phytoplankton are in the subtropical gyres with values down to 0.44 µmol C l^{-1}. Zooplankton are also an important component of the ecosystem, top-down regulating phytoplankton biomass.

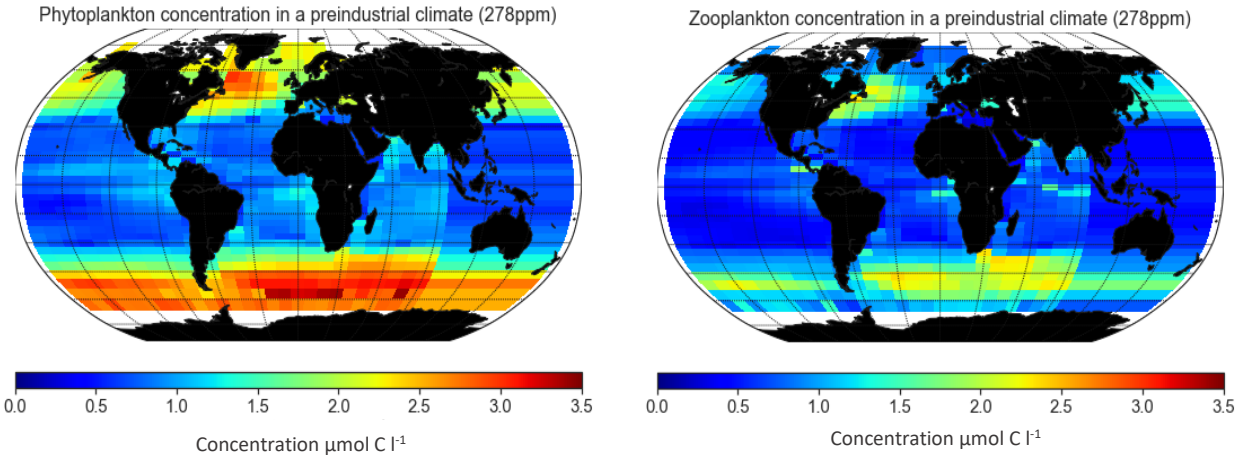

Figure 7, phytoplankton (left) and zooplankton (right) concentrations (µmol C l^{-1}) in our model when under preindustrial conditions

Zooplankton make up a considerable percentage of the global plankton biomass (~35%) with a global biomass of 0.57 GtC. Concentrations in the model follow similar distribution to total phytoplankton, with high concentrations in the North Atlantic (2.31 µmol C l^{-1}) and the northern part of the Southern Ocean (2.37 µmol C l^{-1}). Zooplankton have however slightly higher concentrations in upwelling equatorial regions when compared to phytoplankton (figure 7). These are particularly noticeable in the Indian Ocean (1.48 µmol C l^{-1}), Western Africa (1.61 µmol C l^{-1}) and around Costa Rica and Panama (1.82 µmol C l^{-1}). In addition, there are noticeably lower concentrations of zooplankton relative to phytoplankton around the Greenland, Iceland and Norwegian seas (GIN seas) where concentrations drop down to 0.4 µmol C l^{-1}, which is considerably lower than the average phytoplankton concentrations in that region (~2.5 µmol C l^{-1}).

4.1.3 Diatoms

In our model diatoms represent 78% of the total phytoplankton biomass and just over 50% of the global plankton community (0.82 Gt C) in the model. Much of this biomass is present in the Southern Ocean and North Atlantic with average concentrations of 2.72 µmol C l^{-1} and 2.37 µmol C l^{-1}

respectively (figure 8). Diatoms also have relatively high concentrations in upwelling equatorial region, particularly off the western coast of Africa with concentrations around 1.06 µmol C l^{-1}. Diatom concentrations are the lowest in the subtropical gyres with concentrations as low as 0.35 mmol C m^{-3} in the South Pacific and Indonesia. Like total phytoplankton distribution, diatom distribution matches PO4 concentrations. Silicate, however, does not influence diatoms to the same degree. This is due to diatoms - in this model - having low silicate requirements (qmin = 0.002 mmol Si (mmol C)$^{-1}$) and therefore it is never a limiting nutrient. Despite this, diatoms in this model show good distribution and concentration when compared to other models being used (figure 8). The North Pacific, however, does show lower diatom concentrations in our model compared to MIT Darwin model (Tréguer *et al.*, 2018), likely due to the lower silica levels in their model. With less silicate uptake by diatoms due to their low requirements, less is exported as opal in key regions – such as the North Atlantic - meaning redistribution to regions such as the North Pacific is reduced and increasing the silicate concentration at the surface.

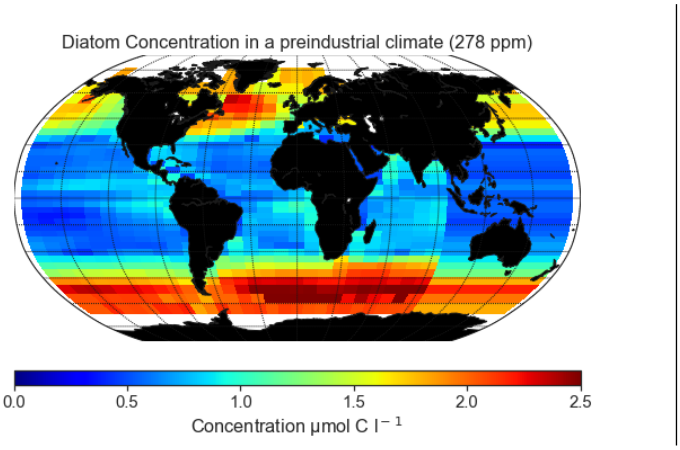

Figure 8, concentration of diatoms (µmol C l^{-1}) in cGEnIE (left) under preindustrial conditions, compared to the MIT Darwin model (right). The Darwin model uses mmol C m^{-3}, however when converted, this is the same as µmol C l^{-1}- which is used in the cGEnIE model.

The size spectrum in our model shows that the 10-µm diatom size class dominates most of the concentration in the higher latitudes – making up 85-95% of the concentration in the GIN seas and 50% in the waters south of Greenland (figure 9). This size class also shows complete dominance on the ice edge surrounding the Southern Ocean where they make up 100% of total diatom

concentration. The 10 µm diatom size class also dominate the North Pacific where they can make up over 80% of the total concentration of diatoms. The 100 µm diatom size class also contribute significantly with ~30% of the concentration below Greenland as well as being prominent in the north part of the Southern Ocean (contributing to 25% of concentration). The smallest size class (1 µm) are at their lowest concentration (0.01 – 0.14 µmol C l^{-1}) in the Southern Ocean where 10 µm diatoms are dominant (up to 100% of the total concentration). It is in the lower latitudes where this size class is most dominant, with concentrations in equatorial regions reaching up to 0.52 mol C m^{-3} – accounting for around 75% of the total diatom concentration and up to 100% in patches. Another key finding from initial analysis is the inability of the model to grow the 1000 µm phytoplankton size class. The exact cause of this issue is not known, with further research being needed to pinpoint the problem. Due to this, 1000 µm phytoplankton and diatoms were not looked at for the remainder of this paper.

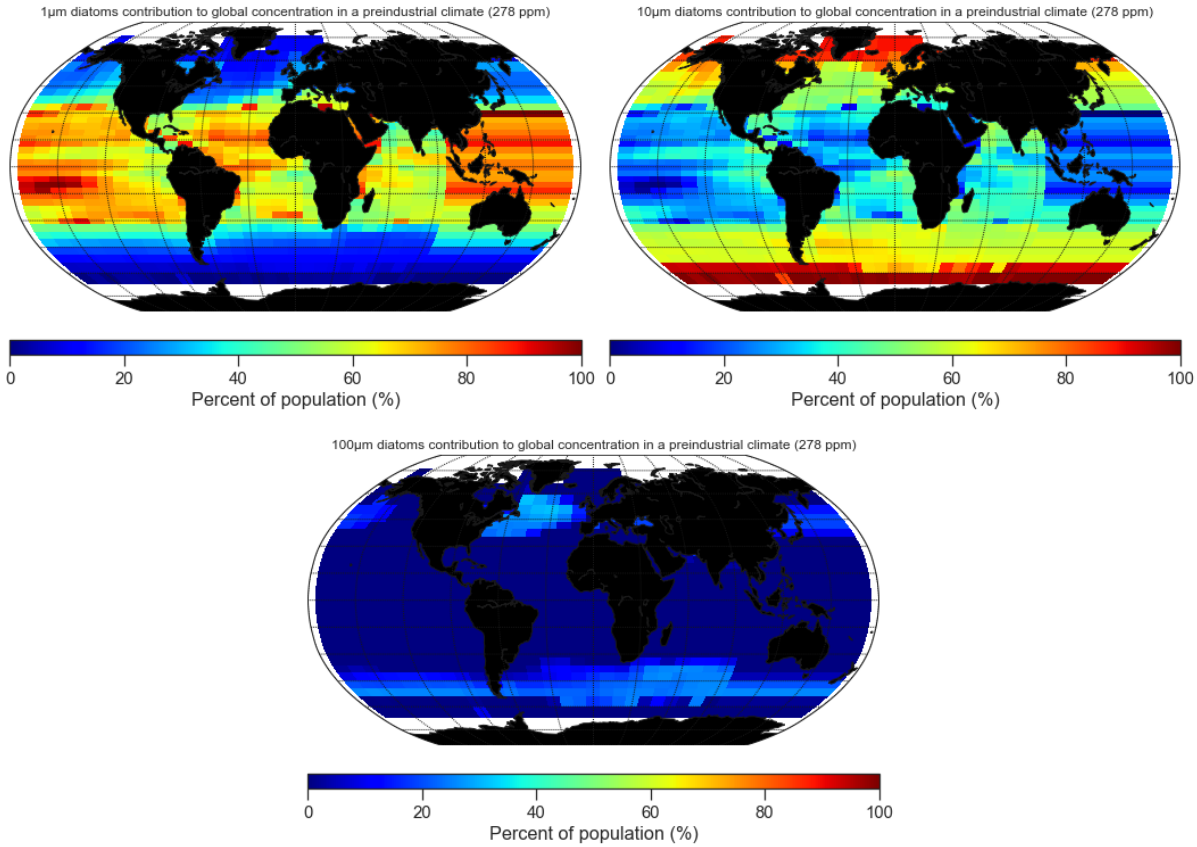

*Figure 9, the contribution of size classes (%) to the global concentration depicted in figure 8. Showing 1µm diatoms (top left), 10µm diatoms (top right) and 100µm diatoms (bottom). The contribution of each size class was calculated using a simple percentage calculation ((x / y) * 100) where **x** is the concentration of the selected size class and **y** is the overall diatom concentration*

4.1.4 Effect of climate

Here I look at the effect of different climates on the model plankton communities, with a focus on diatoms. I contrast a warming and a cooling climate experiment – using the preindustrial climate as a proxy for change. For this, I investigate the change of concentration and overall biomass of plankton groups, as well as the different size classes of diatoms. This will give an insight to not only possible future changes to these communities, but also see if different size classes of diatoms should be focused on in future studies. Finally, I look at how this effects biological carbon export and the possible drivers of change. In this thesis, there has been no change to forcing's, ocean physics or geographical boundaries in the model. This was done in order to focus solely on the effect of an altered pCO_2 concentration on the diatom community. If I were to be focusing on a specific timeframe in more detail, such as the LGM, then alterations to the geography, physics and starting

ocean chemistry would be an important consideration to make – but for the purpose of this study, these change are not needed.

4.1.5 Colder climate experiment (190 ppm)

In the colder climate experiment, the reduction of pCO_2 - to LGM levels - leads to a mean SST reduction of 1.2^{o}C. This is at the lower end of predictions for the LGM where SST is predicted to have dropped by between 1 – 3^{o} C (Stott *et al.*, 2002; Lea, Pak and Spero, 2000). In this study, a reduction in pCO_2 leads to phytoplankton biomass increasing globally by 4.62%, reaching 1.1 Gt C. Overall, the increase is homogeneous with more intense changes surrounding Iceland in the North Atlantic with up to a 15% increase (figure 10). Decreases in concentration can be seen in sparse patches of the Southern Ocean - ranging from 1 – 18% - however alongside this, are increases by similar amounts.

When looking at a cooler climates effect on zooplankton, we see similar patterns with the North Atlantic seeing an overall increase – up to 28% in some regions – higher than that of phytoplankton. There is also a similar increase in biomass by 3.1% reaching 0.59 Gt C. However, in comparison to phytoplankton, zooplankton see a far more widespread decrease in concentration in the Southern Ocean (figure 10). Here we can see decreases in concentration of up to 30% with the overall trend leaning toward a decrease in concentrations.

The overall change to diatom concentration (figure 10), unsurprisingly, is very similar to that of phytoplankton. Here global biomass of diatoms increased from 0.82 – 0.86 Gt C, a 4.9% increase. Concentration also shows global increase, with small patches of lowered concentration in the Southern Ocean ranging between 1.2 and 21.5%.

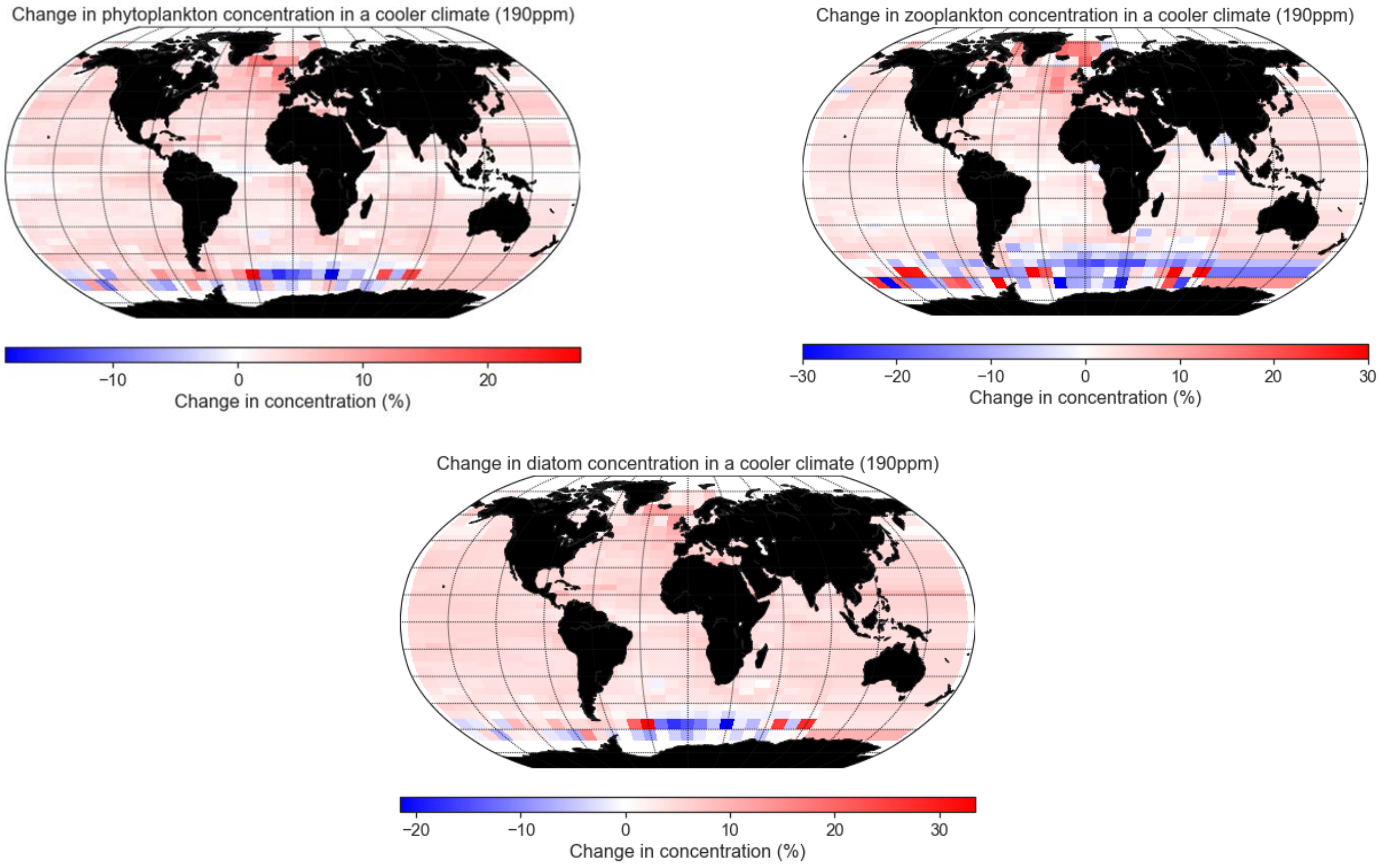

*Figure 10, results showing the change in PFT concentrations between a cool climate and the preindustrial environment. The percentage change in concentration was calculated as follows: ((concentration at 190ppm – concentration at 278ppm) / concentration at 278ppm) *100. A full comparison of these functional type's concentration with the preindustrial environment can be found in Appendix 1.*

Within the size classes, the 1 µm diatom concentration experiences a small overall increase of 1.6%. Most of the variation occurs in the Southern Ocean (figure 11), yet this size class still dominates the concentration in the lower latitudes - making up 60-100% of the concentration here. In the high latitudes of the northern hemisphere, however, there is a decrease in concentration, ranging from 0.1 – 32%. The 10 µm phytoplankton size class experiences a far more uniform change increasing in concentration by 5.4% globally, with little alteration to distribution being seen. There are some small patches of high increase, particularly in the Mediterranean however, due to this ocean only being represented by one grid square, this region is not accurately portrayed. This size class still dominates the Southern Ocean contributing up to 100% of the concentration. They also still dominate the

North Pacific (up to 85%) and the North Atlantic Ocean (60 – 70%), particularly the GIN seas (up to 97%).

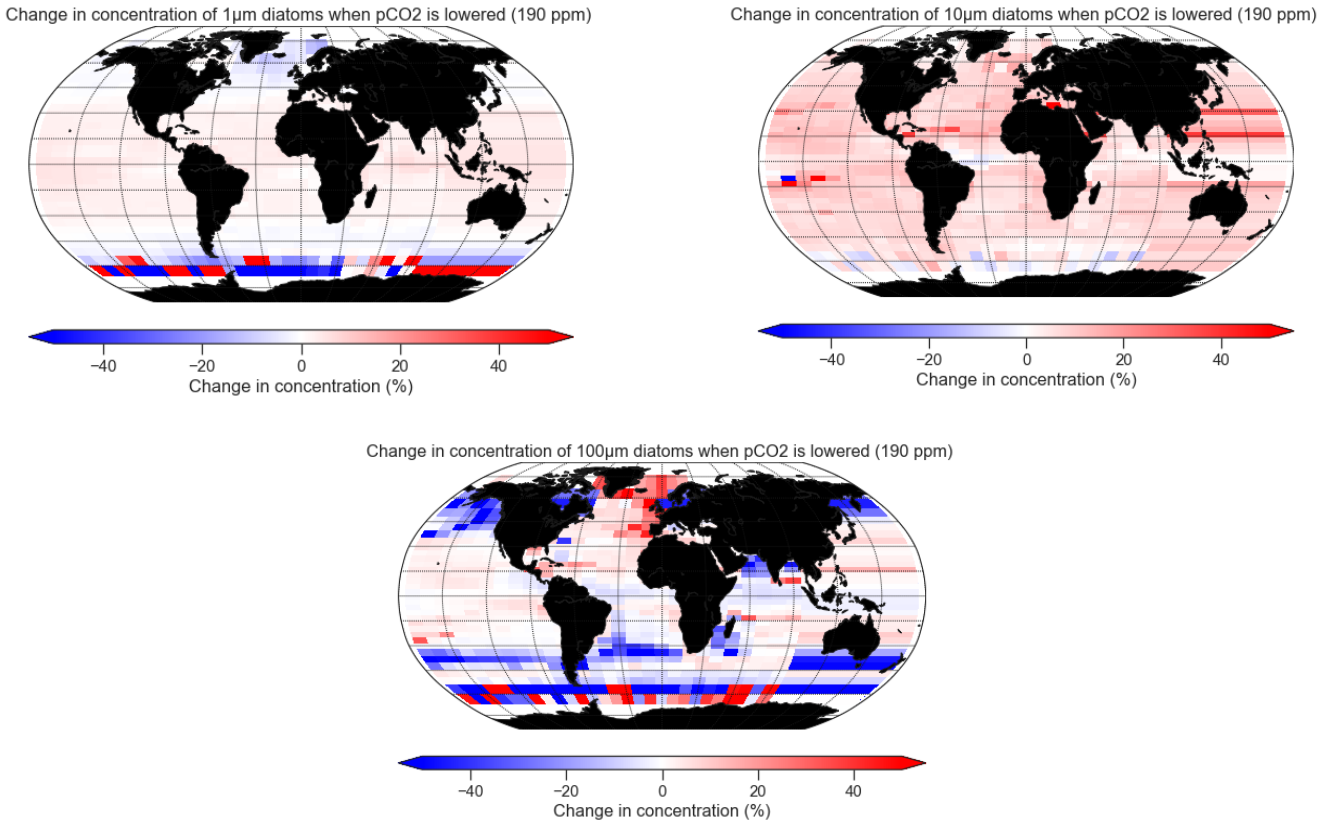

*Figure 11, changes in diatom size class concentrations between the cooler environment and the preindustrial run – with blue indicating a reduciton in concentration and red showing an increase. These changes were calculated as follows: ((size class concetration at 190ppm - size class concetration at 278ppm) / size class concetration at 278ppm) * 100.*

The 100 µm diatom size class experiences the most extreme changes for both distribution and concentration. Firstly, they show a large decrease in concentration in the Southern Ocean and lower mid-latitudes (>100% change in patches), but still make up 25% of the concentration here. In the Northern hemisphere we also see reduced concentration in the North Pacific up to 49%, with their contribution to concentration declining by 2%. Finally, there are some increases in concentration of this size class most notably in the North Atlantic Ocean and GIN seas where concentration increases by up to 53%, with the average being 14%.

With an increase in overall plankton biomass during the 190 ppm experiment, it is no surprise that we see a global increase in POC export (1.4%). A majority of the POC increase in my colder climate experiment occurs in the North Atlantic, in particular, the Norwegian sea. Here we found a 13% increase in POC export, coupled with an increase in all plankton functional type biomass. This increase was not seen across all size classes however, with the smaller 1 μm classes decreasing in biomass. The larger 100 μm size class saw the greatest increase in biomass across the PFTs in this region. Equatorial regions see little change with slight decreases being seen in the Indian Ocean (0.5 – 3% decrease) and off the west coast of Africa (0.8 – 3.5%). In the Southern Ocean we see POC decreasing in large proportions of the region. This can be seen in figure 12 where there is a decrease of between 1% and 26%. This region also sees sporadic patches of increase – sometimes by up to 46% - however, the overall trend for this region is a decrease in export.

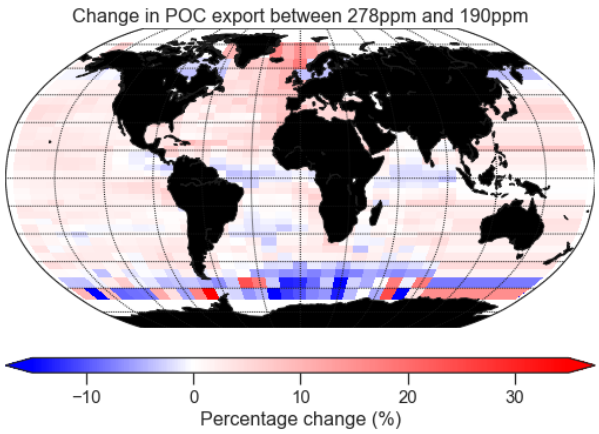

*Figure 12, changes to POC export between the cooler environment and the preindustrial environment, with blue indicating a reduction in export and red an increase. This was calculated as follows: ((POC export in cooler environment – POC export in preindustrial environment) / POC export in preindustrial environment * 100*

4.1.6 Warmer climate experiment (425 ppm)

A warmer climate – with the average SST increasing by 1.4^{o}C from preindustrial conditions - appears to have a far greater impact on phytoplankton than when temperature is reduced. Global biomass decreases, dropping from 1.04 Gt C in the preindustrial experiment to 0.93 Gt C. We also see a global decrease in concentration of 5.1% with the main source of this coming from the GIN seas and off the west coast of the UK - where concentration dropped by up to 30% (figure 13). There are, however, increases in concentration in the Southern Ocean, the highest of which (10% increase) is in the Indian sector of the Southern Ocean, south of Australia. Zooplankton also experience large decreases in concentration globally (5% decrease). Again, this is mostly for the North Atlantic – particularly through the GIN seas - where concentration dropped by as much as 47%. Like phytoplankton, the rest of the globe also has a general low decrease in concentration, with the Southern Ocean being the only exception. Here, the model shows increase in zooplankton concentration by up to 118%, but for the most part, increases are far smaller (<10%). As my colder climate experiment, overall diatom concentration changes mimic total phytoplankton changes. Globally, the biomass of diatoms decreased from 0.82 Gt C to 0.73 Gt C, with the highest levels of decreases in the North Atlantic Ocean, and the Southern Ocean showing an increase.

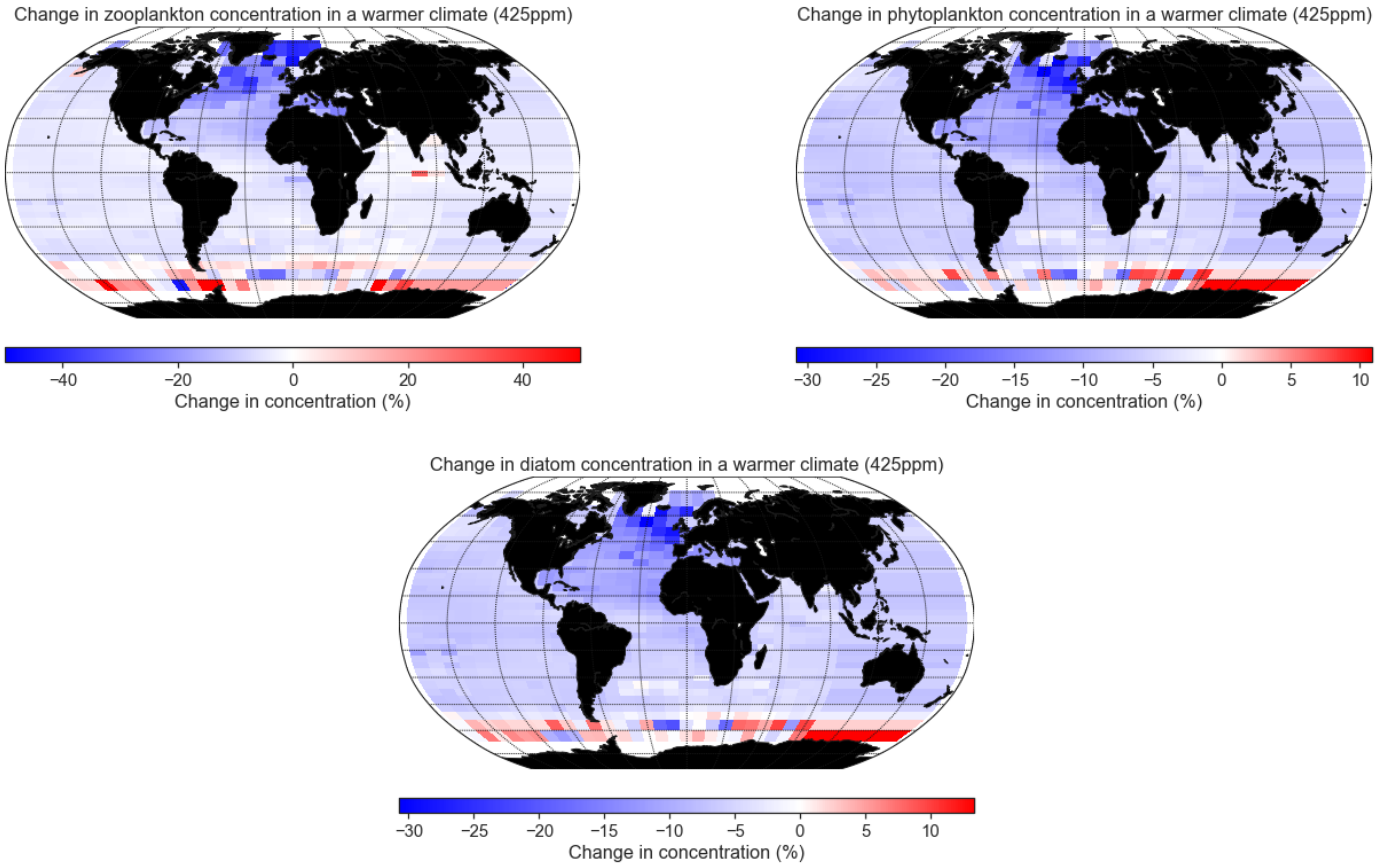

*Figure 13, results showing the change in PFT concentrations between a warm climate and the preindustrial environment. The percentage change in concentration was calculated as follows: ((concentration at 425 ppm – concentration at 278 ppm) / concentration at 278 ppm) *100. A full comparison of these functional type's concentration with the preindustrial environment can be found in Appendix 2.*

The different size classes of diatoms have a more complex pattern in change of concentration. Firstly, 1 µm diatom size class experiences a small decrease in global concentration of around 2%. A majority of this decrease is in the equatorial regions where this size class dominates (figure 14). They do, however, show increase in concentration in the higher latitudes. In the Southern Ocean, 1 µm diatoms now contribute up to 9% of the concentration, where they previously provided 0%. There is also an increase in concentration in the waters surrounding Iceland, with the greatest increase being by 112%. These changes also enhance their contribution to concentration by up to 25% in patches, indicating a shift in 1 µm diatom community structure. 10 µm diatoms do not show such dramatic changes, in fact the global decrease is uniform, with a 7.6% reduction globally. Finally, 100 µm diatoms experience a small 0.6% increase in global concentration. However, like the 1 µm size class, 100 µm diatoms do experience, with a warmer climate, large increases (>100%) in concentration in

the Southern Ocean increasing their contribution to overall concentration by up to 3%. This was also seen in the North Pacific as well as off the east coast of South America, although they still only contribute to 25% of the concentration here. There is, however, a noticeable decrease in the North Atlantic Ocean, where concentration in general drops by >20%, with some regions seeing decreases upward of 80%. This reduces their contribution to overall concentration by up to 4% as they become less prominent in this region.

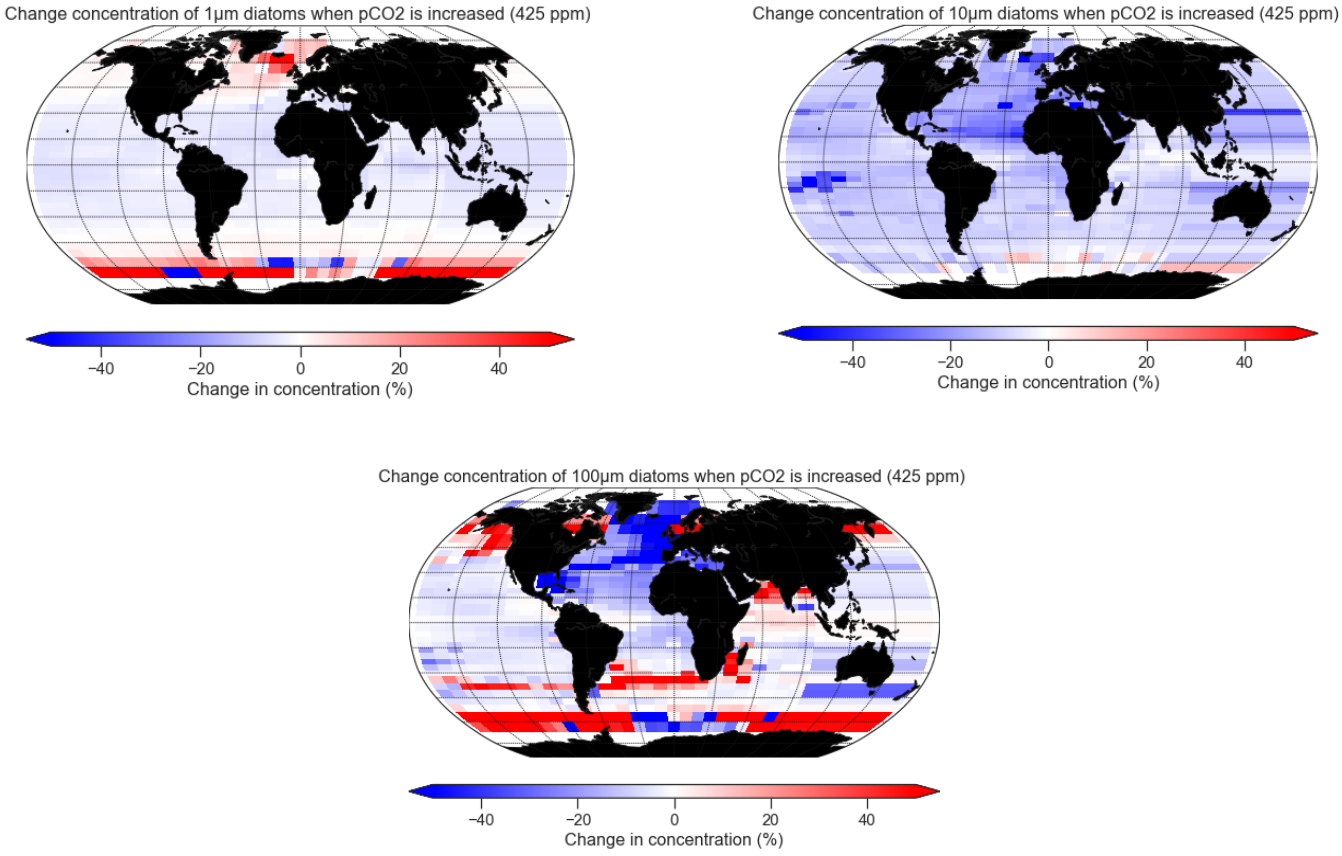

*Figure 14, changes in diatom size class concentrations between the warmer environment and the preindustrial run – with blue indicating a reduciton in concentration and red showing an increase. These changes were calculated as follows: ((size class concetration at 425 ppm - size class concetration at 278 ppm) / size class concetration at 27 8ppm) * 100.*

After investigating changes to the ecology of plankton, I show here how these ecosystem changes affects the biological export of carbon (Figure 15). When pCO_2 is increased, there is a more pronounced change in export than in the cooler climate experiment. Globally, POC export decreases by 4.6%. Here a large decrease in the amount of carbon being exported is present in the Northern

hemisphere, especially in the North Atlantic (figure 15). It is the regions surrounding Iceland that sees the most dramatic decreases, with some places experiencing a 60% decline in POC export.

It is between roughly 45°N and 65°N that we see a dramatic decline before a slight rise in the highest latitudes. The only region to experience an increase in POC export is from 60°S – 70°S where the average increase peaked at just over 7%. These patterns show good likeness to the changes in plankton biomass and concentration, highlighting their close coupling.

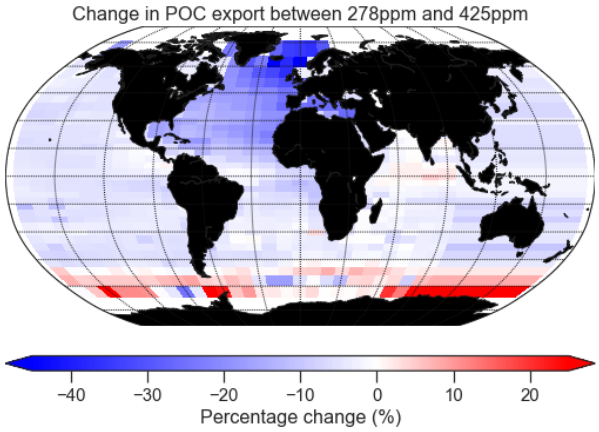

*Figure 15, changes to POC export between the warmer environment and the preindustrial environment, with blue indicating a reduction in export and red an increase. This was calculated as follows: ((POC export in warmer environment – POC export in preindustrial environment) / POC export in preindustrial environment * 100*

Table 4, summary of key findings

	Preindustrial climate (278 ppm)	Cooler climate (190 ppm)	Warmer climate (425 ppm)
Average SST	**17.5 °C**	**16.3 °C** *(-1.2 °C)*	**18.9 °C** *(+1.4 °C)*
PO_4	**0.01 – 1.6 µmol kg^{-1}**	**+3.15%** *(Globally)*	**-8.12%** *(Globally)*
Global diatom biomass	**0.82 Gt C**	**0.86 Gt C** *(+4.9%)*	**0.73 Gt C** *(-12.04%)*
1µm (average conc.) (Rounded to 2 dp)	**0.38**	**0.39** *(+1.6%)*	**0.37** *(-2%)*
10µm (average conc.) (Rounded to 2 dp)	**0.67**	**0.70** *(5.4%)*	**0.62** *(-7.6%)*
100µm (average conc.) (Rounded to 3 dp)	**0.082**	**0.080** *(-2%)*	**0.082** *(0.6%)*
POC	**2.92**	**2.96** *(+1.4%)*	**2.79** *(-4.6%)*

4.2 Causes of change

After describing the changes to the ecological component, I investigate here the possible causes, including changes to ocean physics, chemistry, and nutrient concentrations under the new environmental conditions.

Firstly, I look at the effect of temperature with these warming and cooling experiments. While changing pCO_2, SST changes accordingly more or less uniformly across the globe, with slightly larger changes at the poles. In our cooler climate experiment, the global average SST drops by 1.2 ^oC with the largest decrease being 1.78 ^oC. When warming the environment, global average SST increases by 1.4 ^oC, with some regions of the Southern Ocean increasing by up to 2.15 ^oC. These changes do not however, help explain the alteration that plankton and in particular diatoms experience. With increased temperature, we would expect an increase in metabolic rate and therefore, an increase in diatom growth and concentration. Likewise, a decreased SST should reduce metabolism and therefore decrease growth.

Another possible cause of change is nutrient supply, which depends on ocean currents that deliver nutrients from the deep ocean to surface waters. These are in the model represented by upwelling and convective mixing. I investigate first how wind induced upwelling changes in our climate experiments. Figure 16 shows the pattern of vertical currents at the pre-industrial state with blue (negative) characteristic of downwelling and red (positive) of upwelling regions.

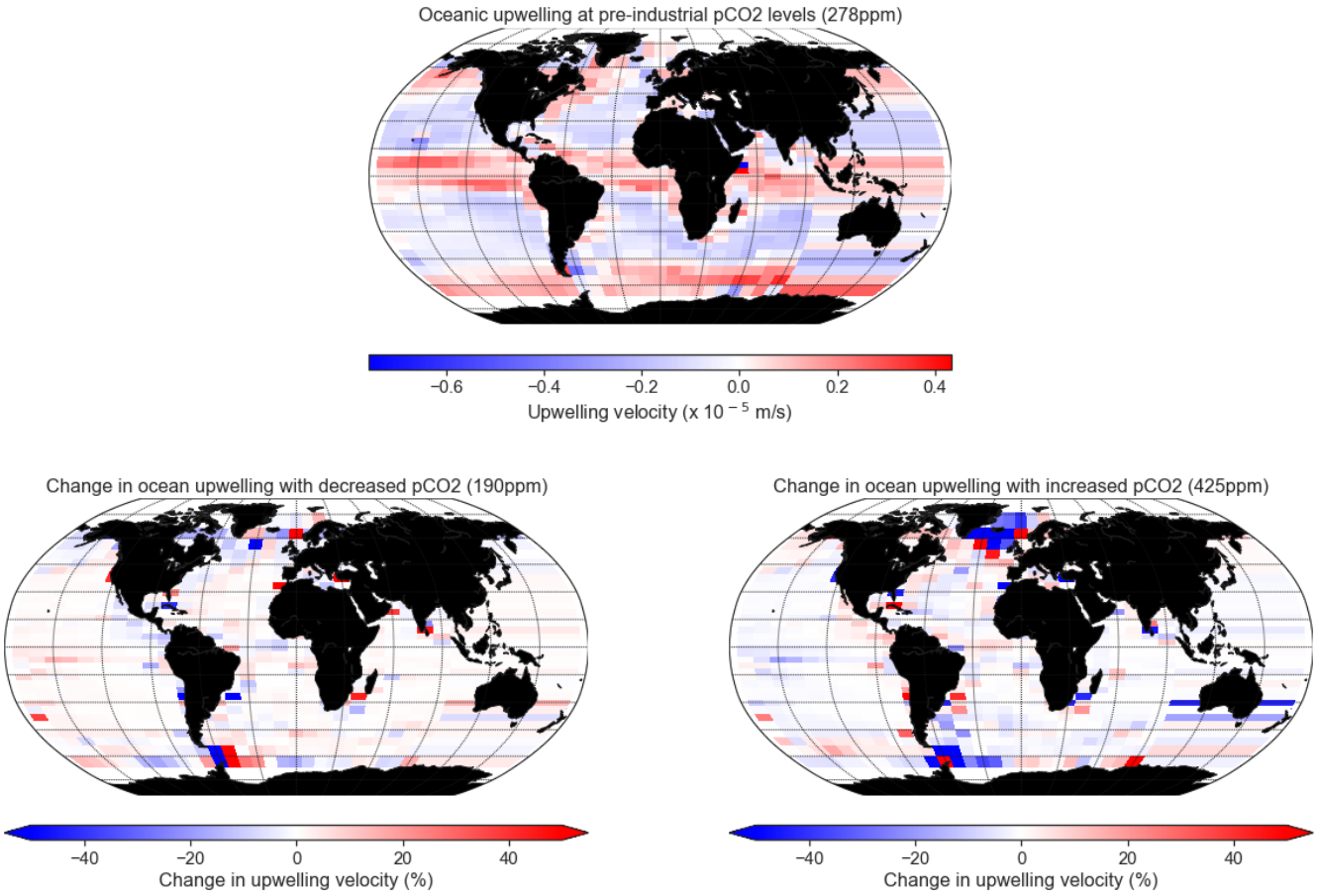

*Figure 16, the change in upwelling velocity between the preindustrial climate (top) and the cooler (bottom left) and warmer climate (bottom right). Changes were calculated as follows: ((Upwelling in cooler / warmer climate – upwelling in preindustrial conditions) / upwelling in preindustrial conditions) *100. The changes in upwelling are limited to between -100% and 100%. This is due to a few select points showing large changes in velocity thus, when the scale is set to include these, numerous other data points become ineligible.*

In the colder climate experiment with pCO_2 of 190 ppm, the overall global upwelling increases by 472%, with large portions of the ocean experiencing an increase in upwelling velocity (each grid point on average increased by 0.5%) (figure 16). There is an increase in downwelling velocity around South America as well as a decrease in upwelling in Drake Passage. Most importantly, the North Atlantic and Norwegian sea have an increase in upwelling off the coast of Norway. This increase in upwelling pumps nutrient-rich deep water to the surface, thus increasing plankton biomass in the region. In the warmer climate experiment, global upwelling decreases by 199%.

The North Atlantic Ocean experiences large changes to upwelling velocity, decreasing dramatically (>100%) over a large area. As upwelling slows, nutrient supply reduces coinciding with the reduced plankton biomass that we observed in the North Atlantic. The Southern Ocean also experiences a reduced upwelling velocity, but this is not as severe as the reduction in the North Atlantic.

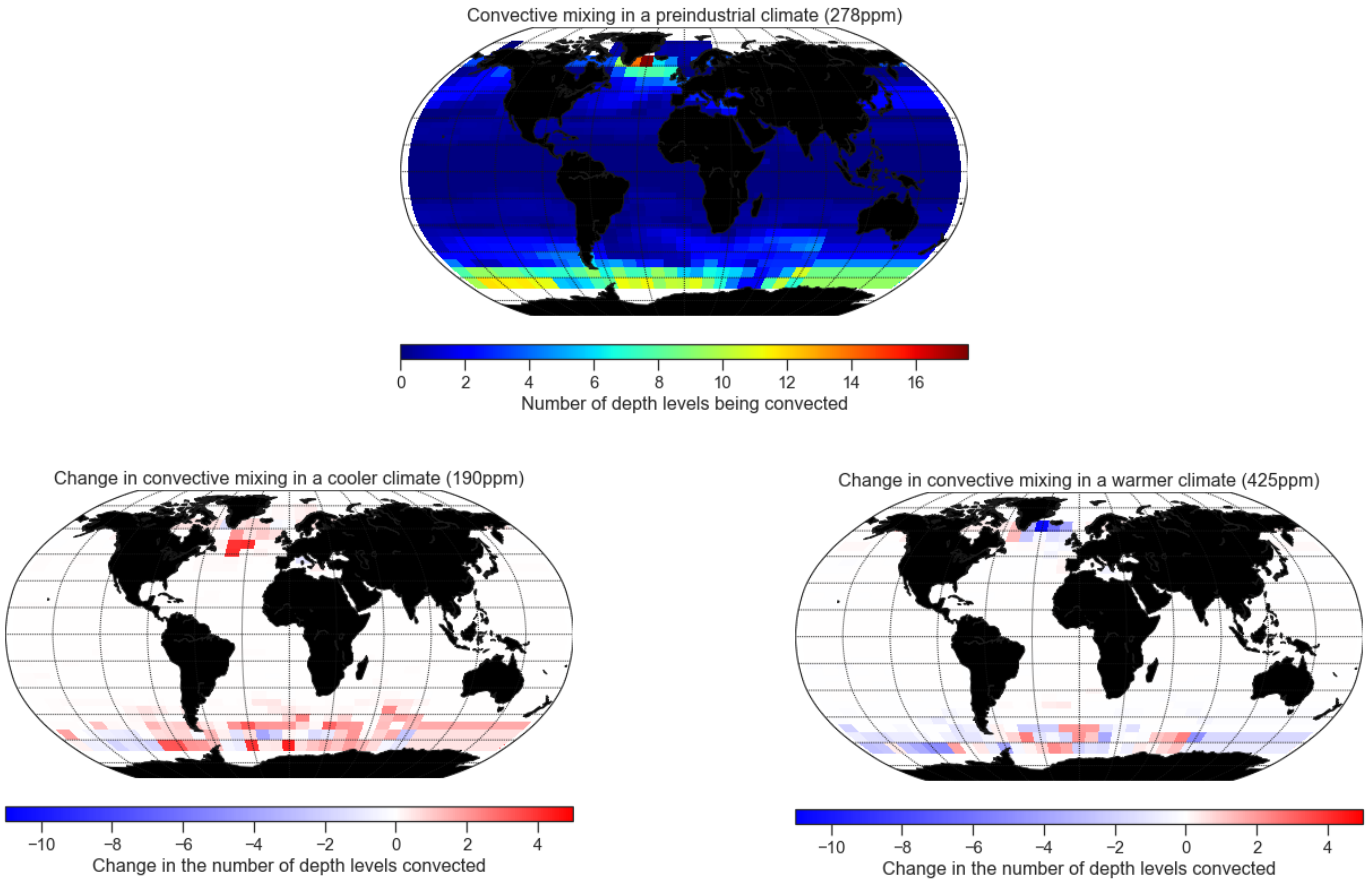

*Figure 17, changes in convective mixing between preindustrial (top) and cooler (bottom left) and warmer environment (bottom right). Changes were calculated as follows: ((Convective mixing in cooler / warmer climate – convective mixing in preindustrial conditions) / convective mixing in preindustrial conditions) *100.*

As well as wind induced mixing of the oceans, this model incorporates mixing caused by temperature and water density. In the cooled climate experiment, the North Atlantic sees an increase in the number of layers being mixed, which coincides with the increase MLD (figure 18) and upwelling velocity in this area (figure 16).

Furthermore, the Southern Ocean becomes better mixed with more layers being convected throughout. On the other hand, in the warmer climate experiment the number of layers being mixed decreases in the North Atlantic, supporting the reduction in upwelling velocity.

The mixed layer depth (MLD) is a good marker for the exchange of nutrients between the surface and deep ocean. In a pre-industrial climate, the MLD is generally below 200 m, and increases up to 1000 m (regions of deep mixing) in the Southern Ocean and North Atlantic Ocean (figure 18). MLD shows little variation in a majority of the oceans when the environment was warmed or cooled. Two regions that do, however, are the regions of deep mixing. In the Southern Ocean, a cooling climate led to both shallowing (up to 580 m) and deepening (up to 444 m) of the mixed layer depth. The warmer climate saw similar, but more extreme changes to MLD, with areas shallowing by over 900 m and deepening by 800 m. The warmer climate – unlike the cooler climate – also led to changes in the North Atlantic Oceans mixed layer, with it shallowing by almost 400 m. The shoaling of MLD usually results in an increase in light intensity, which may lead to the increase in phytoplankton biomass, but is often not the main driver of change (Leung, Cabré and Marinov, 2015; Laufkötter *et al.*, 2015). This supports our findings in the North Atlantic where shallowing did not lead to increased PP, indicating that the main cause of diatom reduction here is nutrient limitation. In the Southern Ocean however, changes in MLD show conformity with hypothesis, with shallowing MLD often coinciding with reduced diatom concentration and vice versa. This seems to effect 1 µm and 100 µm diatoms the most, likely due to their lower maximum photosynthetic rates making them more dependent on higher light levels. In the warmer climate, reduction of sea ice cover would also increase light availability. Again, this appears to coincide with the increased concentration of 1 µm and 100µm diatoms in the Southern Ocean.

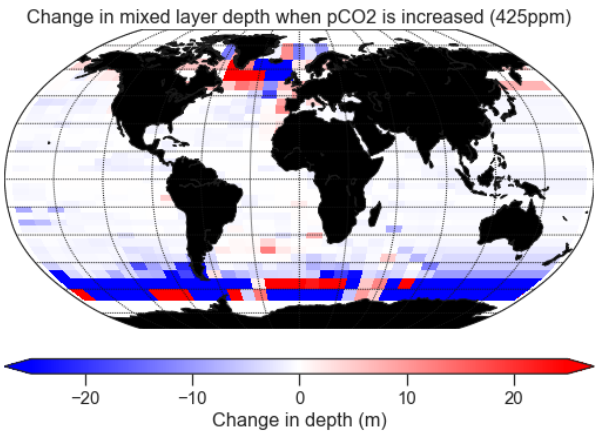

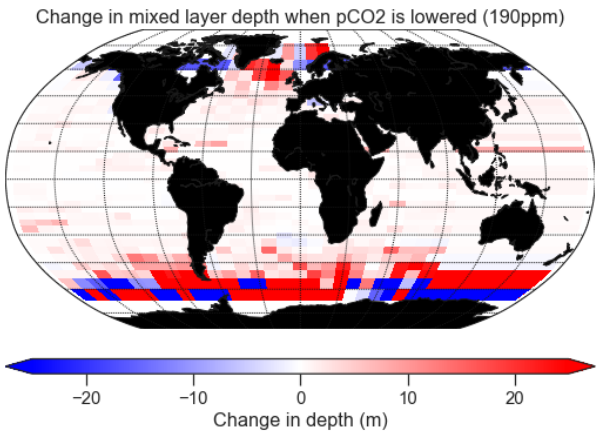

*Figure 18, changes in MLD between the preindustrial environment and the cooler (left) and warmer (right) environment. This was calculated as follows: ((MLD in cooler / warmer climate – MLD in preindustrial conditions) / MLD in preindustrial conditions) *100.*

I now investigate how these physical changes might affect nutrient supply in the surface waters of the model. In our pre-industrial experiment, concentrations of PO_4 are higher around the Southern Ocean and in the North Atlantic Ocean. In our colder climate experiment, the model experiences an overall global increase in PO_4 concentration by 3.15% (figure 19). This increase is more or less global with larger increase in North Atlantic, just south of Svalbard where concentration increased by 50%. This increase matches up with changes to ocean physics in the North Atlantic Ocean. The increased convective mixing and upwelling velocity here would likely move nutrients from the deeper waters, into the surface waters. In the other deep mixing region, the Southern Ocean, there was a decrease in PO_4 concentration. Although there is a slight decrease in upwelling here, another factor could be increased sea ice cover (figure 20) which would reduce the available surface waters.

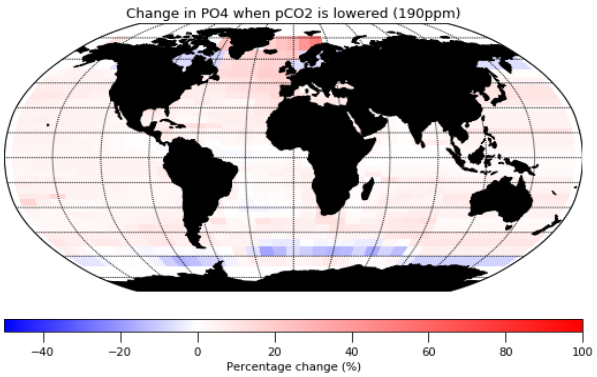

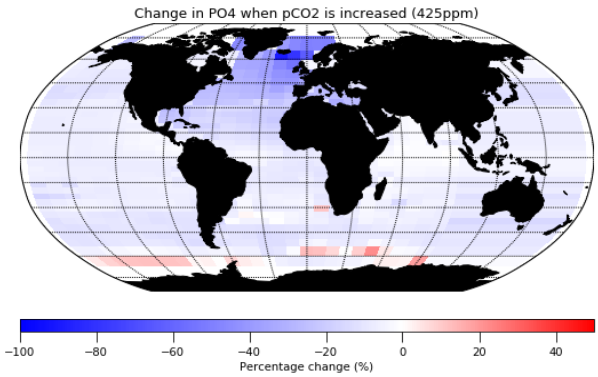

*Figure 19, change in surface PO_4 concentration between preindustrial climate and the cooler (left) and warmer (right) environments. This was calculated as follows: ((PO_4 in cooler / warmer climate – PO_4 in preindustrial conditions) / PO_4 in preindustrial conditions) *100.*

In the warmer climate experiment, PO_4 concentrations decrease globally by 8.12%. Again, much of this change comes from the North Atlantic Ocean where there are decreases of almost 90% in patches, with the average decrease being by 26.6% (figure 19).

This large change to nutrient input is almost certainly caused by the reduced mixing and upwelling velocities here, similar to ocean stratification. There are patches of small increase in the Southern Ocean and again, this could be linked with changes in sea ice cover (figure 20).

Iron concentration during the preindustrial run was mainly concentrated around the North Atlantic, Mediterranean Sea and in the most northern parts of the Indian Ocean (Arabian Sea). In the colder climate experiment, global Fe concentration decreases by 0.4% despite a large increase present in most of the Southern Hemisphere. In the 425 ppm experiment, there is a global increase of 6.98% with this occurring in most oceans worldwide. The largest of these increases can be seen off the west coast of Africa in the equatorial region, where on average the Fe concentration increases by 28%. Despite this, these changes seem to have little effect on plankton biomass in this study.

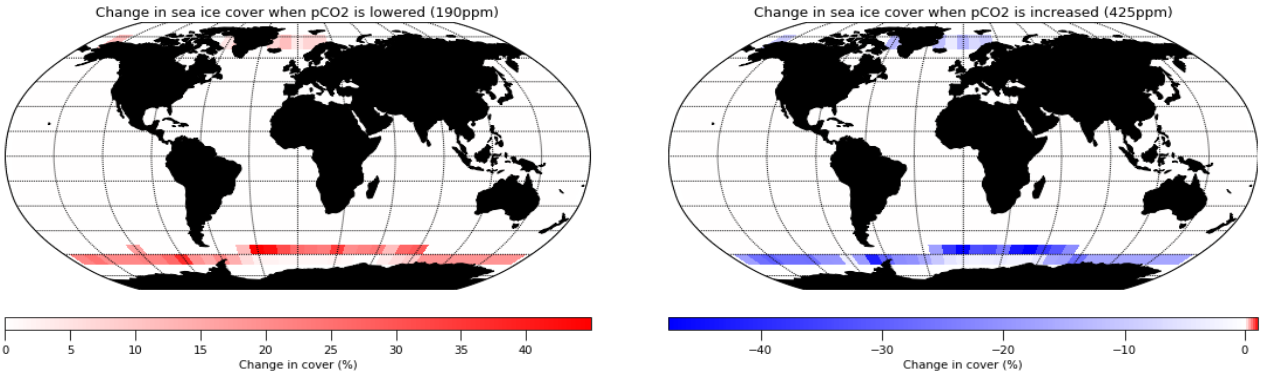

*Figure 20, changes to sea ice cover between the preindustrial environment and the cooler (left) and warmer (right) environments. This was calculated as follows: ((sea ice in cooler / warmer climate – sea ice in preindustrial conditions) / sea ice in preindustrial conditions) *100.*

5 Discussion

This study investigated how differing climate scenarios could impact the abundance, distribution and size structure of diatoms, as well as their ability to export carbon. The effect of a changing climate on primary production is well documented for both future (Wassmann and Reigstad, 2011; Dutkiewicz *et al.*, 2015; Masson-Delmotte *et al.*, 2018) and paleoclimates (Piotrowski *et al.*, 2009; Bradtmiller *et al.*, 2006; Taylor, Whitehead and Domack, 2001) . However, this is the first time that differing size classes of diatoms have been investigated in detail in a modelling study, thus providing a unique overview on the impact of different climates. While Tréguer *et al.* (2018) also represented different diatoms size classes under future climate scenarios, they did not discuss this aspect as they focused on the diatom community as a whole. My study focused on an atmospheric CO_2 concentration of 425 ppm – which is likely to be a reality in the coming decades based off the study by Davis et al. (2010). This caused an average increase of 1.4 ^{o}C, just shy of what is deemed a critical temperature by the IPCC (1.5 ^{o}C) (Adams *et al.*, 2013). Under these differing scenarios I expected different responses. In a colder climate, I expected to see an increase in primary productivity and POC export, with larger sizes of diatoms dominating the primary producers due to increased nutrient and iron supply. As temperature was increased, I hypothesised the opposite effect, with productivity and POC export decreasing and smaller size classes becoming more dominant in the nutrient replete oceans. Finally, I wanted to see if modelling different size classes was necessary, or could we get the same results by just looking at the most common size class (10 µm). In terms of POC export and overall changes to primary production, the results were as expected, with increased export and primary production in the cooler climate and decreases in the warmer climate due to changes in nutrient availability. The changes to size classes, however, were not as expected. Smaller classes increased in concentration in the cooler climate and larger size classes did not dominate global concentration. This was also seen in our warmer climate, where larger size classes increased and smaller classes decreased - the opposite to what was expected.

5.1 – Cooler climate (190 ppm)

The first of my two experiments tested the effect of pCO_2 reduction from 278 ppm to 190 ppm to mimic the effect of glacial-interglacial variation in accordance with ice core data from Monnin et al. (2001).

The first output that was investigated was the effect on overall diatom biomass. This showed a global increase in diatom biomass of 4.37%, as well as other functional types similarly seeing an increase. For diatoms, this increase in biomass was seen across all size classes with 10 μm diatoms seeing the largest increase (6.1%) and larger cells (100 μm) seeing only a 0.94% increase. Originally, I hypothesised that the larger diatom size classes would become the more dominant and see the largest increase in biomass, with smaller diatoms decreasing due to the lower expected SST. This assumption was based off the temperature size relationships suggested by Bergmann (1847), James (1970) and Atkinson (1995). However, my results showed some compliance with these rules, with 100 μm diatoms being found in the lower latitudes and 1 μm diatoms being found in the mid-high latitudes. Diatoms conformity with this rule has been investigated in numerous studies (Li *et al.*, 2009; Morán *et al.*, 2010; Yvon-Durocher *et al.*, 2011; Rüger and Sommer, 2012; Adams *et al.*, 2013) with mixed results. It has been suggested, that unless being smaller is significantly more advantageous - in terms of competition and acquisition of resources - there may not be a change in size with temperature (Adams *et al.*, 2013). Additionally, in natural environments, the complex trophic interactions these organisms encounter can further reduce the impact of temperature on size (Rüger and Sommer, 2012). Therefore, it can be assumed that in this experiment, there was no additional limitation imposed on smaller sizes and no clear advantage of being a larger species – leading to a global increase of all size classes.

Regionally, I observed that greatest changes in concentration and biomass occur in the North Atlantic Ocean and the Southern Ocean. The Greenland, Iceland and Norwegian (GIN) seas have

often been regarded as important regulators of Northern Hemisphere heat transport and CO_2 exchange (Broecker and Denton, 1989; Boyle, 1988; Dickson *et al.*, 1988). The colder climate model experiment supported this view, because the GIN region exports the largest amount of carbon in the model. Investigations into the ocean chemistry and physics of this region in the model showed increased upwelling velocity and convective mixing along the coast of Norway. With this, PO_4 saw a largest increase (50%). This upwelling of Atlantic water is likely the source of these additional nutrients. Past studies using foraminifera in the LGM have also suggested a similar pattern, induced by Atlantic upwelling (Knies, Vogt and Stein, 1998; Nørgaard-Pedersen *et al.*, 2003). Additional upwelling was also predicted in this region during the LGM due to increased sea ice cover. An increase in sea ice has been predicted to cause additional ice-edge upwelling (Smith *et al.*, 1987) further enhancing nutrient supply.

The Southern Ocean was the only region to have a noticeable decrease in the concentration throughout all functional types, with zooplankton seeing the greatest decrease during the colder climate experiment. This region showed a minor decrease in PO_4 which is likely to have contributed to the reduction in concentration here. Furthermore, there was a noticeable increase in convective mixing, as well as a deepening of MLD across a large proportion of the region. This change in mixed layer depth will have effected light supply to phytoplankton and again, could have reduced concentration. The cause of these changes likely results from temperature changes as well as increased ice cover altering salinity.

Another key process I looked at in these experiments was POC export. With diatoms being a key driver of surface export in the modern ocean (Nelson *et al.*, 1995; Treguer *et al.*, 1995) changes to community structure could impact the amount of POC being exported from surface waters. The model showed an overall increase in POC export coupled with the increases seen in diatom concentration. The only decrease that was observed during the colder climate experiment was in the Southern Ocean. Again, this is likely linked to the reduced overall concentration of diatoms,

particularly of the 100 µm size class. In addition to this it seems likely that the reduced POC export here is linked to the reduction in zooplankton. Following on from the work of Turner and Ferrante (1979), it has been showing that zooplankton faecal pellets can play a large part in surface export due to their high sinking rate. A reduction in their abundance, could therefore cause the reduction in POC export in the Southern Ocean. This reduction in POC export in the Southern Ocean was not expected, with my hypothesis being for an increase in export in the region, similar to that of LGM predictions. It has been suggested that during the LGM export production was higher than in modern oceans, causing most of the observed draw down of pCO_2. This is also seen in our experiment, with global POC export increasing by 1.41%. There are numerous theories as to why this drawdown of CO_2 occurs in the LGM, one being the silica leakage theory. Although this model was set to replicate an LGM climate, many other factors were missing to make reliable comparisons to the silica leakage hypothesis and give an accurate representation of the ocean in this time period. For example, it is hypothesised that primary production in the Southern Ocean increased due to a reduction in iron limitation due to an increased iron flux. In our model we see an increase in iron throughout the Southern Ocean, yet this did not lead to an increase in diatom concentration. This was not expected, with increased iron often stimulating higher diatoms growth rates (Coale *et al.*, 1996; Boyd *et al.*, 2007; Smetacek *et al.*, 2012). However, iron concentration in our experiment through the Southern Ocean (0.2 – 0.3 nmol l^1) is far lower than that found in ice core data of the LGM (1.5 nmol l^{-1}) (Martin, 1990) and in fertilisation experiments (Smetacek *et al.*, 2012). This is due to iron input in our model being a fixed constant, whereas iron supply during the LGM would have had an increased supply. This is a key factor in LGM modelling and in theories such as the silica leakage hypothesis, and in order to model it accurately, we would need to add this additional iron flux to the model. Additionally, alterations to the Si:C ratio with iron presence would be key. This is due to one of the key responses to increased iron being an alteration of Si:N. In the silica leakage hypothesis, an increase in iron is said to have caused a shift from modern day Si:N ratios (~4:1) to those found under adequate light and nutrient conditions (1:1). With this shift, we would have

expected to see a propagation of silica into the mid-latitudes increasing its surface concentration. Therefore, without these changes I am unable to accurately test such theories and portray a true LGM environment, but for the purpose of this study, simulating the LGM climate was adequate.

5.2 – Warmer climate experiment (425 ppm)

In this second experiment, pCO_2 increased to 425 ppm. As expected, this experiment showed contrasting results to that of the cooling experiment with the overall biomass of diatoms dropping 10.65%. Again, we observed that the size classes in the model did not conform to the temperature-size rules previously highlighted. I had hypothesised, that the smallest size-classes would thrive in these conditions, and a noticeable shift to smaller sizes would be seen. This was not the case, with 1 μm and 10 μm diatoms decreasing in biomass and the larger, 100 μm diatoms increasing in biomass. As temperature increased, I would have expected to see an increase in metabolic rate. The observed higher biomass, required additional nutrients and therefore, being of a smaller size with a larger surface to cell mass ratio, would be more advantageous (Atkinson, Ciotti and Montagnes, 2003). In this experiment however, there was - in general - no clear advantage to being of a smaller size.

POC export in this experiment decreased across a majority of the globe, with the Southern Ocean being the only acceptation. The open ocean saw an overall reduction in POC export, which has also been observed in other modelling experiments (Bopp *et al.*, 2013; Steinacher *et al.*, 2010). As with the cooling experiment, much of the change occurs in the North Atlantic. Here we observed a dramatic decrease with POC export reducing by up to 60% in places, coinciding with the reduction of all PFTs - with phytoplankton seeing the greatest reduction. Due to the coupling of the primary productivity and POC export, a reduction in one, will affect the other. The cause of this decrease in primary productivity likely to resonates from alterations to the ocean physics effecting nutrient input

to the region. One of the key drivers of this change is likely the stratification and shallowing of the mixed layer depth making the region more oligotrophic. This effect can been seen on a seasonal scale in the natural environment, with increased solar irradiance, reduced mixing and increased fresh water input leading to intense blooms which can strip surface waters of their nutrients (Holt *et al.*, 2012). On a seasonal scale, this increases productivity. But if these waters remain stratified and upwelling continues to decrease, these nutrient replete waters will remain limiting and plankton growth will not recover. This is supported by data showing a negative relationship between SST and PP when the ocean is permanently stratified (Behrenfeld *et al.*, 2006) and has occurred in numerous similar studies (Steinacher *et al.*, 2010; Holt *et al.*, 2012; Chust *et al.*, 2014). Furthermore, this stratification is likely to lead to reduced ventilation and indirectly effect oxygen supply to the euphotic zone, further limiting plankton growth (Plattner, Joos and Stocker, 2002). In our model, stratification caused up to a 90% reduction in PO_4 concentration as well as a reduction in SiO_2. Despite this reduction in SiO_2 being an additional limitation, diatoms did not decrease as much as phytoplankton. This could be down to their other traits such as higher growth rates, being more beneficial in these conditions. We also see an increase in iron supply to the Atlantic, which would normally induce an increase in phytoplankton growth, however, iron is no longer the limiting nutrient in the region thus, it cannot stimulate growth as it would under nutrient replete conditions.

Although the overall biomass of plankton in the North Atlantic decreased, this was not replicated across all size classes. The smallest size class (1 μm) of both phytoplankton and diatoms both presented an increase in the North Atlantic, when all other size classes declined. In these stratified conditions with lowered nutrients, smaller, faster growing size classes are favoured. This is due to a higher nutrient affinity that comes with a smaller size. Furthermore, smaller phytoplankton have a reduced sinking rate, this will keep them in the surface waters for longer, allowing them to collect more nutrients and removing less nutrients from the surface waters.

In the Southern Ocean we begin to see an increase in both primary productivity and carbon export with average increases of up to 7% along the highest latitudes. The increase in biomass is seen across all PFTs, although it is zooplankton and diatoms that appear to see the largest increases. The size classes of these PFTs do not all increase to the same extent, with the more abundant 10 μm diatom seeing more of a decrease in biomass. It is the larger (100 μm) and smaller (1 μm) size classes that see the greatest change in biomass. The cause of this increase is not as clear, there is a slight increase of PO_4 in the already nutrient-rich water, but both SiO_2 and Fe see slight decreases. Changes to the physical process in the Southern Ocean are erratic with no distinct pattern. There is an increase in the MLD and in the number of convected layers in the Atlantic sector of the Southern Ocean which would allow for increased plankton biomass if we assume an homogenous distribution throughout (Behrenfeld, 2010). This additional mixing will have been driven by increased SST, reducing the stratification. Furthermore, this increased SST will not only allow for increased growth rates, but also, alleviate any potential temperature limitations on the plankton in the region. There is also increased zooplankton biomass, increasing grazing pressure as temperature increases. A study by Laufkötter et al. (2015) also found increased grazing of primary producers with increased temperature – as well as with increased nutrient limitation. This could be the cause of the reduction in 10 μm diatoms. If zooplankton size classes did in fact follow the same patterns of biomass change (increases in 1 μm & 100 μm and a decrease in 10 μm) this would leave 1 μm diatoms with reduced grazing pressure – as there are lower levels of 10μm zooplankton- and it would lead to an increase in grazing pressure on 10 μm diatoms and phytoplankton. With the 1000 μm size classes in our model often not being produced, grazing is expected to have a lesser impact on 100 μm size classes and therefore their change would be due to bottom-up controls. This increase in primary production and carbon export in the Southern Ocean has been seen in a number of studies (Laufkötter *et al.*, 2015; Leung, Cabré and Marinov, 2015; Hauck *et al.*, 2015) but as with this model, these studies struggle to pinpoint the exact cause of these increases.

5.3 – Does size class matter?

After running the two climate experiments, it became clear that the 10-µm diatom size class was the dominant one, and likely governed a majority of the global carbon export. However, my study also showed that 1 µm and 100 µm diatoms were affected by changing environment to a greater degree than 10 µm. These dramatic changes could be vital when looking at hypotheses such as the silica leakage theory and other carbon export related studies. During this study I also noticed that, despite relatively high concentrations (~0.5 – 1 µmol C l^{-1}) of 1µm diatoms in equatorial regions, the export of carbon here was low. I therefore ran a series of additional experiments to include a ballasting effect on plankton. At present, a majority of small size classes organic matter is likely recycled in the microbial loop. However, with the inclusion of ballasting, a proportion of this organic matter appears be exported to the deep ocean, making smaller diatom classes more effective exporters of carbon. Currently in the model, small size classes have little impact on POC export, but with ballasting, they could be more effective, which conforms with field observations (Richardson and Jackson, 2007).

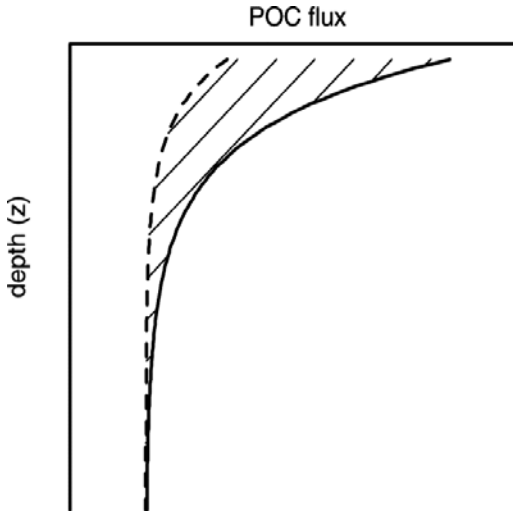

Figure 21, the total flux of POC (solid line) and the POC flux associated with ballast materials (dashed line). The crosshatched partition of these two lines represents "excess" POC that would be remineralized in the surface / upper water column (image taken from Armstrong et al.*, (2001))*

It has been suggested that the export of organic carbon is impacted by the presence of ballast mineral, including opal (Francois *et al.*, 2002). To test the impact of this hypothesis, I implement here the ballasting relationship between export flux with opal flux, proposed by Klaas and Archer (2002). This splits POC export into two components, normal POC export, which decays in the upper kilometre of the ocean, and the ballast-material (figure 21) and can be written as:

(13)

$$F_T = F_E + \not{\beta} \cdot F_B$$

Where F_T is the total POC export flux, F_E is the "excess" POC flux, F_B is the total ballast associated export and $\mathcal{f}$ is the carrying capacity of the ballast material. Therefore, with additional ballast material we will begin to see an increase in total export. This ballast material also has an increased sinking rate and can provide protection from degradation, causing more POC to reach the deep ocean. This model uses three ballast minerals; calcium carbonate, opal and detritus material, however, with no coccolithophores to provide additional calcium carbonate, opal is the main contributor to ballast for this experiment.

The addition of the ballasting effect has a dramatic effect on global carbon export in my model experiment, particularly in the mid-low latitudes (Figure 22). Ballasting due to opal production results to up to 175% increase in POC export in the South Pacific.

This increase in carbon export is correlated with 1 µm diatom concentrations in this region, indicating that small diatoms can play a key role. Furthermore, the addition of this ballast effect should also influence nutrient distribution and consequentially, plankton distribution and biomass. Therefore, in future experiments I think it is vital to explore this effect in more depth especially when exploring carbon export.

Additionally, ballasting will increase the export of opal, allowing for its redistribution – which in turn, will affect the distribution and biomass of diatoms. These will all be vital factors when attempting to accurately simulate the LGM and test the silica leakage hypothesis.

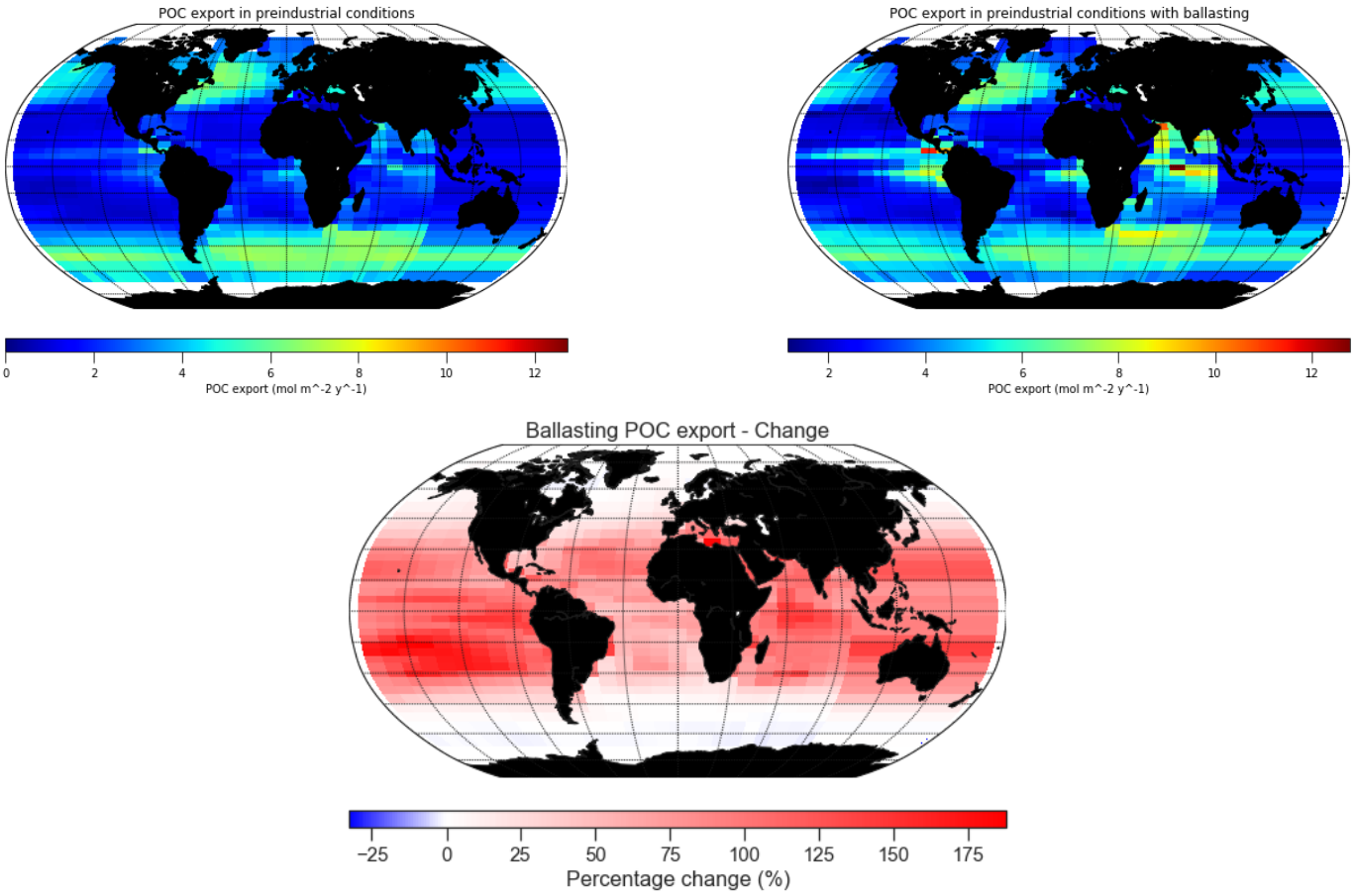

*Figure 22, a comparison of POC export with ballasting effect off (top left) and when it is switched on (top right) under pre-industrial conditions. The percentage change between these two states is also shown, and was calculated as follows; ((POC with ballasting - POC export without ballasting) / POC export without ballasting) *100*

5.4 – Future investigations

Building on this thesis, it seems the addition of ballasting could be a key focus point for future studies. Additionally, looking at size dependant sinking would provide a better understanding of the role of size classes distribution in carbon export. With this implemented, in depth investigations could then be conducted looking at an accurate LGM environment as well as future climate scenarios (RPC6, 8.5 etc.). Investigations into the LGM, especially looking at the silica leakage theory,

would require multiple adaptations to the base configuration of the model, as well as adding coccolithophores. With these changes in place, we would be able to better portray the silica leakage theory, and investigate this different size classes, something not done before.

With this addition of diatoms, it would also be interesting to distinguish the role of pennate and centric diatoms in future work. With pennate and centric diatoms undertaking different modes of sexual reproduction and motility (Round, Crawford and Mann, 1990) as well as their ability to form chains (Amato *et al.*, 2005); these key defining traits could provide further insight into diatom community structures.

6 Conclusion

This study aimed to investigate the effect of temperature on the distribution, abundance, size and carbon export of diatoms under two dramatically different climatic conditions. The cooling experiment ran at 190 ppm to mimic an LGM climate and showed an increase in productivity and global carbon export as expected. However, it was the changes to distribution and size that did not conform in the way that I expected. There was no noticeable shift towards larger diatoms under these conditions. Size classes did show good overall distribution however, acting as expected, with larger diatoms being found in the polar regions and smaller size classes in the open ocean and oceanic gyres. With the warming experiment there was a decrease in productivity and carbon export, as expected, due to upwelling and MLD reducing nutrients to regions, the North Atlantic in particular. Again, size classes didn't act as expected, with smaller size classes decreasing and larger ones seeing an increase in biomass. The exact cause of this was hard to pinpoint, but it likely due to the increased nutrients, reduced sea ice cover and changes to MLD in the Southern Ocean creating preferable conditions for larger diatoms. With this increased primary productivity in the Southern Ocean, a subsequent increase in carbon export was seen, something I had not previously hypothesised.

Overall, I believe this study gave a good basic representation of changes to diatoms productivity and carbon export potential under the different climatic conditions studied. Comparing the pre-industrial experiment used in this study to other models such as Tréguer et al. (2018), it showed that distribution and concentration of diatoms was the same as other models for our preindustrial run. The increase in productivity and carbon export seen in our 190 ppm experiment fits in well with current literature on this paleo-environment, as does the warming experiment. However, there were discrepancies between the change in size class seen in our model and literature. However, with the addition of the ballasting effect and further investigation, the use of different size classes could prove vital in predicting the role of diatoms in POC export.

There were limitations to my study, and improvements on these could give a more accurate portrayal of the conditions modelled. Firstly, alterations need to be made to diatom silica requirements in order to accurately represent silica and diatom distribution. Furthermore, the simulations of the different climatic conditions were very basic. The next step for future climates would be to model them as a perturbated system, running for 100 – 200 years, rather than the steady state environment used in this study. Also, for our paleo-experiment, a more accurate depiction of the LGM could have been used. In doing so, I would have a better representation of the diatom community during this time and have increased confidence in exploring hypothesis such as the silica leakage theory. With this, adding additional functional types would have been beneficial, particularly coccolithophores, as these are a foundation for the silica leakage theory. Another limitation was the model's inability to simulate larger plankton size classes (>1000μm). It is known that diatoms can grow to this size, and therefore, if we want to truly understand diatom communities under these different conditions, we need to be able to add them to our model. Pennate diatoms are also an important group of diatoms and adding these to the model would further improve accuracy. Additionally, including more size classes could help in seeing changes in distribution and abundance more clearly. A final improvement to this study would be to look at additional future scenarios. The one used in this study was one of the less extreme future scenarios. Looking at more extreme future emission scenarios such as RCP6.5 & 8.5 would help to better understand the impact of climate warming on diatom communities.

Despite this, I believe this work has formed a good foundation for future studies using diatoms of different size classes. Investigations into more accurate LGM environments and more extreme warming events could be a point of study, particularly in investigation of the silica leakage hypothesis. Furthermore, additional work on the parameterisation of diatoms behaviour in terms of chain formation, flocculation and buoyancy adaptations could prove to be important factors in carbon export potential. Finally, with warming scenarios, looking into seasonal variability on the

impacts of diatoms would be an important aspect of study, particularly for industries such as fisheries who depend on seasonal blooms.

7 References

Adams, G.L., Pichler, D.E., Cox, E.J., O'Gorman, E.J., Seeney, A., Woodward, G. and Reuman, D.C. (2013) Diatoms can be an important exception to temperature-size rules at species and community levels of organization. *Global Change Biology* [online]. pp. n/a-n/a. Available from: http://doi.wiley.com/10.1111/gcb.12285doi:10.1111/gcb.12285.

Aké-Castillo, J., Hernandez-Becerril, D., Meave del Castillo, M. and Bravo-Sierra, E. (2001) Species of Minidiscus (Bacillariophyceae) in the Mexican Pacific Ocean. *Cryptogamie Algologie* [online]. 22 (1), pp. 101–107. Available from: http://linkinghub.elsevier.com/retrieve/pii/S0181156800010515doi:10.1016/S0181-1568(00)01051-5.

Alvain, S., Moulin, C., Dandonneau, Y. and Loisel, H. (2008) Seasonal distribution and succession of dominant phytoplankton groups in the global ocean: A satellite view. *Global Biogeochemical Cycles* [online]. 22 (3), pp. n/a-n/a. Available from: http://doi.wiley.com/10.1029/2007GB003154doi:10.1029/2007GB003154.

Amato, A., Orsini, L., D'Alelio, D. and Montresor, M. (2005) LIFE CYCLE, SIZE REDUCTION PATTERNS, AND ULTRASTRUCTURE OF THE PENNATE PLANKTONIC DIATOM PSEUDO-NITZSCHIA DELICATISSIMA (BACILLARIOPHYCEAE)1. *Journal of Phycology* [online]. 41 (3), pp. 542–556. Available from: http://doi.wiley.com/10.1111/j.1529-8817.2005.00080.xdoi:10.1111/j.1529-8817.2005.00080.x.

Anderson, R.F., Chase, Z., Fleisher, M.Q. and Sachs, J. (2002) The Southern Ocean's biological pump during the Last Glacial Maximum. *Deep Sea Research Part II: Topical Studies in Oceanography*. 49 (9–10), pp. 1909–1938. doi:10.1016/S0967-0645(02)00018-8.

Anderson, T.R. (2005) Plankton functional type modelling: running before we can walk? *Journal of Plankton Research* [online]. 27 (11), pp. 1073–1081. Available from:

http://academic.oup.com/plankt/article/27/11/1073/1576286/Plankton-functional-type-modelling-running-beforedoi:10.1093/plankt/fbi076.

Archer, D. (1996) A data-driven model of the global calcite lysocline. *Global Biogeochemical Cycles*. 10 (3), pp. 511–526. doi:10.1029/96GB01521.

Armstrong, R.A., Lee, C., Hedges, J.I., Honjo, S. and Wakeham, S.G. (2001) A new, mechanistic model for organic carbon fluxes in the ocean based on the quantitative association of POC with ballast minerals. *Deep Sea Research Part II: Topical Studies in Oceanography* [online]. 49 (1–3), pp. 219–236. Available from: https://linkinghub.elsevier.com/retrieve/pii/S0967064501001011doi:10.1016/S0967-0645(01)00101-1.

Asadi Zarch, M.A., Sivakumar, B., Malekinezhad, H. and Sharma, A. (2017) Future aridity under conditions of global climate change. *Journal of Hydrology* [online]. 554 pp. 451–469. Available from: https://linkinghub.elsevier.com/retrieve/pii/S0022169417305796doi:10.1016/j.jhydrol.2017.08.043.

Assmy, P., Smetacek, V., Montresor, M., Klaas, C., Henjes, J., Strass, V.H., Arrieta, J.M., Bathmann, U., Berg, G.M., Breitbarth, E., Cisewski, B., Friedrichs, L., Fuchs, N., Herndl, G.J., et al. (2013) Thick-shelled, grazer-protected diatoms decouple ocean carbon and silicon cycles in the iron-limited Antarctic Circumpolar Current. *Proceedings of the National Academy of Sciences* [online]. 110 (51), pp. 20633–20638. Available from: http://www.pnas.org/cgi/doi/10.1073/pnas.1309345110doi:10.1073/pnas.1309345110.

Atkinson, D. (1995) Effects of temperature on the size of aquatic ectotherms: Exceptions to the general rule. *Journal of Thermal Biology* [online]. 20 (1–2), pp. 61–74. Available from: http://linkinghub.elsevier.com/retrieve/pii/030645659400028Hdoi:10.1016/0306-4565(94)00028-H.

Atkinson, D., Ciotti, B.J. and Montagnes, D.J.S. (2003) Protists decrease in size linearly with temperature: ca. 2.5% C-1. *Proceedings of the Royal Society B: Biological Sciences* [online]. 270 (1533), pp. 2605–2611. Available from: http://rspb.royalsocietypublishing.org/cgi/doi/10.1098/rspb.2003.2538doi:10.1098/rspb.2003.2538.

Azam, F., Fenchel, T., Field, J.G., Gray, J.S., Meyer-Reil, L.A. and Thingstad, F. (1983) The Ecological Role of Water-Column Microbes in the Sea. *Marine Ecology Progress Series* [online]. 10 (3), pp. 257–263. Available from: http://www.jstor.org/stable/24814647.

Bannon, C.C. and Campbell, D.A. (2017) Sinking towards destiny: High throughput measurement of phytoplankton sinking rates through time-resolved fluorescence plate spectroscopy Rajagopal Subramanyam (ed.). *PLOS ONE* [online]. 12 (10), pp. e0185166. Available from: http://dx.plos.org/10.1371/journal.pone.0185166doi:10.1371/journal.pone.0185166.

Banse, K. (1982) Cell volumes, maximal growth rates of unicellular algae and ciliates, and the role of ciliates in the marine pelagial. *Limnology and Oceanography* [online]. 27 (6), pp. 1059–1071. Available from: http://doi.wiley.com/10.4319/lo.1982.27.6.1059doi:10.4319/lo.1982.27.6.1059.

Baretta, J.W., Ebenhöh, W. and Ruardij, P. (1995) The European regional seas ecosystem model, a complex marine ecosystem model. *Netherlands Journal of Sea Research* [online]. 33 (3–4), pp. 233–246. Available from: http://linkinghub.elsevier.com/retrieve/pii/0077757995900470doi:10.1016/0077-7579(95)90047-0.

Beaufort, L., Garidel-Thoron, T., Mix, A. and Pisias, N. (2001) ENSO-like Forcing on Oceanic Primary Production During the Late Pleistocene. *Science* [online]. 293 (5539), pp. 2440–2444. Available from: http://www.sciencemag.org/cgi/doi/10.1126/science.293.5539.2440doi:10.1126/science.293.5

539.2440.

Behrenfeld, M.J. (2010) Abandoning Sverdrup's Critical Depth Hypothesis on phytoplankton blooms. *Ecology* [online]. 91 (4), pp. 977–989. Available from: http://doi.wiley.com/10.1890/09-1207.1doi:10.1890/09-1207.1.

Behrenfeld, M.J., O'Malley, R.T., Siegel, D.A., McClain, C.R., Sarmiento, J.L., Feldman, G.C., Milligan, A.J., Falkowski, P.G., Letelier, R.M. and Boss, E.S. (2006) Climate-driven trends in contemporary ocean productivity. *Nature* [online]. 444 (7120), pp. 752–755. Available from: https://doi.org/10.1038/nature05317doi:10.1038/nature05317.

Bell, T. and Kalff, J. (2001) The contribution of picophytoplankton in marine and freshwater systems of different trophic status and depth. *Limnology and Oceanography*. 46 (5), pp. 1243–1248. doi:10.4319/lo.2001.46.5.1243.

Van Den Berg, A.J., Ridderinkhof, H., Riegman, R., Ruardij, P. and Lenhart, H. (1996) Influence of variability in water transport on phytoplankton biomass and composition in the southern North Sea: a modelling approach (FYFY). *Continental Shelf Research* [online]. 16 (7), pp. 907–931. Available from: http://linkinghub.elsevier.com/retrieve/pii/0278434395000232doi:10.1016/0278-4343(95)00023-2.

Bergkvist, J., Thor, P., Jakobsen, H.H., Wängberg, S.-Å. and Selander, E. (2012) Grazer-induced chain length plasticity reduces grazing risk in a marine diatom. *Limnology and Oceanography* [online]. 57 (1), pp. 318–324. Available from: http://doi.wiley.com/10.4319/lo.2012.57.1.0318doi:10.4319/lo.2012.57.1.0318.

Bergmann, C. (1847) *About the relationships between heat conservation and body size of animals*. 1 (1), pp. 595–708.

Beucher, C.P., Brzezinski, M.A. and Crosta, X. (2007) Silicic acid dynamics in the glacial sub-Antarctic:

Implications for the silicic acid leakage hypothesis. *Global Biogeochemical Cycles* [online]. 21 (3), . Available from: http://doi.wiley.com/10.1029/2006GB002746doi:10.1029/2006GB002746.

Blanco, S., Borrego-Ramos, M. and Olenici, A. (2017) Disentangling diatom species complexes: does morphometry suffice? *PeerJ* [online]. 5 pp. e4159. Available from: https://peerj.com/articles/4159doi:10.7717/peerj.4159.

Bopp, L., Resplandy, L., Orr, J.C., Doney, S.C., Dunne, J.P., Gehlen, M., Halloran, P., Heinze, C., Ilyina, T., Séférian, R., Tjiputra, J. and Vichi, M. (2013) Multiple stressors of ocean ecosystems in the 21st century: projections with CMIP5 models. *Biogeosciences* [online]. 10 (10), pp. 6225–6245. Available from: https://www.biogeosciences.net/10/6225/2013/doi:10.5194/bg-10-6225-2013.

Boyd, P.W., Jickells, T., Law, C.S., Blain, S., Boyle, E.A., Buesseler, K.O., Coale, K.H., Cullen, J.J., de Baar, H.J.W., Follows, M., Harvey, M., Lancelot, C., Levasseur, M., Owens, N.P.J., et al. (2007) Mesoscale Iron Enrichment Experiments 1993-2005: Synthesis and Future Directions. *Science* [online]. 315 (5812), pp. 612–617. Available from: http://www.sciencemag.org/cgi/doi/10.1126/science.1131669doi:10.1126/science.1131669.

Boyd, P.W., Strzepek, R., Fu, F. and Hutchins, D.A. (2010) *Environmental control of open-ocean phytoplankton groups : Now and in the future*. 55 (3), pp. 1353–1376. doi:10.4319/lo.2010.55.3.1353.

Boyd, P.W., Watson, A.J., Law, C.S., Abraham, E.R., Trull, T., Murdoch, R., Bakker, D.C.E., Bowie, A.R., Buesseler, K.O., Chang, H., Charette, M., Croot, P., Downing, K., Frew, R., et al. (2000) A mesoscale phytoplankton bloom in the polar Southern Ocean stimulated by iron fertilization. *Nature* [online]. 407 pp. 695. Available from: https://doi.org/10.1038/35037500.

Boyle, E.A. (1988) Vertical oceanic nutrient fractionation and glacial/interglacial CO2cycles. *Nature* [online]. 331 (6151), pp. 55–56. Available from:

https://doi.org/10.1038/331055a0doi:10.1038/331055a0.

Bradtmiller, L.I., Anderson, R.F., Fleisher, M.Q. and Burckle, L.H. (2006) Diatom productivity in the equatorial Pacific Ocean from the last glacial period to the present: A test of the silicic acid leakage hypothesis. *Paleoceanography* [online]. 21 (4), . Available from: http://doi.wiley.com/10.1029/2006PA001282doi:10.1029/2006PA001282.

Broecker, W.S. and Denton, G.H. (1989) The role of ocean-atmosphere reorganizations in glacial cycles. *Geochimica et Cosmochimica Acta* [online]. 53 (10), pp. 2465–2501. Available from: https://linkinghub.elsevier.com/retrieve/pii/0016703789901233doi:10.1016/0016-7037(89)90123-3.

Brzezinski, M.A. (1985) THE Si:C:N RATIO OF MARINE DIATOMS: INTERSPECIFIC VARIABILITY AND THE EFFECT OF SOME ENVIRONMENTAL VARIABLES1. *Journal of Phycology* [online]. 21 (3), pp. 347–357. Available from: http://doi.wiley.com/10.1111/j.0022-3646.1985.00347.xdoi:10.1111/j.0022-3646.1985.00347.x.

Brzezinski, M.A., Olson, R.J. and Chisholm, S.W. (1990) Silicon availability and cell-cycle progression in marine diatoms. *Marine Ecology Progress Series* [online]. 67 (1), pp. 83–96. Available from: http://www.jstor.org/stable/24816749.

Brzezinski, M.A., Pride, C.J., Franck, V., Sigman, D., Gruber, N., Rau, G. and Coale, K.H. (2002) A switch from Si(OH) 4 to NO 3 − depletion in the glacial Southern Ocean. *Geophysical Research Letters* [online]. 29 (12), pp. 1564. Available from: http://doi.wiley.com/10.1029/2001GL014349doi:10.1029/2001GL014349.

Buesseler, K.O. (1998) The decoupling of production and particulate export in the surface ocean. *Global Biogeochemical Cycles* [online]. 12 (2), pp. 297–310. Available from: http://doi.wiley.com/10.1029/97GB03366doi:10.1029/97GB03366.

Buesseler, K.O. and Boyd, P.W. (2003) CLIMATE CHANGE: Will Ocean Fertilization Work? *Science*

[online]. 300 (5616), pp. 67–68. Available from: http://www.sciencemag.org/cgi/doi/10.1126/science.1082959doi:10.1126/science.1082959.

Burrows, M.T., Schoeman, D.S., Richardson, A.J., Molinos, J.G., Hoffmann, A., Buckley, L.B., Moore, P.J., Brown, C.J., Bruno, J.F., Duarte, C.M., Halpern, B.S., Hoegh-Guldberg, O., Kappel, C. V., Kiessling, W., et al. (2014) Geographical limits to species-range shifts are suggested by climate velocity. *Nature*. 507 (7493), pp. 492–495. doi:10.1038/nature12976.

Butenschön, M., Clark, J., Aldridge, J.N., Icarus Allen, J., Artioli, Y., Blackford, J., Bruggeman, J., Cazenave, P., Ciavatta, S., Kay, S., Lessin, G., Van Leeuwen, S., Van Der Molen, J., De Mora, L., et al. (2016) ERSEM 15.06: A generic model for marine biogeochemistry and the ecosystem dynamics of the lower trophic levels. *Geoscientific Model Development*. 9 (4), pp. 1293–1339. doi:10.5194/gmd-9-1293-2016.

Cabré, A., Marinov, I. and Leung, S. (2015) Consistent global responses of marine ecosystems to future climate change across the IPCC AR5 earth system models. *Climate Dynamics* [online]. 45 (5–6), pp. 1253–1280. Available from: http://link.springer.com/10.1007/s00382-014-2374-3doi:10.1007/s00382-014-2374-3.

Cao, L., Eby, M., Ridgwell, A., Caldeira, K., Archer, D., Ishida, A., Joos, F., Matsumoto, K., Mikolajewicz, U., Mouchet, A., Orr, J., Plattner, G., Schlitzer, R., Tokos, K., et al. (2009) *The role of ocean transport in the uptake of anthropogenic CO 2*. pp. 375–390.

Chust, G., Allen, J.I., Bopp, L., Schrum, C., Holt, J., Tsiaras, K., Zavatarelli, M., Chifflet, M., Cannaby, H., Dadou, I., Daewel, U., Wakelin, S.L., Machu, E., Pushpadas, D., et al. (2014) Biomass changes and trophic amplification of plankton in a warmer ocean. *Global Change Biology* [online]. 20 (7), pp. 2124–2139. Available from: http://doi.wiley.com/10.1111/gcb.12562doi:10.1111/gcb.12562.

Di Cicco, A., Sammartino, M., Marullo, S. and Santoleri, R. (2017) Regional Empirical Algorithms for

an Improved Identification of Phytoplankton Functional Types and Size Classes in the Mediterranean Sea Using Satellite Data. *Frontiers in Marine Science* [online]. 4 . Available from: http://journal.frontiersin.org/article/10.3389/fmars.2017.00126/fulldoi:10.3389/fmars.2017.00126.

Cipollini, P., Vignudelli, S. and Benveniste, J. (2014) The Coastal Zone: A Mission Target for Satellite Altimeters. *Eos, Transactions American Geophysical Union* [online]. 95 (8), pp. 72–72. Available from: http://doi.wiley.com/10.1002/2014EO080006doi:10.1002/2014EO080006.

Coale, K.H., Johnson, K.S., Fitzwater, S.E., Gordon, R.M., Tanner, S., Chavez, F.P., Ferioli, L., Sakamoto, C., Rogers, P., Millero, F., Steinberg, P., Nightingale, P., Cooper, D., Cochlan, W.P., et al. (1996) A massive phytoplankton bloom induced by an ecosystem-scale iron fertilization experiment in the equatorial Pacific Ocean. *Nature* [online]. 383 pp. 495. Available from: https://doi.org/10.1038/383495a0.

Cushing, D.H. (1990) *Plankton Production and Year-class Strength in Fish Populations: an Update of the Match/Mismatch Hypothesis*. In: [online]. pp. 249–293. Available from: https://linkinghub.elsevier.com/retrieve/pii/S0065288108602023doi:10.1016/S0065-2881(08)60202-3.

Davis, S.J., Caldeira, K. and Matthews, H.D. (2010) Future CO 2 Emissions and Climate Change from Existing Energy Infrastructure. *Science* [online]. 329 (5997), pp. 1330–1333. Available from: http://www.sciencemag.org/lookup/doi/10.1126/science.1188566doi:10.1126/science.1188566.

DeMaster, D.J. (2002) The accumulation and cycling of biogenic silica in the Southern Ocean: revisiting the marine silica budget. *Deep Sea Research Part II: Topical Studies in Oceanography* [online]. 49 (16), pp. 3155–3167. Available from: http://linkinghub.elsevier.com/retrieve/pii/S0967064502000760doi:10.1016/S0967-0645(02)00076-0.

Dickson, R.R., Meincke, J., Malmberg, S.-A. and Lee, A.J. (1988) The “great salinity anomaly” in the Northern North Atlantic 1968–1982. *Progress in Oceanography* [online]. 20 (2), pp. 103–151. Available from: https://linkinghub.elsevier.com/retrieve/pii/0079661188900493doi:10.1016/0079-6611(88)90049-3.

Droop, M.R. (1974) The nutrient status of algal cells in continuous culture. *Journal of the Marine Biological Association of the United Kingdom* [online]. 54 (04), pp. 825. Available from: http://www.journals.cambridge.org/abstract_S002531540005760Xdoi:10.1017/S002531540005760X.

Droop, M.R. (1968) Vitamin B12 and Marine Ecology. IV. The Kinetics of Uptake, Growth and Inhibition in Monochrysis Lutheri. *Journal of the Marine Biological Association of the United Kingdom* [online]. 48 (03), pp. 689. Available from: http://www.journals.cambridge.org/abstract_S0025315400019238doi:10.1017/S002531540019238.

Drum, R.W. and Hopkins, J.T. (1966) Diatom locomotion: An explanation. *Protoplasma*. 62 (1), pp. 1–33. doi:10.1007/BF01254629.

Dufour, C.O., Griffies, S.M., de Souza, G.F., Frenger, I., Morrison, A.K., Palter, J.B., Sarmiento, J.L., Galbraith, E.D., Dunne, J.P., Anderson, W.G. and Slater, R.D. (2015) Role of Mesoscale Eddies in Cross-Frontal Transport of Heat and Biogeochemical Tracers in the Southern Ocean. *Journal of Physical Oceanography* [online]. 45 (12), pp. 3057–3081. Available from: http://journals.ametsoc.org/doi/10.1175/JPO-D-14-0240.1doi:10.1175/JPO-D-14-0240.1.

Durbin, E.G. (1977) STUDIES ON THE AUTECOLOGY OF THE MARINE DIATOM THALASSIOSIRA NORDENSKIOELDII. II. THE INFLUENCE OF CELL SIZE ON GROWTH RATE, AND CARBON, NITROGEN, CHLOROPHYLL a AND SILICA CONTENT. *Journal of Phycology* [online]. 13 (2), pp. 150–155. Available from: http://doi.wiley.com/10.1111/j.1529-

8817.1977.tb02904.xdoi:10.1111/j.1529-8817.1977.tb02904.x.

Dutkiewicz, S., Morris, J.J., Follows, M.J., Scott, J., Levitan, O., Dyhrman, S.T. and Berman-Frank, I. (2015) Impact of ocean acidification on the structure of future phytoplankton communities. *Nature Climate Change* [online]. 5 pp. 1002. Available from: https://doi.org/10.1038/nclimate2722.

Edwards, N.R. and Marsh, R. (2005) *Uncertainties due to transport-parameter sensitivity in an efficient 3-D ocean-climate model*. pp. 415–433. doi:10.1007/s00382-004-0508-8.

Falkowski, P.G., Barber, R. and Smetacek, V. (1998) Biogeochemical Controls and Feedbacks on Ocean Primary Production. *Science* [online]. 281 (5374), pp. 200–206. Available from: http://www.sciencemag.org/cgi/doi/10.1126/science.281.5374.200doi:10.1126/science.281.5374.200.

Finkel, Z. V., Katz, M.E., Wright, J.D., Schofield, O.M.E. and Falkowski, P.G. (2005) Climatically driven macroevolutionary patterns in the size of marine diatoms over the Cenozoic. *Proceedings of the National Academy of Sciences* [online]. 102 (25), pp. 8927–8932. Available from: http://www.pnas.org/cgi/doi/10.1073/pnas.0409907102doi:10.1073/pnas.0409907102.

Foster, R.A., Subramaniam, A. and Zehr, J.P. (2009) Distribution and activity of diazotrophs in the Eastern Equatorial Atlantic. *Environmental Microbiology* [online]. 11 (4), pp. 741–750. Available from: http://doi.wiley.com/10.1111/j.1462-2920.2008.01796.xdoi:10.1111/j.1462-2920.2008.01796.x.

Francois, R., Honjo, S., Krishfield, R. and Manganini, S. (2002) Factors controlling the flux of organic carbon to the bathypelagic zone of the ocean. *Global Biogeochemical Cycles* [online]. 16 (4), pp. 34-1-34–20. Available from: http://doi.wiley.com/10.1029/2001GB001722doi:10.1029/2001GB001722.

Fu, W., Randerson, J.T. and Moore, J.K. (2016) Climate change impacts on net primary production

(NPP) and export production (EP) regulated by increasing stratification and phytoplankton community structure in the CMIP5 models. *Biogeosciences* [online]. 13 (18), pp. 5151–5170. Available from: https://www.biogeosciences.net/13/5151/2016/doi:10.5194/bg-13-5151-2016.

Fulton, E., Smith, A. and Johnson, C. (2003) Effect of complexity on marine ecosystem models. *Marine Ecology Progress Series* [online]. 253 pp. 1–16. Available from: http://www.int-res.com/abstracts/meps/v253/p1-16/doi:10.3354/meps253001.

Garcia, H., Weathers, K.W., Paver, C.R., Smolyar, I., Boyer, T.P., Locarnini, R.A., Zweng, M.M., Mishonov, A.V., Baranova, O.K., Seidov, D. and Reagan, J.R. (2019) *NOAA Atlas NESDIS 82 WORLD OCEAN ATLAS 2018 Volume 2 : Salinity NOAA National Centers for Environmental Information*. 2 (September), .

Geider, R.J., MacIntyre, H.L. and Kana, T.M. (1998) A dynamic regulatory model of phytoplanktonic acclimation to light, nutrients, and temperature. *Limnology and Oceanography*. 43 (4), pp. 679–694. doi:10.4319/lo.1998.43.4.0679.

Gregg, W.W., Ginoux, P., Schopf, P.S. and Casey, N.W. (2003) Phytoplankton and iron: validation of a global three-dimensional ocean biogeochemical model. *Deep Sea Research Part II: Topical Studies in Oceanography* [online]. 50 (22–26), pp. 3143–3169. Available from: http://linkinghub.elsevier.com/retrieve/pii/S096706450300184Xdoi:10.1016/j.dsr2.2003.07.013.

Guiry, M.D. (2012) HOW MANY SPECIES OF ALGAE ARE THERE? *Journal of Phycology*. 48 (5), pp. 1057–1063. doi:10.1111/j.1529-8817.2012.01222.x.

Hamm, C.E., Merkel, R., Springer, O., Jurkojc, P., Maier, C., Prechtel, K. and Smetacek, V. (2003) Architecture and material properties of diatom shells provide effective mechanical protection. *Nature* [online]. 421 pp. 841. Available from: https://doi.org/10.1038/nature01416.

Hargreaves, J.C., Annan, J.D., Edwards, N.R. and Marsh, R. (2004) *An efficient climate forecasting*

method using an intermediate complexity Earth System Model and the ensemble Kalman filter. pp. 745–760. doi:10.1007/s00382-004-0471-4.

Harrison, K.G. (2007) *Role of increased marine silica input on paleo-pC02 levels*. 15 (3), pp. 1–7. Available from: papers2://publication/uuid/B43D221B-C0E6-41CB-90BE-D73076C8B335.

Hauck, J., Völker, C., Wolf-Gladrow, D.A., Laufkötter, C., Vogt, M., Aumont, O., Bopp, L., Buitenhuis, E.T., Doney, S.C., Dunne, J., Gruber, N., Hashioka, T., John, J., Quéré, C. Le, et al. (2015) On the Southern Ocean CO 2 uptake and the role of the biological carbon pump in the 21st century. *Global Biogeochemical Cycles* [online]. 29 (9), pp. 1451–1470. Available from: https://onlinelibrary.wiley.com/doi/abs/10.1002/2015GB005140doi:10.1002/2015GB005140.

Hays, G., Richardson, A. and Robinson, C. (2005) Climate change and marine plankton. *Trends in Ecology & Evolution* [online]. 20 (6), pp. 337–344. Available from: https://linkinghub.elsevier.com/retrieve/pii/S0169534705000650doi:10.1016/j.tree.2005.03.004.

Hays, J. (1977) *A review of the late Quaternary climatic history of Antarctic seas*.

Heinle, A. and Slawig, T. (2013) Internal dynamics of NPZD type ecosystem models. *Ecological Modelling* [online]. 254 pp. 33–42. Available from: https://linkinghub.elsevier.com/retrieve/pii/S0304380013000392doi:10.1016/j.ecolmodel.2013.01.012.

Holt, J., Butenschön, M., Wakelin, S.L., Artioli, Y. and Allen, J.I. (2012) Oceanic controls on the primary production of the northwest European continental shelf: model experiments under recent past conditions and a potential future scenario. *Biogeosciences* [online]. 9 (1), pp. 97–117. Available from: https://www.biogeosciences.net/9/97/2012/doi:10.5194/bg-9-97-2012.

Honjo, S., Manganini, S.J. and Cole, J.J. (1982) Sedimentation of biogenic matter in the deep ocean. *Deep Sea Research Part A. Oceanographic Research Papers*. 29 (5), pp. 609–625.

doi:10.1016/0198-0149(82)90079-6.

Hutchins, D.A. and Bruland, K. (1998) *Iron-limited diatom growth and Si:N uptake ratios in a coastal upwelling regime*. 393 (June), pp. 65–68. doi:10.1038/31203.

James, F.C. (1970) Geographic Size Variation in Birds and Its Relationship to Climate. *Ecology* [online]. 51 (3), pp. 365–390. Available from: http://doi.wiley.com/10.2307/1935374doi:10.2307/1935374.

Javaheri, N., Dries, R., Burson, A., Stal, L.J., Sloot, P.M.A. and Kaandorp, J.A. (2015) Temperature affects the silicate morphology in a diatom. *Scientific Reports* [online]. 5 (1), pp. 11652. Available from: http://www.nature.com/articles/srep11652doi:10.1038/srep11652.

Jickells, T.D., An, Z.S., Andersen, K.K., Baker, A., Bergametti, G., Brooks, N., Cao, J., Boyd, P.W., Duce, R., Hunter, K., Kawahata, H., Kubilay, N., LaRoche, J., Liss, P., et al. (2005) Global Iron Connections Between Desert Dust, Ocean Biogeochemistry, and Climate. *Science* [online]. 308 (5718), pp. 67–71. Available from: http://www.sciencemag.org/cgi/doi/10.1126/science.1105959doi:10.1126/science.1105959.

Jones, R., Hendry, K., Wilson, J., Death, R. and Ridgwell, A. (no date) *Calibration of the cGENIE-muffin v.0.9 Earth System Model for marine biogeochemical cycling of silicon*.

Kemp, A.E.., Pike, J., Pearce, R.B. and Lange, C.B. (2000) The “Fall dump” — a new perspective on the role of a “shade flora” in the annual cycle of diatom production and export flux. *Deep Sea Research Part II: Topical Studies in Oceanography* [online]. 47 (9–11), pp. 2129–2154. Available from: http://linkinghub.elsevier.com/retrieve/pii/S0967064500000199doi:10.1016/S0967-0645(00)00019-9.

Kemp, A.E.S. and Villareal, T.A. (2018) The case of the diatoms and the muddled mandalas: Time to recognize diatom adaptations to stratified waters. *Progress in Oceanography* [online]. 167 pp. 138–149. Available from:

https://linkinghub.elsevier.com/retrieve/pii/S0079661118301095doi:10.1016/j.pocean.2018.08.002.

Kienast, S.S., Kienast, M., Jaccard, S., Calvert, S.E. and François, R. (2006) Testing the silica leakage hypothesis with sedimentary opal records from the eastern equatorial Pacific over the last 150 kyrs. *Geophysical Research Letters* [online]. 33 (15), pp. L15607. Available from: http://doi.wiley.com/10.1029/2006GL026651doi:10.1029/2006GL026651.

Kiørboe, T. (2008) *A Mechanistic Approach to Plankton Ecology*. (no place) Princeton University Press.

Klaas, C. and Archer, D.E. (2002) Association of sinking organic matter with various types of mineral ballast in the deep sea: Implications for the rain ratio. *Global Biogeochemical Cycles* [online]. 16 (4), pp. 63-1-63–14. Available from: http://doi.wiley.com/10.1029/2001GB001765doi:10.1029/2001GB001765.

Knies, J., Vogt, C. and Stein, R. (1998) Late Quaternary growth and decay of the Svalbard/Barents Sea ice sheet and paleoceanographic evolution in the adjacent Arctic Ocean. *Geo-Marine Letters* [online]. 18 (3), pp. 195–202. Available from: https://doi.org/10.1007/s003670050068doi:10.1007/s003670050068.

Kooistra, W.H.C.F., Gersonde, R., Medlin, L.K. and Mann, D.G. (2007) The Origin and Evolution of the Diatoms: Their Adaptation to a Planktonic Existence. In: *Evolution of Primary Producers in the Sea* [online]. (no place) Elsevier. pp. 207–249. Available from: http://linkinghub.elsevier.com/retrieve/pii/B9780123705181500126doi:10.1016/B978-012370518-1/50012-6.

Krause, J.W. and Lomas, M.W. (2020) Understanding Diatoms' Past and Future Biogeochemical Role in High-Latitude Seas. *Geophysical Research Letters* [online]. 47 (1), . Available from: https://onlinelibrary.wiley.com/doi/abs/10.1029/2019GL085602doi:10.1029/2019GL085602.

Lancelot, C., Spitz, Y., Gypens, N., Ruddick, K., Becquevort, S., Rousseau, V., Lacroix, G. and Billen, G. (2005) Modelling diatom and Phaeocystis blooms and nutrient cycles in the Southern Bight of the North Sea: The MIRO model. *Marine Ecology Progress Series*. 289 pp. 63–78. doi:10.3354/meps289063.

Laufkötter, C., Vogt, M., Gruber, N., Aita-Noguchi, M., Aumont, O., Bopp, L., Buitenhuis, E., Doney, S.C., Dunne, J., Hashioka, T., Hauck, J., Hirata, T., John, J., Le Quéré, C., et al. (2015) Drivers and uncertainties of future global marine primary production in marine ecosystem models. *Biogeosciences* [online]. 12 (23), pp. 6955–6984. Available from: https://www.biogeosciences.net/12/6955/2015/doi:10.5194/bg-12-6955-2015.

Lavaud, J., Rousseau, B. and Etienne, A.-L. (2004) General features of photoprotection by energy dissipation in planktonic diatoms (Bacillariophyceae). *Journal of Phycology* [online]. 40 (1), pp. 130–137. Available from: http://doi.wiley.com/10.1046/j.1529-8817.2004.03026.xdoi:10.1046/j.1529-8817.2004.03026.x.

Lea, D.W., Pak, D. and Spero, H. (2000) Climate Impact of Late Quaternary Equatorial Pacific Sea Surface Temperature Variations. *Science* [online]. 289 (5485), pp. 1719–1724. Available from: http://www.sciencemag.org/cgi/doi/10.1126/science.289.5485.1719doi:10.1126/science.289.5485.1719.

Lehahn, Y., D'Ovidio, F. and Koren, I. (2018) A Satellite-Based Lagrangian View on Phytoplankton Dynamics. *Annual Review of Marine Science* [online]. 10 (1), pp. 99–119. Available from: http://www.annualreviews.org/doi/10.1146/annurev-marine-121916-063204doi:10.1146/annurev-marine-121916-063204.

Lenhart, H.J., Radach, G. and Ruardij, P. (1997) The effects of river input on the ecosystem dynamics in the continental coastal zone of the North Sea using ERSEM. *Journal of Sea Research*. 38 (3–4), pp. 249–274. doi:10.1016/S1385-1101(97)00049-X.

Lenton, T.M., Marsh, R., Price, A.R., Lunt, D.J., Aksenov, Y., Annan, J.D., Cooper-Chadwick, T., Cox, S.J., Edwards, N.R., Goswami, S., Hargreaves, J.C., Harris, P.P., Jiao, Z., Livina, V.N., et al. (2007) Effects of atmospheric dynamics and ocean resolution on bi-stability of the thermohaline circulation examined using the Grid ENabled Integrated Earth system modelling (GENIE) framework. *Climate Dynamics* [online]. 29 (6), pp. 591–613. Available from: https://doi.org/10.1007/s00382-007-0254-9doi:10.1007/s00382-007-0254-9.

Leung, S., Cabré, A. and Marinov, I. (2015) A latitudinally banded phytoplankton response to 21st century climate change in the Southern Ocean across the CMIP5 model suite. *Biogeosciences* [online]. 12 (19), pp. 5715–5734. Available from: https://www.biogeosciences.net/12/5715/2015/doi:10.5194/bg-12-5715-2015.

Lewis, J. (1955) Silicon metabolism in diatoms. II. Sources of silicon for growth of Navicula pelliculosa. *Plant Physiol*. 30 pp. 129–134.

Li, F., Beardall, J. and Gao, K. (2018) Diatom performance in a future ocean: interactions between nitrogen limitation, temperature, and CO2-induced seawater acidification Shubha Sathyendranath (ed.). *ICES Journal of Marine Science* [online]. 75 (4), pp. 1451–1464. Available from: https://academic.oup.com/icesjms/article/75/4/1451/4788789doi:10.1093/icesjms/fsx239.

Li, G. and Campbell, D.A. (2013) Rising CO2 Interacts with Growth Light and Growth Rate to Alter Photosystem II Photoinactivation of the Coastal Diatom Thalassiosira pseudonana Rajagopal Subramanyam (ed.). *PLoS ONE* [online]. 8 (1), pp. e55562. Available from: https://dx.plos.org/10.1371/journal.pone.0055562doi:10.1371/journal.pone.0055562.

Li, W.K.W., McLaughlin, F.A., Lovejoy, C. and Carmack, E.C. (2009) Smallest Algae Thrive As the Arctic Ocean Freshens. *Science* [online]. 326 (5952), pp. 539–539. Available from: http://www.sciencemag.org/cgi/doi/10.1126/science.1179798doi:10.1126/science.1179798.

Litchman, E. and Klausmeier, C.A. (2001) Competition of Phytoplankton under Fluctuating Light. *The American Naturalist* [online]. 157 (2), pp. 170–187. Available from: https://www.journals.uchicago.edu/doi/10.1086/318628doi:10.1086/318628.

Litchman, E., Klausmeier, C.A., Miller, J.R., Schofield, O.M. and Falkowski, P.G. (2006) *Multi-nutrient, multi-group model of present and future oceanic phytoplankton communities*.

Litchman, E., Klausmeier, C.A., Schofield, O.M. and Falkowski, P.G. (2007) The role of functional traits and trade-offs in structuring phytoplankton communities: scaling from cellular to ecosystem level. *Ecology Letters*. 10 (12), pp. 1170–1181. doi:10.1111/j.1461-0248.2007.01117.x.

Litchman, E., Klausmeier, C.A. and Yoshiyama, K. (2009) Contrasting size evolution in marine and freshwater diatoms. *Proceedings of the National Academy of Sciences* [online]. 106 (8), pp. 2665–2670. Available from: http://www.pnas.org/lookup/doi/10.1073/pnas.0810891106doi:10.1073/pnas.0810891106.

Long, S.P., Humphries, S. and Falkowski, P.G. (1994) Photoinhibition of. *Annu. Rev. Plant Physiol. Plant Mol. Biol.* 45 pp. 633–662.

Luo, M., Algeo, T.J., Chen, L., Shi, X. and Chen, D. (2018) Role of dust fluxes in stimulating Ethmodiscus rex giant diatom blooms in the northwestern tropical Pacific during the Last Glacial Maximum. *Palaeogeography, Palaeoclimatology, Palaeoecology* [online]. 511 pp. 319–331. Available from: https://linkinghub.elsevier.com/retrieve/pii/S0031018218305297doi:10.1016/j.palaeo.2018.08.017.

Mann, D.G. and Droop, S.J.M. (1996) Biodiversity, biogeography and conservation of diatoms. In: Jørgen Kristiansen (ed.). *Biogeography of Freshwater Algae: Proceedings of the Workshop on Biogeography of Freshwater Algae, held during the Fifth International Phycological Congress, Qingdao, China, June 1994* [online]. Dordrecht: Springer Netherlands. pp. 19–32. Available

from: https://doi.org/10.1007/978-94-017-0908-8_2doi:10.1007/978-94-017-0908-8_2.

Marañón, E., Cermeño, P., López-Sandoval, D.C., Rodríguez-Ramos, T., Sobrino, C., Huete-Ortega, M., Blanco, J.M. and Rodríguez, J. (2012) Unimodal size scaling of phytoplankton growth and the size dependence of nutrient uptake and use Gregor Fussmann (ed.). *Ecology Letters* [online]. 16 (3), pp. 371–379. Available from: http://doi.wiley.com/10.1111/ele.12052doi:10.1111/ele.12052.

Marsh, R., Muller, S., Yool, A. and Edwards, N.R. (2011) *Incorporation of the C-GOLDSTEIN efficient climate model into the GENIE framework : " eb go gs "*. doi:10.5194/gmd-4-957-2011.

Martin, J.H. (1990) Glacial-interglacial CO 2 change: The Iron Hypothesis. *Paleoceanography* [online]. 5 (1), pp. 1–13. Available from: http://doi.wiley.com/10.1029/PA005i001p00001doi:10.1029/PA005i001p00001.

Masson-Delmotte, V., Zhai, P., Pörtner, H.-O., Roberts, D., Skea, J., Shukla, P.R., Pirani, A., Moufouma-Okia, W., Péan, C., Pidcock, R., Connors, S., Matthews, J.B.R., Chen, Y., Zhou, X., et al. (2018) *Global warming of 1.5°C An IPCC Special Report* [online].

Matsumoto, K. and Sarmiento, J.L. (2008) A corollary to the silicic acid leakage hypothesis. *Paleoceanography* [online]. 23 (2), pp. n/a-n/a. Available from: http://doi.wiley.com/10.1029/2007PA001515doi:10.1029/2007PA001515.

Matsumoto, K., Sarmiento, J.L. and Brzezinski, M.A. (2002) Silicic acid leakage from the Southern Ocean: A possible explanation for glacial atmospheric p CO 2. *Global Biogeochemical Cycles* [online]. 16 (3), pp. 5-1-5–23. Available from: http://doi.wiley.com/10.1029/2001GB001442doi:10.1029/2001GB001442.

McCave, I.N. (1975) Vertical flux of particles in the ocean. *Deep Sea Research and Oceanographic Abstracts*. 22 (7), pp. 491–502. doi:10.1016/0011-7471(75)90022-4.

Meyer, K.M., Ridgwell, A. and Payne, J.L. (2016) *The influence of the biological pump on ocean*

chemistry : implications for long-term trends in marine redox chemistry , the global carbon cycle , and marine animal ecosystems. pp. 207–219. doi:10.1111/gbi.12176.

Monnin, E., Indermühle, A., Dällenbach, A., Flückiger, J., Stauffer, B., Stocker, T., Raynaud, D. and Barnola, J.M. (2001) Atmospheric CO2 Concentrations over the Last Glacial Termination. *Science* [online]. 291 (5501), pp. 112–114. Available from: http://www.sciencemag.org/cgi/doi/10.1126/science.291.5501.112doi:10.1126/science.291.5501.112.

Montagnes, D.J.S. and Franklin, M. (2001) Effect of temperature on diatom volume, growth rate, and carbon and nitrogen content: Reconsidering some paradigms. *Limnology and Oceanography* [online]. 46 (8), pp. 2008–2018. Available from: http://doi.wiley.com/10.4319/lo.2001.46.8.2008doi:10.4319/lo.2001.46.8.2008.

Monteiro, F.M., Pancost, R.D., Ridgwell, A. and Donnadieu, Y. (2012) *Nutrients as the dominant control on the spread of anoxia and euxinia across the Cenomanian-Turonian oceanic anoxic event (OAE2): Model-data comparison*. 27 pp. 1–17. doi:10.1029/2012PA002351.

Moore, J.K. and Abbott, M.R. (2002) Surface chlorophyll concentrations in relation to the Antarctic Polar Front: seasonal and spatial patterns from satellite observations. *Journal of Marine Systems* [online]. 37 (1–3), pp. 69–86. Available from: http://linkinghub.elsevier.com/retrieve/pii/S0924796302001963doi:10.1016/S0924-7963(02)00196-3.

Moore, J.K., Doney, S.C., Kleypas, J.A., Glover, D.M. and Fung, I.Y. (2002) An intermediate complexity marine ecosystem model for the global domain. *Deep-Sea Research Part II: Topical Studies in Oceanography*. 49 (1–3), pp. 403–462. doi:10.1016/S0967-0645(01)00108-4.

Moore, J.K., Doney, S.C. and Lindsay, K. (2004) Upper ocean ecosystem dynamics and iron cycling in a global three-dimensional model. *Global Biogeochemical Cycles* [online]. 18 (4), pp. n/a-n/a.

Available from: http://doi.wiley.com/10.1029/2004GB002220doi:10.1029/2004GB002220.

MORÁN, X.A.G., LÓPEZ-URRUTIA, Á., CALVO-DÍAZ, A. and LI, W.K.W. (2010) Increasing importance of small phytoplankton in a warmer ocean. *Global Change Biology* [online]. 16 (3), pp. 1137–1144. Available from: http://doi.wiley.com/10.1111/j.1365-2486.2009.01960.xdoi:10.1111/j.1365-2486.2009.01960.x.

Nakamura, Y. and Oka, A. (2019) CMIP5 model analysis of future changes in ocean net primary production focusing on differences among individual oceans and models. *Journal of Oceanography* [online]. 75 (5), pp. 441–462. Available from: http://link.springer.com/10.1007/s10872-019-00513-wdoi:10.1007/s10872-019-00513-w.

Nelson, D.M., Tréguer, P., Brzezinski, M.A., Leynaert, A. and Quéguiner, B. (1995) Production and dissolution of biogenic silica in the ocean: Revised global estimates, comparison with regional data and relationship to biogenic sedimentation. *Global Biogeochemical Cycles* [online]. 9 (3), pp. 359–372. Available from: http://doi.wiley.com/10.1029/95GB01070doi:10.1029/95GB01070.

Niyogi, K.K. (2000) Safety valves for photosynthesis. *Current Opinion in Plant Biology* [online]. 3 (6), pp. 455–460. Available from: http://linkinghub.elsevier.com/retrieve/pii/S1369526600001138doi:10.1016/S1369-5266(00)00113-8.

NOAA (2018) *Trends in Atmospheric Carbon Dioxide*. Available from: https://www.esrl.noaa.gov/gmd/ccgg/trends/monthly.html.

Nørgaard-Pedersen, N., Spielhagen, R.F., Erlenkeuser, H., Grootes, P.M., Heinemeier, J. and Knies, J. (2003) Arctic Ocean during the Last Glacial Maximum: Atlantic and polar domains of surface water mass distribution and ice cover. *Paleoceanography* [online]. 18 (3), pp. n/a-n/a. Available from: http://doi.wiley.com/10.1029/2002PA000781doi:10.1029/2002PA000781.

Nozaki, Y. and Yamamoto, Y. (2001) South China Sea and a silicon-induced " alkalinity pump " hypothesis the continental shelves of the southeast Asian Seas are strong sources to much lesser extent , which are largely transported by the surface currents into the Indian The vertical profiles. *Global Biogeochemical Cycles*. 15 (3), pp. 555–567.

O'Neill, B.C., Tebaldi, C., van Vuuren, D.P., Eyring, V., Friedlingstein, P., Hurtt, G., Knutti, R., Kriegler, E., Lamarque, J.-F., Lowe, J., Meehl, G.A., Moss, R., Riahi, K. and Sanderson, B.M. (2016) The Scenario Model Intercomparison Project (ScenarioMIP) for CMIP6. *Geoscientific Model Development* [online]. 9 (9), pp. 3461–3482. Available from: https://www.geosci-model-dev.net/9/3461/2016/doi:10.5194/gmd-9-3461-2016.

Paasche, E. (1980) *Silicon content of five marine plankton measured with a rapid filter method1 diatom species*. 25 (3), pp. 474–480.

Pappas, J.L. and Stoermer, E.F. (2003) Legendre shape descriptors and shape group determination of specimens in the Cymbella cistula species complex. *Phycologia* [online]. 42 (1), pp. 90–97. Available from: https://www.tandfonline.com/doi/full/10.2216/i0031-8884-42-1-90.1doi:10.2216/i0031-8884-42-1-90.1.

Pierella Karlusich, J.J., Ibarbalz, F.M. and Bowler, C. (2020) Phytoplankton in the Tara Ocean. *Annual Review of Marine Science* [online]. 12 (1), pp. 233–265. Available from: https://www.annualreviews.org/doi/10.1146/annurev-marine-010419-010706doi:10.1146/annurev-marine-010419-010706.

Piotrowski, A.M., Banakar, V.K., Scrivner, A.E., Elderfield, H., Galy, A. and Dennis, A. (2009) Indian Ocean circulation and productivity during the last glacial cycle. *Earth and Planetary Science Letters* [online]. 285 (1–2), pp. 179–189. Available from: https://linkinghub.elsevier.com/retrieve/pii/S0012821X09003422doi:10.1016/j.epsl.2009.06.007.

Plattner, G.-K., Joos, F. and Stocker, T.F. (2002) Revision of the global carbon budget due to changing air-sea oxygen fluxes. *Global Biogeochemical Cycles* [online]. 16 (4), pp. 43-1-43–12. Available from: http://doi.wiley.com/10.1029/2001GB001746doi:10.1029/2001GB001746.

Pondaven, P., Gallinari, M., Chollet, S., Bucciarelli, E., Sarthou, G., Schultes, S. and Jean, F. (2007) Grazing-induced Changes in Cell Wall Silicification in a Marine Diatom. *Protist* [online]. 158 (1), pp. 21–28. Available from: http://linkinghub.elsevier.com/retrieve/pii/S1434461006000988doi:10.1016/j.protis.2006.09.002.

Pondaven, P., Ragueneau, O., Tréguer, P., Hauvespre, A., Dezileau, L. and Reyss, J.L. (2000a) Resolving the 'opal paradox' in the Southern Ocean. *Nature* [online]. 405 (6783), pp. 168–172. Available from: http://www.nature.com/articles/35012046doi:10.1038/35012046.

Pondaven, P., Ruiz-Pino, D., Fravalo, C., Tréguer, P. and Jeandel, C. (2000b) Interannual variability of Si and N cycles at the time-series station KERFIX between 1990 and 1995 – a 1-D modelling study. *Deep Sea Research Part I: Oceanographic Research Papers* [online]. 47 (2), pp. 223–257. Available from: http://linkinghub.elsevier.com/retrieve/pii/S0967063799000539doi:10.1016/S0967-0637(99)00053-9.

Prants, S.V., Lobanov, V.B., Budyansky, M.V. and Uleysky, M.Y. (2016) Lagrangian analysis of formation, structure, evolution and splitting of anticyclonic Kuril eddies. *Deep Sea Research Part I: Oceanographic Research Papers* [online]. 109 pp. 61–75. Available from: https://linkinghub.elsevier.com/retrieve/pii/S0967063715300546doi:10.1016/j.dsr.2016.01.003.

Quere, C. Le, Harrison, S.P., Colin Prentice, I., Buitenhuis, E.T., Aumont, O., Bopp, L., Claustre, H., Cotrim Da Cunha, L., Geider, R., Giraud, X., Klaas, C., Kohfeld, K.E., Legendre, L., Manizza, M., et al. (2005) Ecosystem dynamics based on plankton functional types for global ocean

biogeochemistry models. *Global Change Biology* [online]. pp. 051013014052005-??? Available from: http://doi.wiley.com/10.1111/j.1365-2486.2005.1004.xdoi:10.1111/j.1365-2486.2005.1004.x.

Rhee, G.-Y. (1978) Effects of N:P atomic ratios and nitrate limitation on algal growth, cell composition, and nitrate uptake 1. *Limnology and Oceanography* [online]. 23 (1), pp. 10–25. Available from: http://doi.wiley.com/10.4319/lo.1978.23.1.0010doi:10.4319/lo.1978.23.1.0010.

Richardson, A.J. and Schoeman, D.S. (2004) Climate Impact on Plankton Ecosystems in the Northeast Atlantic. *Science* [online]. 305 (5690), pp. 1609–1612. Available from: http://www.sciencemag.org/cgi/doi/10.1126/science.1100958doi:10.1126/science.1100958.

Richardson, T.L. and Jackson, G.A. (2007) Small Phytoplankton and Carbon Export from the Surface Ocean. *Science* [online]. 315 (5813), pp. 838–840. Available from: http://www.sciencemag.org/cgi/doi/10.1126/science.1133471doi:10.1126/science.1133471.

Richman, S. and Rogers, J.N. (1969) The feeding of Calanus helgolandicus on synchronously growing populations of the marine diatom Ditylum brightwellii. *Limnology and Oceanography* [online]. 14 (5), pp. 701–709. Available from: http://doi.wiley.com/10.4319/lo.1969.14.5.0701doi:10.4319/lo.1969.14.5.0701.

Ridgwell, A., Hargreaves, J.C., Edwards, N.R., Annan, J.D., Lenton, T.M., Yool, A., Watson, A., Ridgwell, A., Hargreaves, J.C., Edwards, N.R., Annan, J.D. and Lenton, T.M. (2007) *Marine geochemical data assimilation in an efficient Earth System Model of global biogeochemical cycling To cite this version : HAL Id : hal-00297599 Biogeosciences Marine geochemical data assimilation in an efficient Earth System Model of global biogeoch*.

Ridgwell, A. and Schmidt, D.N. (2010) Past constraints on the vulnerability of marine calcifiers to massive carbon dioxide release. *Nature Geoscience* [online]. 3 (3), pp. 196–200. Available

from: http://dx.doi.org/10.1038/ngeo755doi:10.1038/ngeo755.

Romann, J., Valmalette, J.C., Chauton, M.S., Tranell, G., Einarsrud, M.A. and Vadstein, O. (2015) Wavelength and orientation dependent capture of light by diatom frustule nanostructures. *Scientific Reports* [online]. 5 (7491), pp. 1–6. Available from: http://dx.doi.org/10.1038/srep17403doi:10.1038/srep17403.

Round, F.E., Crawford, R.M. and Mann, D.G. (1990) *Diatoms: Biology and Morphology of the Genera* [online]. (no place) Cambridge University Press.

Rueler, J.G. and Ades., D.R. (1987) The role of iron nutrition in photosynthesis and nitrogen assimilation in SCENEDESMUS QUADRICAUDA (Chlorophyceae). *Journal of Phycology* [online]. 23 (3), pp. 452–457. Available from: http://doi.wiley.com/10.1111/j.1529-8817.1987.tb02531.xdoi:10.1111/j.1529-8817.1987.tb02531.x.

Rüger, T. and Sommer, U. (2012) Warming does not always benefit the small – Results from a plankton experiment. *Aquatic Botany* [online]. 97 (1), pp. 64–68. Available from: https://linkinghub.elsevier.com/retrieve/pii/S0304377011001744doi:10.1016/j.aquabot.2011.12.001.

Rynearson, T.A., Richardson, K., Lampitt, R.S., Sieracki, M.E., Poulton, A.J., Lyngsgaard, M.M. and Perry, M.J. (2013) Major contribution of diatom resting spores to vertical flux in the sub-polar North Atlantic. *Deep Sea Research Part I: Oceanographic Research Papers*. 82 pp. 60–71. doi:10.1016/j.dsr.2013.07.013.

Sabater, S. (2009) Diatoms. In: *Encyclopedia of Inland Waters* [online]. (no place) Elsevier. pp. 149–156. Available from: https://linkinghub.elsevier.com/retrieve/pii/B9780123706263001356doi:10.1016/B978-012370626-3.00135-6.

Sánchez, C., Cristóbal, G. and Bueno, G. (2019) Diatom identification including life cycle stages

through morphological and texture descriptors. *PeerJ* [online]. 7 pp. e6770. Available from: https://peerj.com/articles/6770doi:10.7717/peerj.6770.

Sarmiento, J.L., Slater, R., Barber, R., Bopp, L., Doney, S.C., Hirst, A.C., Kleypas, J., Matear, R., Mikolajewicz, U., Monfray, P., Soldatov, V., Spall, S.A. and Stouffer, R. (2004) Response of ocean ecosystems to climate warming. *Global Biogeochemical Cycles* [online]. 18 (3), pp. n/a-n/a. Available from: http://doi.wiley.com/10.1029/2003GB002134doi:10.1029/2003GB002134.

Sarthou, G., Timmermans, K.R., Blain, S. and Tréguer, P. (2005) Growth physiology and fate of diatoms in the ocean: a review. *Journal of Sea Research* [online]. 53 (1–2), pp. 25–42. Available from: https://linkinghub.elsevier.com/retrieve/pii/S1385110104000644doi:10.1016/j.seares.2004.01.007.

Schmittner, A., Oschlies, A., Matthews, H.D. and Galbraith, E.D. (2008) Future changes in climate, ocean circulation, ecosystems, and biogeochemical cycling simulated for a business-as-usual CO 2 emission scenario until year 4000 AD. *Global Biogeochemical Cycles* [online]. 22 (1), pp. n/a-n/a. Available from: http://doi.wiley.com/10.1029/2007GB002953doi:10.1029/2007GB002953.

Six, K.D. and Maier-Reimer, E. (1996) Effects of plankton dynamics on seasonal carbon fluxes in an ocean general circulation model. *Global Biogeochemical Cycles* [online]. 10 (4), pp. 559–583. Available from: http://doi.wiley.com/10.1029/96GB02561doi:10.1029/96GB02561.

Smayda, T.J. (1971) Normal and accelerated sinking of phytoplankton in the sea. *Marine Geology*. 11 (2), pp. 105–122. doi:10.1016/0025-3227(71)90070-3.

Smetacek, V. (1999) Bacteria and silica cycling. *Nature* [online]. 397 pp. 475. Available from: https://doi.org/10.1038/17219.

Smetacek, V. and Cloern, J.E. (2008) OCEANS: On Phytoplankton Trends. *Science* [online]. 319

(5868), pp. 1346–1348. Available from: http://www.sciencemag.org/cgi/doi/10.1126/science.1151330doi:10.1126/science.1151330.

Smetacek, V., Klaas, C., Strass, V.H., Assmy, P., Montresor, M., Cisewski, B., Savoye, N., Webb, A., D'Ovidio, F., Arrieta, J.M., Bathmann, U., Bellerby, R., Berg, G.M., Croot, P., et al. (2012) Deep carbon export from a Southern Ocean iron-fertilized diatom bloom. *Nature* [online]. 487 (7407), pp. 313–319. Available from: http://dx.doi.org/10.1038/nature11229%5Cnpapers2://publication/doi/10.1038/nature11229doi:10.1038/nature11229 https://www.nature.com/articles/nature11229#supplementary-information.

Smith, H.E.K., Poulton, A.J., Garley, R., Hopkins, J., Lubelczyk, L.C., Drapeau, D.T., Rauschenberg, S., Twining, B.S., Bates, N.R. and Balch, W.M. (2017) The Influence of Environmental Variability on the Biogeography of Coccolithophores and Diatoms in the Great Calcite Belt. *Biogeosciences Discussions*. (April), pp. 1–35. doi:10.5194/bg-2017-110.

Smith, W.O., Baumann, M.E.M., Wilson, D.L. and Aletsee, L. (1987) Phytoplankton biomass and productivity in the marginal ice zone of the Fram Strait during summer 1984. *Journal of Geophysical Research* [online]. 92 (C7), pp. 6777. Available from: http://doi.wiley.com/10.1029/JC092iC07p06777doi:10.1029/JC092iC07p06777.

Sommer, U., Charalampous, E., Genitsaris, S. and Moustaka-Gouni, M. (2016) Benefits, costs and taxonomic distribution of marine phytoplankton body size. *Journal of Plankton Research* [online]. Available from: https://academic.oup.com/plankt/article-lookup/doi/10.1093/plankt/fbw071doi:10.1093/plankt/fbw071.

Steinacher, M., Joos, F., Frölicher, T.L., Bopp, L., Cadule, P., Cocco, V., Doney, S.C., Gehlen, M., Lindsay, K., Moore, J.K.K., Schneider, B. and Segschneider, J. (2010) Projected 21st century decrease in marine productivity: a multi-model analysis. *Biogeosciences* [online]. 7 (3), pp. 979–1005. Available from: http://www.biogeosciences.net/7/979/2010/doi:10.5194/bg-7-979-

2010.

Stott, L., Poulsen, C., Lund, S. and Thunell, R. (2002) Super ENSO and Global Climate Oscillations at Millennial Time Scales. *Science* [online]. 297 (5579), pp. 222–226. Available from: http://www.sciencemag.org/cgi/doi/10.1126/science.1071627doi:10.1126/science.1071627.

Taylor, A.H., Allen, J.I. and Clark, P.A. (2002) *Extraction of a weak climatic signal by an ecosystem*. 416 (April), pp. 629–632.

Taylor, F., Whitehead, J. and Domack, E. (2001) Holocene paleoclimate change in the Antarctic Peninsula: evidence from the diatom, sedimentary and geochemical record. *Marine Micropaleontology* [online]. 41 (1–2), pp. 25–43. Available from: https://linkinghub.elsevier.com/retrieve/pii/S0377839800000499doi:10.1016/S0377-8398(00)00049-9.

Tréguer, P., Bowler, C., Moriceau, B., Dutkiewicz, S., Gehlen, M., Aumont, O., Bittner, L., Dugdale, R., Finkel, Z., Iudicone, D., Jahn, O., Guidi, L., Lasbleiz, M., Leblanc, K., et al. (2018) Influence of diatom diversity on the ocean biological carbon pump. *Nature Geoscience* [online]. 11 (1), pp. 27–37. Available from: https://doi.org/10.1038/s41561-017-0028-xdoi:10.1038/s41561-017-0028-x.

Treguer, P., Nelson, D.M., Van Bennekom, A.J., DeMaster, D.J., Leynaert, A. and Queguiner, B. (1995) The Silica Balance in the World Ocean: A Reestimate. *Science* [online]. 268 (5209), pp. 375–379. Available from: http://www.sciencemag.org/cgi/doi/10.1126/science.268.5209.375doi:10.1126/science.268.5209.375.

Tréguer, P.J. (2014) The Southern Ocean silica cycle. *Comptes Rendus Geoscience* [online]. 346 (11–12), pp. 279–286. Available from: https://linkinghub.elsevier.com/retrieve/pii/S1631071314000972doi:10.1016/j.crte.2014.07.0

03.

Tréguer, P.J. and De La Rocha, C.L. (2013) The World Ocean Silica Cycle. *Annual Review of Marine Science* [online]. 5 (1), pp. 477–501. Available from: http://www.annualreviews.org/doi/10.1146/annurev-marine-121211-172346doi:10.1146/annurev-marine-121211-172346.

Turner, J.T. and Ferrante, J.G. (1979) Zooplankton Fecal Pellets in Aquatic Ecosystems. *BioScience* [online]. 29 (11), pp. 670–677. Available from: https://academic.oup.com/bioscience/article-lookup/doi/10.2307/1307591doi:10.2307/1307591.

Turpin H., D. (1988) Physiological mechanisms in phytoplankton resource competition. *Growth and reproductive strategies of freshwater phytoplankton* [online]. Available from: http://ci.nii.ac.jp/naid/10020144957/en/ [Accessed 13 December 2018].

Vanormelingen, P., Verleyen, E. and Vyverman, W. (2008) The diversity and distribution of diatoms: from cosmopolitanism to narrow endemism. *Biodiversity and Conservation* [online]. 17 (2), pp. 393–405. Available from: https://doi.org/10.1007/s10531-007-9257-4doi:10.1007/s10531-007-9257-4.

Villareal, T.A. (1992) Buoyancy properties of the giant diatom Ethmodiscus. *Journal of Plankton Research* [online]. 14 (3), pp. 459–463. Available from: https://academic.oup.com/plankt/article-lookup/doi/10.1093/plankt/14.3.459doi:10.1093/plankt/14.3.459.

Villareal, T.A., Brown, C.G., Brzezinski, M.A., Krause, J.W. and Wilson, C. (2012) Summer Diatom Blooms in the North Pacific Subtropical Gyre: 2008–2009 Myron Peck (ed.). *PLoS ONE* [online]. 7 (4), pp. e33109. Available from: http://dx.plos.org/10.1371/journal.pone.0033109doi:10.1371/journal.pone.0033109.

Waite, A., Fisher, A., Thompson, P. and Harrison, P. (1997) Sinking rate versus cell volume

relationships illuminate sinking rate control mechanisms in marine diatoms. *Marine Ecology Progress Series* [online]. 157 pp. 97–108. Available from: http://www.int-res.com/abstracts/meps/v157/p97-108/doi:10.3354/meps157097.

Waite, A.M., Thompson, P.A. and Harrison, P.J. (1992) Does energy control the sinking rates of marine diatoms? *Limnology and Oceanography* [online]. 37 (3), pp. 468–477. Available from: http://doi.wiley.com/10.4319/lo.1992.37.3.0468doi:10.4319/lo.1992.37.3.0468.

Ward, B.A., Dutkiewicz, S. and Follows, M.J. (2014) Modelling spatial and temporal patterns in size-structured marine plankton communities: top–down and bottom–up controls. *Journal of Plankton Research* [online]. 36 (1), pp. 31–47. Available from: http://academic.oup.com/plankt/article/36/1/31/1527116/Modelling-spatial-and-temporal-patterns-indoi:10.1093/plankt/fbt097.

Ward, B.A., Dutkiewicz, S., Jahn, O. and Follows, M.J. (2012) A size-structured food-web model for the global ocean. *Limnology and Oceanography*. 57 (6), pp. 1877–1891. doi:10.4319/lo.2012.57.6.1877.

Ward, B.A., Wilson, J.D., Death, R.M., Monteiro, F.M., Yool, A. and Ridgwell, A. (2018) *EcoGEnIE 1 . 0 : plankton ecology in the cGEnIE Earth system model*. pp. 4241–4267.

Wassmann, P. and Reigstad, M. (2011) Future Arctic Ocean Seasonal Ice Zones and Implications for Pelagic-Benthic Coupling. *Oceanography* [online]. 24 (3), pp. 220–231. Available from: http://www.jstor.org/stable/24861317.

Watson, S.B., McCauley, E. and Downing, J.A. (1997) Patterns in phytoplankton taxonomic composition across temperate lakes of differing nutrient status. *Limnology and Oceanography* [online]. 42 (3), pp. 487–495. Available from: http://doi.wiley.com/10.4319/lo.1997.42.3.0487doi:10.4319/lo.1997.42.3.0487.

Weber, T.S. and Deutsch, C. (2010) Ocean nutrient ratios governed by plankton biogeography.

Nature [online]. 467 (7315), pp. 550–554. Available from: http://www.nature.com/articles/nature09403doi:10.1038/nature09403.

Wilson, D.L., Smith, W.O. and Nelson, D.M. (1986) Phytoplankton bloom dynamics of the western Ross Sea ice edge—I. Primary productivity and species-specific production. *Deep Sea Research Part A. Oceanographic Research Papers* [online]. 33 (10), pp. 1375–1387. Available from: http://linkinghub.elsevier.com/retrieve/pii/0198014986900415doi:10.1016/0198-0149(86)90041-5.

Wroblewski, J.S., Sarmiento, J.L. and Flierl, G.R. (1988) An Ocean Basin Scale Model of plankton dynamics in the North Atlantic: 1. Solutions For the climatological oceanographic conditions in May. *Global Biogeochemical Cycles* [online]. 2 (3), pp. 199–218. Available from: http://doi.wiley.com/10.1029/GB002i003p00199doi:10.1029/GB002i003p00199.

Yoder, J.A. (1979) EFFECT OF TEMPERATURE ON LIGHT-LIMITED GROWTH AND CHEMICAL COMPOSITION OF SKELETONEMA COSTATUM (BACILLARIOPHYCEAE). *Journal of Phycology* [online]. 15 (4), pp. 362–370. Available from: http://doi.wiley.com/10.1111/j.1529-8817.1979.tb00706.xdoi:10.1111/j.1529-8817.1979.tb00706.x.

YVON-DUROCHER, G., MONTOYA, J.M., TRIMMER, M. and WOODWARD, G. (2011) Warming alters the size spectrum and shifts the distribution of biomass in freshwater ecosystems. *Global Change Biology* [online]. 17 (4), pp. 1681–1694. Available from: http://doi.wiley.com/10.1111/j.1365-2486.2010.02321.xdoi:10.1111/j.1365-2486.2010.02321.x.

8 Appendix

Appendix 1, a comparison of global concentration between preindustrial climate (left) and the cooler climate (right) showing all functional types

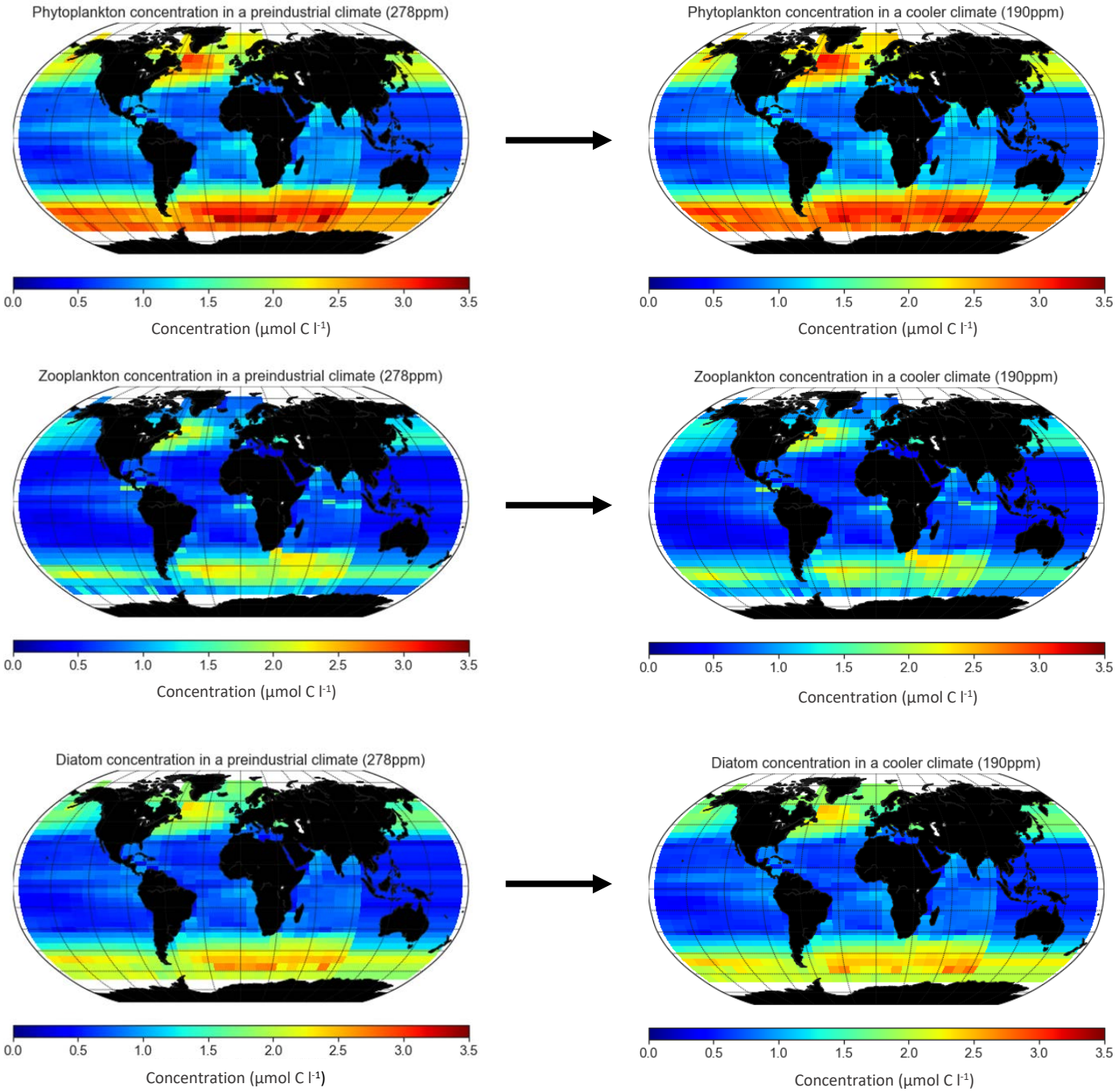

Appendix 2, a comparison of global concentration between preindustrial climate (left) and the cooler climate (right) showing all functional types